THE EFFECT OF COEFFICIENT OF FRICTION BETWEEN RAIL VEHICLE WHEELS AND RAIL TRACK ON OPERATION POWER CONSUMPTION

BY

NUR SHAHIBRAHIM BIN MAHAMUDIN

A thesis submitted in fulfillment of the requirement for the degree of Master of Science in Engineering

Kulliyyah of Engineering
International Islamic University Malaysia

JANUARY 2024

ABSTRACT

The daily cost of rail operation is increasing due to the increase in rail network size. Therefore, reducing operation power consumption is important for rail operators to optimize daily operation costs. Operation power consumption in rail operation can be divided into 80% traction power, such as vehicle propulsion system, and 20% non-traction power, such as station electrical consumption. Many research has already been carried out on advanced traction systems, such as regenerative braking storage systems, hybrid batteries, and others, which aim to reduce operation power consumption. However, very few addresses the concern about track condition and maintenance. This research focuses on the interaction between the rail vehicle wheels and the rail track and how the coefficient of friction affects the rail operation power consumption. Train resistance can be expressed in the Davis equation, which is the mathematical model used in rail industries to find train performance, therefore Davis equation is use in the research to determining the operation power consumption of variable track kinetic coefficient of friction. As rail grinding is an essential rail preventive maintenance to improve track surface, indirectly coefficient of friction has shown an improvement. Our findings indicate that the application of the rail grinding method had successfully reduced the track kinetic coefficient of friction from $\mu = 0.5$ to 0.3, therefore reducing 9% in operation power consumption. The reduction of the track kinetic coefficient of friction has led to a decrease in train running resistance, consequently resulting in a reduction in operation power consumption.

ملخص البحث

الزيادة في التكلفة اليومية لتشغيل السكك الحديدة سببه زيادة وتوسع حجم شبكة السكك الحديدية. ولذلك، فإن الحد من استهلاك الطاقة التشغيلية أمر هام بالنسبة لمشغلي السكك الحديدية لتحقيق المستوى الأمثل لتكاليف التشغيل اليومية. ويمكن تقسيم استهلاك الطاقة العاملة في مجال تشغيل السكك الحديدية إلى 80% من طاقة الجر الآلي، كما في نظام دفع المركبات، و20% من طاقة غير الجر الآلي، كما في استهلاك المحطات الكهربائية. وقد أُجريت العديد من البحوث على نظم متقدمة للجر، مثل نظم تخزين المكابح التجديدية، والبطاريات الهجينة، وغيرها، التي تهدف إلى الحد من استهلاك الطاقة التشغيلية. ومع ذلك، هناك عدد قليل جدًا من الأبحاث التي تعالج القلق بشأن حالة المسار وصيانته. لهذا,يركز هذا البحث على التفاعل بين عجلات عربات السكك الحديدية ومسار السكك الحديدية وكيف يؤثر معامل الاحتكاك على استهلاك طاقة تشغيل السكك الحديدية.ويمكن التعبير عن مقاومة السكة بمعادلة ديفيس، وهي النموذج الرياضي المستخدم في قطاع السكك الحديدية لإيجاد مستوى فعالية وأداء القطارات، لذلك تستخدم معادلة ديفيس في البحوث لتحديد استهلاك قوة التشغيل لمعامل الاحتكاك الحركي ذو المسار المتغير. وبما أن طحن السكك الحديدية وهو صيانة وقائية أساسية للسكك الحديدية لتحسين سطح المسار، فإن معامل الاحتكاك أظهر تحسناً بصورة غير مباشرة. وتشير النتائج التي توصلنا إليها في هذه الدارسة إلى أن تطبيق طريقة طحن السكك الحديدية قد أدى بنجاح إلى خفض معامل الاحتكاك الحركي في المسار من 0.5 إلى 0.3 ميكرو، وبالتالي خفض 9 في المائة من استهلاك الطاقة التشغيلية. وقد أدى انخفاض معامل الاحتكاك الحركي للمسار إلى انخفاض في مقاومة تشغيل القطارات، مما أدى إلى انخفاض في استهلاك الطاقة التشغيلية.

APPROVAL PAGE

I certify that I have supervised and read this study and that in my opinion, it conforms to acceptable standards of scholarly presentation and is fully adequate, in scope and quality, as a dissertation for the degree of Master of Science in Engineering

…….
Fadly Jashi Darsivan
Supervisor

I certify that I have read this study and that in my opinion it conforms to acceptable standards of scholarly presentation and is fully adequate, in scope and quality, as a dissertation for the degree of Master of Science in Engineering

…….
Tengku Nordayana Akma
Examiner

…….
Jamaluddin Mahmud
External Examiner

This thesis was submitted to the Department of Mechanical and Aerospace Engineering and is accepted as a fulfilment of the requirement for the degree of Master of Science in Engineering

…….
Hanan Mokhtar
Head, Department of Mechanical and Aerospace Engineering

This thesis was submitted to the Kulliyyah of Engineering and is accepted as a fulfillment of the requirement for the degree of Master of Science in Engineering

…….
Sany Izan Ihsan
Dean, Kulliyyah of Engineering

DECLARATION

I hereby declare that this thesis is the result of my own investigations, except where otherwise stated. I also declare that it has not been previously or concurrently submitted as a whole for any other degrees at IIUM or other institutions.

Nur Shahibrahim bin Mahamudin

Signature…… Date…….09/01/2024…….

INTERNATIONAL ISLAMIC UNIVERSITY MALAYSIA

DECLARATION OF COPYRIGHT AND AFFIRMATION OF FAIR USE OF UNPUBLISHED RESEARCH

THE EFFECT OF COEFFICIENT OF FRICTION BETWEEN RAIL VEHICLE WHEELS AND RAIL TRACK ON OPERATION POWER CONSUMPTION

I declare that the copyright holder of this thesis/dissertation are jointly owned by the student and IIUM.

By signing this form, I acknowledged that I have read and understand the IIUM Intellectual Property Right and Commercialization policy.

Affirmed by Nur Shahibrahim bin Mahamudin

…… ……...09/01/2024……

Signature Date

This thesis is dedicated to my parents for laying the foundation of what I turned out to be in life.

ACKNOWLEDGEMENTS

All glory is due to Allah, the Almighty, whose Grace and Mercies have been with me throughout my program. Although it has been tasking, His Mercies and Blessings on me ease the arduous task of completing this thesis.

I am most indebted to my supervisor, Assoc. Prof. Dr. Fadly Jashi Darsivan, whose enduring disposition, kindness, promptitude, thoroughness, and friendship have facilitated the successful completion of my work. I put on record and appreciate his detailed comments, valuable suggestions, and inspiring queries, which have considerably improved this thesis. His brilliant grasp of the aim and content of this work led to his insightful comments, suggestions, and queries, which helped me a great deal. Despite his commitments, he took the time to listen and attend to me whenever requested. The moral support he extended to me was a boost that helped in build and write the draft of this research work.

Lastly, my gratitude goes to my beloved wife Amira and my lovely children Qaid and Ajda; for their prayers, understanding, and endurance while away.

Once again, we glorify Allah for His endless mercy on us, one of which is enabling us to successfully round off the efforts of writing this thesis. Alhamdulillah.

TABLE OF CONTENTS

LIST OF TABLES

LIST OF FIGURES

LIST OF ABBREVIATION

ATS	Automatic train supervision
BADD	Boarding dedicated doors
BASD	Boarding space division
BATD	Boarding time division
CBTC	Communication base train control
ECS	Environment control system
ESS	Energy saving system
LIM	Linear induction motor
LRT	Light rail transit
MRT	Mass rail transit
OTCS	Optimal train control simulator
VCC	Vehicle control center

LIST OF SYMBOLS

W_a	Adhesive weight (N)
B_e	Breaking force (N)
c_2^r, c_3^r	Coefficient due to track alignment
c_a^r	Coefficient of train body smoothness
n	Engine efficiency
P	Operation power consumption (kW)
R	Resistance force (N)
S	Station-to-station distance (m)
t	Time (s)
μ	Track coefficient of friction
T_E	Tractive force (N)
a	Train acceleration (m/s^2)
m	Train mass (kg)
v	Train velocity (km/h)

CHAPTER ONE

INTRODUCTION

1.1 BACKGROUND OF THE STUDY

Rail transportation is one of Malaysia's important transportation mode. According to the Ministry of Transportation Malaysia, the rail network in Malaysia covers most of the 11 states in Peninsular Malaysia, and it provides connectivity for most Malaysian, especially in Klang Valley (MOT, 2019). It reduces traffic congestion and provides satisfaction for most Malaysian. To ensure the railway network in Malaysia benefits most Malaysian, several future new rail networks projects have been planned, such as the new LRT 3, MRT Putrajaya Line, MRT Circle Line, East coast rail line (ECRL), and Kuala Lumpur high-speed rail (HSR).

There are three essential elements in rail transportation: the train (Rolling stock), the rail track system, and the traffic control system (Paul, 2015). These three essential aspects are crucial in maintaining safe and reliable rail operations. The train propulsion systems can be divided into diesel engines and electric engines. Most urban rail in Malaysia, such as LRT, MRT, and Monorail, have electrical propulsion engines.

According to world trends, the daily cost of rail operation is increasing due to the increase in the national electric energy pricing rate and expanding the size of the rail network (Anupriya, 2020; González-Gil *et al.*, 2014). Therefore, reduction in power consumption has played an essential role in the urban rail industry as electric energy is the primary source of vehicle propulsion and traction power systems (Gu *et al.*, 2010). Power consumption use in urban rail systems is typically classified into traction and non-traction consumptions. Traction power is refers to the power consumption required to operate the rolling stock throughout the system and includes propulsion and onboard auxiliary systems (González-Gil *et al.*, 2014).

Several approaches can be implemented to reduce the energy consumption of rail operations, such as using regenerative braking storage systems, hybrid batteries, and others. These approaches can be costly as they require a large amount of investment

to acquire the technology (González-Gil *et al.*, 2014). However, some solutions do not need a large investment by the company, such as implementing suitable track conditions and maintenance plans such as rail grinding. Suitable track surface kinetic coefficient of friction can improve vehicle wheel and rail track interaction, reduce running resistance, and reduce operation power consumption. One of the strategies to reduce the kinetic coefficient of friction of the rail track surface is by applying good track maintenance, such as track lubrication and rail grinding.

Rail grinding is a vital track maintenance tool essential in removing track corrugation and improving track surfaces (Du *et al*., 2021; Sroba, 2013). As rail grinding is a vital rail track maintenance, i.e., to improve track profile and ease corrugation, its effect to track surface kinetic coefficient of friction is always being neglected and not further investigated by track network engineers as the primary concern in rail grinding is to ease track corrugation and improve track profile. Indirectly, we can use rail grinding as a tool to reduce the kinetic track coefficient of friction; that may results in improving operation power consumption.

1.2 PROBLEM STATEMENT

The electrical energy consumed in daily rail operations can be split into 80% for the traction and 20% for station consumers (Galaï-Dol *et al.*, 2016). Instead of providing safe and reliable services to the public, rail operators must cope with their daily operation expenditure that keeps expanding their services.

Most of the daily operation expenditure of rail services is due to the electrical energy used to generate train traction power. Energy consumption in urban rail systems is defined by various interdependent factors embracing vehicles, infrastructure, and operations. Therefore, a broad understanding of the energy flows within the system is fundamental to developing successful energy efficiency programs (González-Gil *et al.*, 2014). Good energy consumption and optimization plans in daily operation and rail maintenance can save vast amounts of operation costs. According to González-Gil (2014), "Several strategies can be used to minimize energy consumption such as regenerative braking, energy-efficient driving, traction losses reduction, comfort functions optimization, energy metering, smart power management, and renewable energy micro-generation." Large energy efficiencies projects such as regenerative power storage systems, hybrid battery systems, and ECS (energy control systems) require large investment from the company; this may not solve the problem as it may increase the rail operator expenditure on new hardware, but there are several plans and strategies can be taken to reduce energy consumption which does not require large investment from the company.

As the major contribution to the operational cost is traction power consumption, one of the comprehensive ways to reduce traction power consumption is by reducing traction losses of the train operation. The coefficient of friction between the wheel and rail surface is a crucial factor in maintaining the train's acceleration, constant speed, and braking performance. In addition, rail tracks may be exposed to oxidation and deformation, leading to track corrugation and profile defects. Therefore, monitoring the track coefficient of friction to its optimum value is vital to maintain safe train operation and optimum daily operation power consumption (Zhao *et al.*, 2012). Friction between the wheel and rail surface is understood to significantly impact the vehicle's wheel and rail surface wear, lateral (curving) forces, noise, and train power consumption (Vandermarel *et al.*, 2014).

1.3 RESEARCH OBJECTIVES

The main objectives of the research are:

1. Investigate the dynamic characteristics of train motion, including acceleration, constant speed, cruising, and braking, through precise measurements and analysis of operational data in order to enhance understanding of rail operation dynamics.
2. Improve the power consumption profile of the train under various operating conditions and to establish a quantitative understanding of power consumption patterns.
3. Analyse the impact of rail track coefficient of friction on rail operation power consumption, hence to assess the correlation between train running resistance and operation power consumption using theoretical and experimental analysis.

1.4 SIGNIFICANCE OF RESEARCH

The research will contribute more practically to the previous research on rail operation costs. The study will benefit rail operators by reducing daily operation costs without installing new and costly hardware, therefore reducing operator expenditure.

The research highlighted the effect of the track kinetic coefficient of friction on operation power consumption and the application of rail grinding to lower track kinetic coefficient of friction is very practical for rail operators as rail grinding is a regular rail track maintenance technique.

Moreover, the research will redirect rail operators by expanding the focus of rail grinding beyond track corrugation and profile; but also the impact of the activity on operation power consumption.

1.5 SCOPE OF STUDY

The research scope focus on metro rail transport such as LRT Line, which generally refers to rail transport within a metropolitan area with a short distance between stations, operating at low speed (not affected by aerodynamic drag) and operating in maximum passenger load. The research focuses on investigating the relationship between the coefficient of friction of rail track surface and train power consumption, thus relating it to train motion of acceleration, constant speed, and braking.

This research takes part at Kelana Jaya Line Kuala Lumpur Rail transit. The daily operation consists of several 2-car and 4-car train (Bombardier Innova Metro 300: Electric system using linear Induction motor (LIM)) that operates 18 hours daily.

The research include the theoretical analysis and experimental analysis of operation power consumption. Theoretical analysis is focus on analysis of train resistance using Davis equation and experimental analysis is focus on the application of rail grinding to reduce track coefficient of friction.

1.6 RESEARCH METHODOLOGY

The following methodology was used to achieve the research objective. A literature review of journal papers, books, articles, and manuals about rail operation power consumption, resistance, and rail grinding was conducted to understand the topics better. A theoretical analysis of rail operation power consumption using the Davis equation was constructed to understand the study better, and the result was compared with the literature analysis. Therefore, the preliminary outcome of the study was estimated. An experiment was conducted at Kelana Jaya Line LRT, and the result was compared with the theoretical analysis to validate the result.

The Figure 1.1 is the research methodology flow diagram. In addition, the sequent work of the research is as the following:

(i) Theoretical analysis of the different types of station-to-station travel and operation power consumption using the Davis equation.

(ii) Theoretical analysis of operation power consumption with different train loading and track coefficient of friction using the Davis equation.

(iii) Experimental analysis of train operation power consumption for various train loading.

(iv) Experimental analysis of train operation power consumption for different track coefficients of friction with the application of rail grinding to reduce track coefficient of friction.

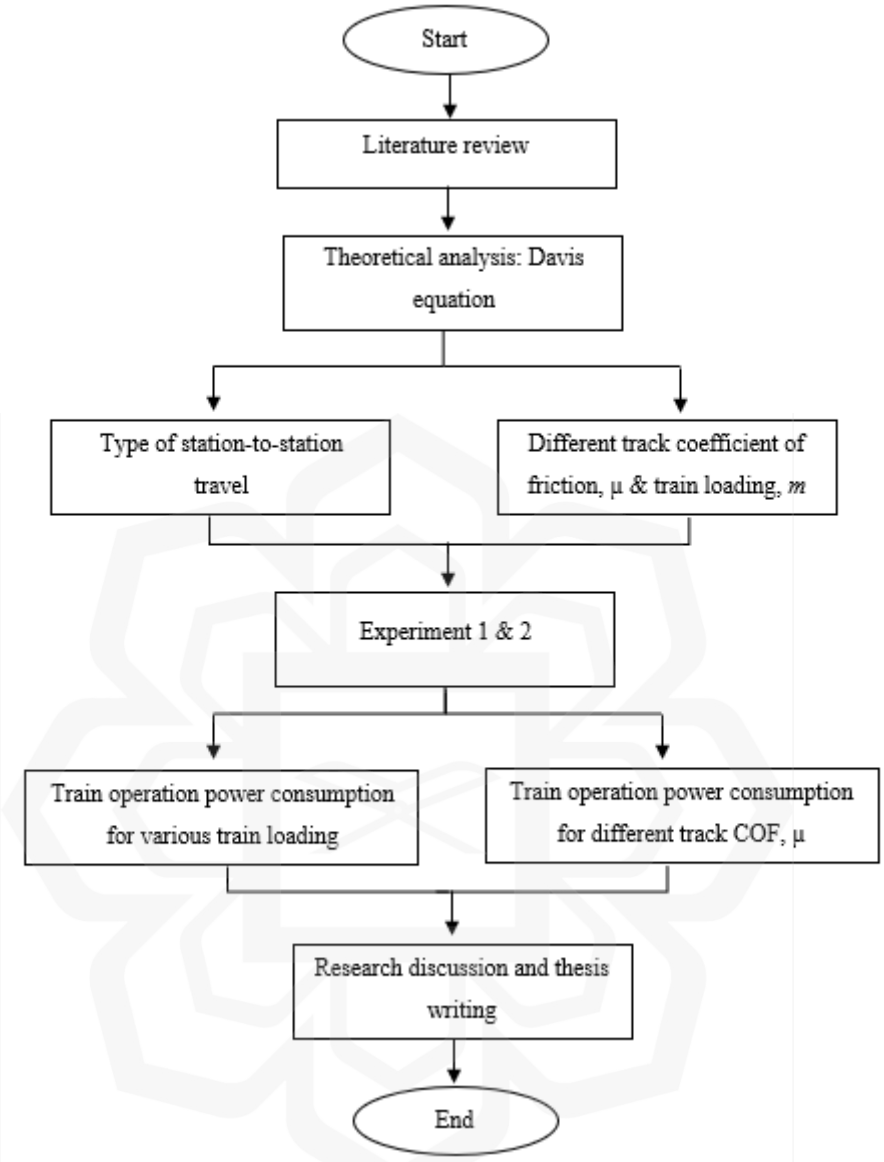

Figure 1.1: Flow diagram of research methodology.

1.7 ORGANIZATION OF THE THESIS

The thesis is organized into chapters so each research objective is well-answered and easily understood. In chapter one, the background of the research was introduced. The problem statement and objective of the research are explained in this chapter. A brief methodology that is used in the research is introduced in this chapter. In addition, the scope of the research is also presented in this chapter.

In chapter two, some previous research and literature are reviewed to gain an understanding of the topics. Several topics on rail operation power consumption, rail station-to-station travel, Davis equation, resistance, and rail grinding are gathered.

In chapter three, the methodology of the research is highlighted. The theoretical and experimental analysis, test procedure and specification are explained in this chapter. A brief introduction of the test application and the methodology chart is shown.

In chapter four, the mathematical model of the study is introduced, and a theoretical analysis is extended using the mathematical model.

In chapter five, the result of the experimental analysis is discussed. The result is compared with the theoretical analysis and literature review for validation.

In chapter six, the research conclusion and recommendations for future improvement were introduced.

CHAPTER TWO

LITERATURE REVIEW

2.1 INTRODUCTION

Most rail operators have been exploring ways to reduce their operational costs; the reduction in rail traction power consumption (Arupiya, 2020); resulting in lowering daily operation power consumption and may gain interest from all the rail operators worldwide.

There are several ways to reduce rail operation power consumption and some of the strategies are already widely implemented by railway operators, such as hybrid battery systems, ECS, ESS, and regenerative braking systems, may more (González-Gil *et al.*, 2014).

According to the Davis equation; a standard equation used in the rail industry to identify train resistance components, a major contribution to rail traction power consumption drawback is the running resistance. Therefore, the reduction of running resistance is expected to bring a positive impact on the system. In addition, there are many contributions to rail resistance, such as aerodynamic resistance and running rail contact resistance (Hansen *et al.*, 2017). The studies by previous researchers on running rail lubrication and wheel profile contact to reduce the resistance value may positively impact the development and design of today's rail system (Vandermarel, 2013).

As for existing rail operators, implementing new designs and hardware may require a large investment in acquisition, testing, commissioning, and approval (González-Gil *et al.*, 2014). Therefore, most rail operators will not consider this method. Some current practices in rail operations are not fully utilized by rail engineers, such as grinding activities. As grinding activities aim to ease rail corrugation and to improve rail profile (Sroba, 2013); for safe rail operation with low noise rate, indirectly some effects seldom being neglected, such as the effect on the rail surface coefficient of friction after rail grinding may affect the train running resistance and the operation power consumption.

2.2 REVIEW ON RAIL OPERATION POWER SYSTEM

Train propulsion is directly fed by the electrical power distribution system using pantographs, or collector shoes, depending on whether the electricity is supplied by an overhead line or conductor rail. Referring to Figure 2.1, 80% major contribution of rail operation power consumption is due to traction power consumption or also known as the power to move trains (González-Gil *et al.*, 2014). Therefore, research in rail operation power consumption should focus on train motion.

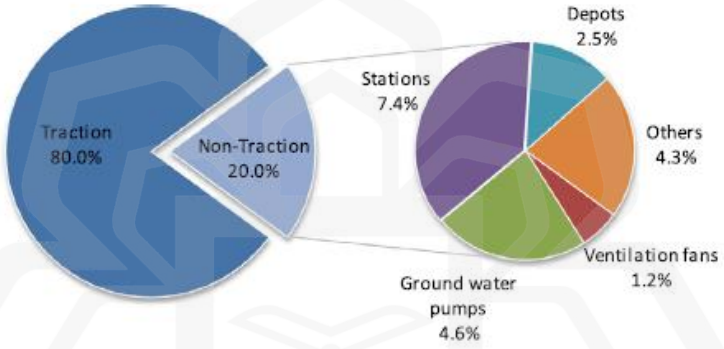

Figure 2.1: Percentage of traction and non-traction power (González-Gil *et al.*, 2014).

In addition, according to Figure 2.2, a major contribution to energy loss is due to energy to overcome the motion resistance of the train, such as aerodynamic opposition and mechanical friction between wheels and rails. Therefore, this area is essential and should be highlighted in the operation power consumption reduction study.

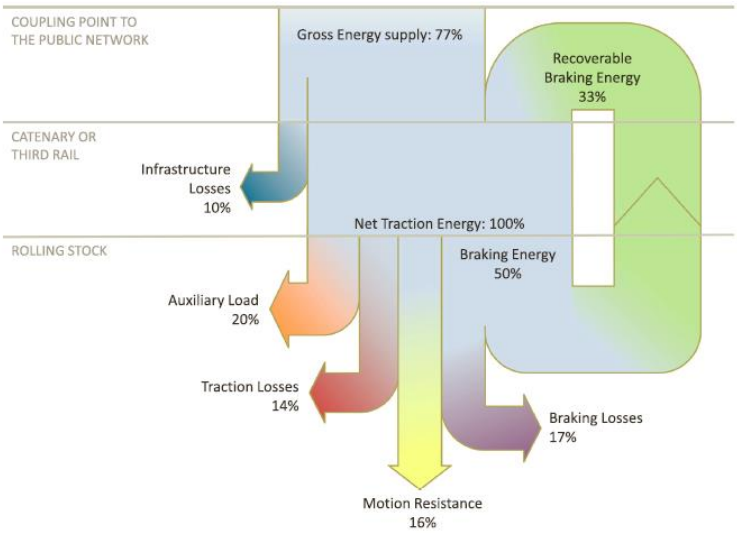

Figure 2.2: Diagram of the percentage of energy loses (González-Gil *et al.*, 2014).

2.2.1 Importance of rail operation power consumption reduction

According to Figure 2.3 and Figure 2.4, the growth of rail transportation contributed to the increase in daily operation expenditure. Therefore, reducing rail operation power consumption is essential in the urban rail industry as electric energy is the primary source of train propulsion and traction power systems.

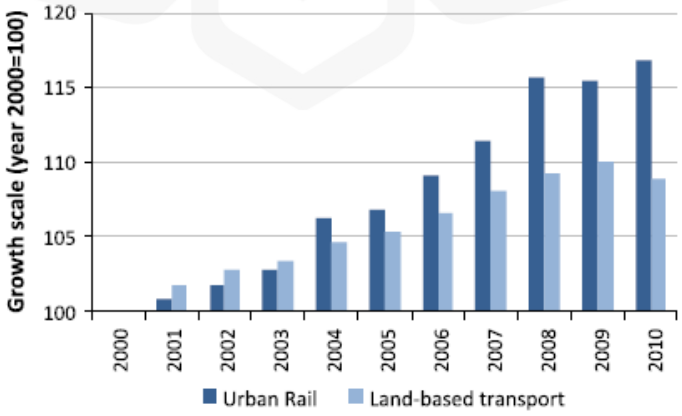

Figure 2.3: Graph of growth scale of rail transport from year 2000 to 2010 (González-Gil *et al.*, 2014).

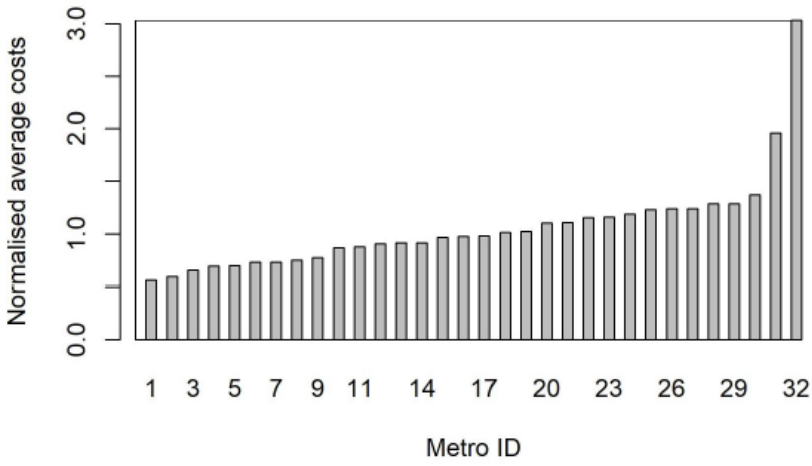

Figure 2.4: Graph of increasing of rail size with expenditure of rail operation (Anupriya, 2020).

Referring to Figure 2.4, metro id refers to the number of metro lines. The research shows the increasing number of metro lines, higher the operation costs. According to a research, China rail operation power consumption in 2021 was about 21.31 billion kWh, an increase of 23.6% from previous year due to expansion of their rail line (Xing *et al.*, 2023). Therefore, rail operators need to reduce their traction power consumption to decrease their daily rail operation power consumption cost. Figure 2.5 shows the basic electrical power distribution system for the rail line.

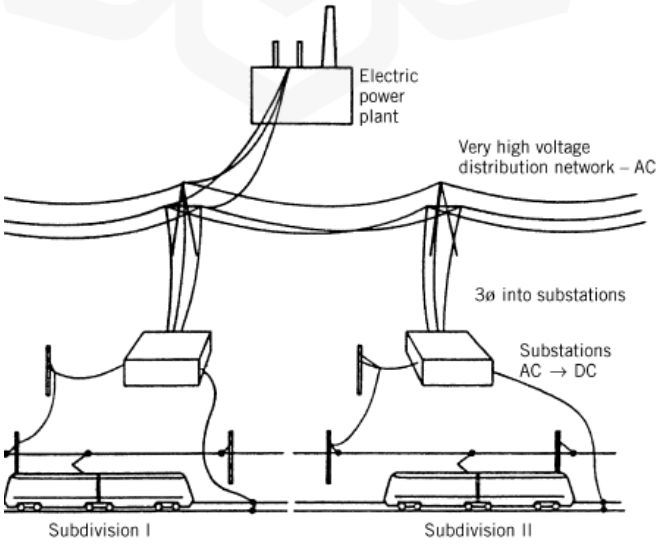

Figure 2.5: Electrical power distribution system of rail line (Vukan, 2007).

2.2.2 Strategies of rail operation power consumption reduction

There are several strategies to reduce rail operation power consumption, and some of the strategies are already widely implemented by railway operators. According to Figure 2.6, many factors contribute to the reduction of operation power consumption, such as the technological base as the implementation of the hybrid battery system, ECS, ESS and traction power regenerative system and operation base, such as timetable and traffic optimization, intelligent energy management, track condition management, and passenger movement optimization (González-Gil *et al.*, 2014).

Figure 2.6: Rail operation power consumption saving strategies (González-Gil *et al.*, 2014).

Based on a journal by Xing *et al.*, 2023 on rail train operation energy-saving optimization framework based on improved brute-force search, the authors emphasise the importance of reducing rail operation power consumption in developing of green and low-carbon environment. He introduced an energy-saving optimization framework that utilised regenerative braking energy and station-to-station operation using a brute-force search algorithm. Several specific intervals of station-to-station travel in

Guangzhou Metro Line 7 are reviewed using the algorithm with the impact of regenerative braking. The journal concludes with a recommended speed curve with the lowest operation power consumption that is suitable for the rail line. However, for conventional ATO rail operation, the station-to-station travel speed curve is automatically generated by the ATC system based on the rail lines parameters such as scheduled timetable, station travel, stopping point, train characteristics and track infrastructure (Bochmann & Jaekel, 2022; Liu *et al.*, 2015). Therefore to set the operation with a recommended speed curve required specific modification to the system by the technical provider.

In addition, most rail lines are not equipped with regenerative braking systems, hence the framework does not apply to most rail lines. Several undiscovered areas can be improved, especially in studying train dynamic characteristics, such as train running resistance and traction losses, to get optimal operation power consumption. As motion resistance and traction losses compromise a major percentage of train power consumption losses (González-Gil *et al.*, 2014), reviewing train dynamic characteristics and connecting them to the existing operation and maintenance procedure will assist researchers in finding ways to reduce operation power consumption.

2.2.2.1 Optimal train control simulator (OCTS)

An optimal train control simulator (OTCS) is designed by Su *et al.*, 2016. Figure 2.7 is the flow diagram of optimal train simulator design using trip distance, time, gradient, resistance, and train mass as the inputs.

The power-efficient train control and power consumption are the output of the design. According to the research, a simulation based on practical data from the Beijing Yizhuang line, several power consumption efficient strategies can be constructed regarding trip time, track gradient, regenerative braking, train mass, and resistance (Su *et al.*, 2016). Figure 2.7 is the input diagram for optimal train control simulator,

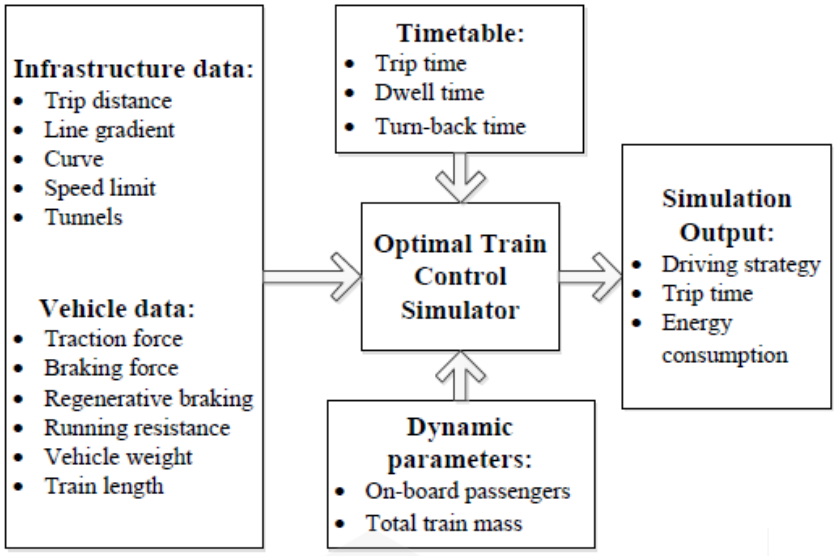

Figure 2.7: Input diagram of OTCS (Su *et al.*, 2016).

Furthermore, research in German railway lines on energy-efficient train driving based on optimal control theory shows that by applying this theory, an average reduction of 37% of their daily operation power consumption is achieved (Heineken *et al.*, 2023). The research stated that it would not be appropriate to apply the optimal control theory on trains that run by the operation timetable because trains that delay need to drive faster to catch up with the timetable and trains that drive too fast will tend to arrive early at the station. In addition, optimal control theory can only attain its full potential if the train is equipped with a regenerative braking system. In the context of this research, applying optimal control theory is not applicable due to the train operation being restricted by the operation timetable.

2.2.2.2 Trip time

Referring to Figure 2.8, the relationship between power consumption and the trip time is in convex function; an increase in trip time will increase power consumption. During off-peak hours, dwell time is sometimes shorter than scheduled dwell time. If the train could close the door immediately after the passenger completes boarding the train, the trip time for the next station-to-station move could be prolonged, and the energy

consumption would be reduced effectively; the power consumption rate can be reduced up to 12.07% for multiple station-to-station movement (Su *et al.*, 2014).

In addition, according to a journal by Gao and Yang, 2019, the trip time and operation power consumption are interrelated. During long train trips time, the train speed is low and the traction force is reduced. Conversely, if the train trip time is short, the train speed is high, and the traction force is increased. Gao and Yang, 2019 also added trip time between stations during off-peak train operations can be increased to decrease operation power consumption. However, most rail operator around the world are restricted with the minimum trip time for their daily operation so that their operation will be more reliable. One way to improve rail operation reliability is by increasing trip time. This is because higher trip time will accommodate any delay during operation and improve operation reliability from the passenger's perspective (Landex, 2012).

Furthermore, two other strategies suggested to reduce operating power consumption in terms of trip time by reducing the trip time by lowering the invalid platform dwell and timetable optimization. The following is the graph of the influences of trip time on operation power consumption.

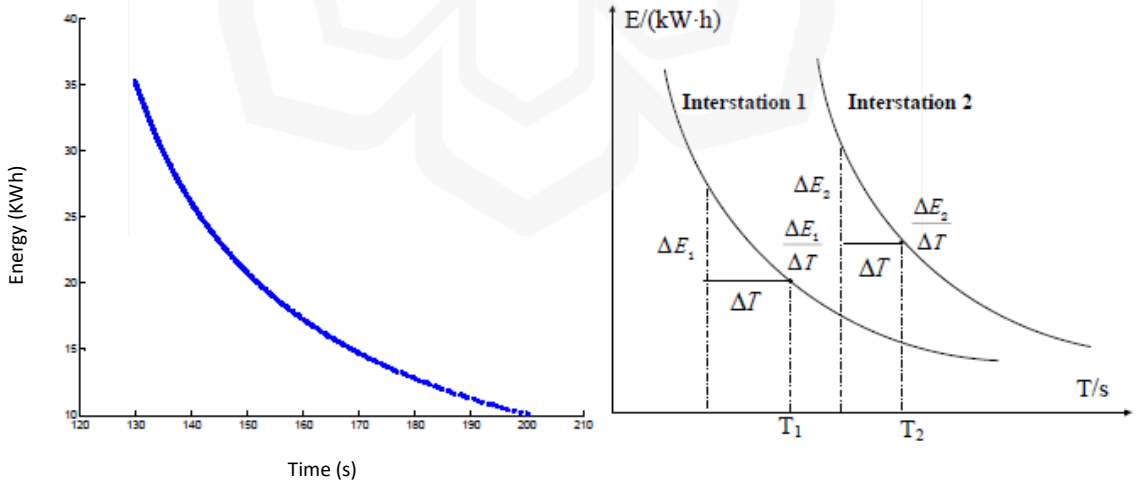

Figure 2.8: Graph effect of trip time to power consumption rate (Su *et al.*, 2016).

2.2.2.3 Gradient

According to the operation power consumption of station-to-station travel between Jiugong and Yizhuangqiao, the compromise of three section changes of gradient from -4% to 11%, from 1% to 15%, and from -5% to 10%, the result shows that more operation power consumption is consumed with an increase of gradient section track design. This is because more traction force must be applied to follow the required trip time for a stepper uphill climb. However, a lower traction force is needed when increasing the gradient at the approaching station section due to less time with a lower braking rate for the train to do the station stop.

In addition, the research shows a higher operation power consumption rate with a higher gradient at the middle section of the track due to the training needs more power consumption to overcome gradient resistance (Su *et al.*, 2016). Therefore, one power consumption efficient strategy that can be concluded in the following research is; designing a rail track that increases in gradient at approaching station and with a proper length of the gradient. Table 2.1 summarizes the power consumption rate for different track gradients. The section in the following table refers to the section of track, which are the start, middle, and end sections.

Table 2.1: Table of power consumption for different track gradients (Su *et al*, 2016).

Section	Parameters	Value							
1	G (‰)	−4	−3	−2	−1	0	1	2	3
	Energy (kWh)	21.0	21.4	21.8	22.2	22.6	23.0	23.3	23.7
	G(‰)	4	5	6	7	8	9	10	11
	Energy (kWh)	24.1	24.5	24.9	25.2	25.6	26.0	26.4	26.8
2	G (‰)	1	2	3	4	5	6	7	8
	Energy (kWh)	21.8	21.8	21.9	21.9	22.0	22.0	22.1	22.1
	G (‰)	9	10	11	12	13	14	15	-
	Energy (kWh)	22.2	22.3	22.4	22.5	22.6	22.7	22.8	-
3	G (‰)	−5	−4	−3	−2	−1	0	1	2
	Energy (kWh)	22.8	22.8	22.7	22.7	22.7	22.6	22.6	22.5
	G (‰)	3	4	5	6	7	8	9	10
	Energy (kWh)	22.5	22.4	22.3	22.2	22.2	22.1	22.1	22.0

2.2.2.4 Regenerative braking

Most modern electrical rail vehicles can convert kinetic energy to electrical energy when braking is applied. According to previous Figure 2.2, approximately 33% of traction power can be recovered using this system. According to research on JSC Russian Railways, the use of regenerative braking systems can reduce up to 30% of operation power consumption (Konstantinova *et al.*, 2022). He added additional advantages of the regenerative braking system such as reduction of brake pads and wheel wear and material cost for braking system maintenance. However, the disadvantage of a regenerative braking system despite the more complicated electrical equipment and control system is the increase in the heating temperature of the braking equipment.

The following Figure 2.9 is the power exchange diagram of a regenerative braking system,

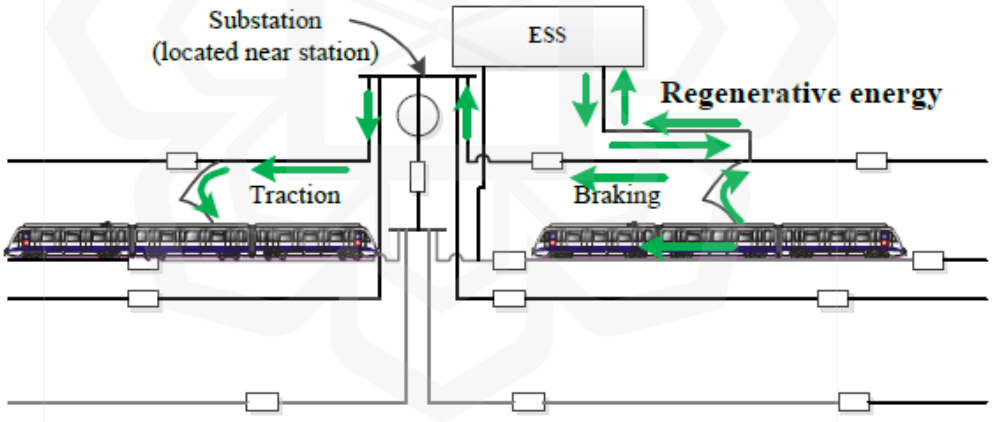

Figure 2.9: Traction power exchange between train and ESS (Su *et al.*, 2016).

2.2.2.5 Train mass

According to the OCTS study, higher train mass consumes more operation power in the same trip time due to higher train mass consuming more traction force and the time of traction force being applied is longer. Reducing train mass is a significant consideration in the railway industry, as it directly influences operation power consumption and

overall train efficiency. For example, in Table 2.2, an increase of 16.8 kWh for 200 tons of train to 31.2 kWh for 400 tons of train; the power consumption rate approximately doubled when train mass increased by 50% (Su *et al.*, 2016).

Therefore, several strategies can be used to achieve a reduction in train mass. For example, utilizing advanced lightweight materials such as aluminium and composite materials for the construction of train components, including car bodies and structural elements, which can significantly reduce overall mass without compromising structural integrity. Employing advanced engineering and design techniques to optimize the structural configuration of train components can lead to a reduction in material usage without sacrificing safety or performance. This includes using efficient load distribution, streamlined shapes, and innovative design solutions. Reducing the size and weight of various train components, such as traction systems, braking systems, and other auxiliary systems, contributes to an overall reduction in mass. Advances in technology allow for the development of more compact and lightweight components without compromising functionality. Designing train interiors with lightweight materials for seats, flooring, and other components contributes to an overall reduction in mass. This can be achieved without compromising passenger comfort and safety (Koizumi, 2013; Rochard, 2004).

In addition, optimized train passenger movement management involves the strategic planning and implementation of measures to ensure efficient and seamless movement of passengers within train systems also can used to reduce train loading during train operation (Yang *et al.*, 2022).

Table 2.2: Power consumption of rail vehicle with different masses (Su *et al.*, 2016).

Train Mass (t)	Energy Consumption (kW·h)	Train Mass (t)	Energy Consumption (kW·h)	Train Mass (t)	Energy Consumption (kW·h)
200	16.8	235	20.8	270	25.6
205	17.2	240	21.2	275	26.4
210	17.6	245	22.0	280	27.2
215	18.4	250	22.8	285	28.0
220	18.8	255	23.2	290	29.2
225	19.2	260	24.0	295	30.0
230	20.0	265	24.8	300	31.2

2.2.2.6 Track surface resistance

Track surface resistance is another factor that influences the OCTS study. Track surface resistance is the resistance the train requires to overcome due to the interaction between the train wheel and the track. It also can be known as the track coefficient of friction.

According to Figure 2.10, the current train power consumption rate of 23.4 kWh for the operation from Jiugong to Yizhuangqiao station is reduced by 0.4 kWh with a decrease of 10% in track surface resistance. The operation power consumption rate is reduced by approximately 3% for every 20% reduction of track surface resistance (Su *et al.*, 2016). Figure 2.10 is the graph of the influence of track resistance on rail operation power consumption rate:

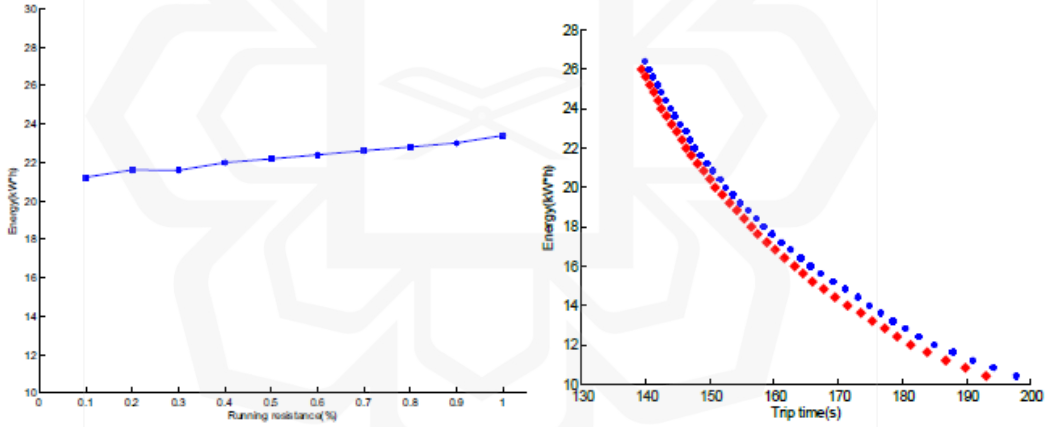

Figure 2.10: Graph effect of track resistance percentage to power consumption (Su *et al.*, 2016).

Several improvements can be made to reduce track surface resistance, such as applying track and wheel lubrication to reduce friction coefficient (International Union of Railways, 2005). In conclusion, operation power consumption is reduced by lowering track surface resistance.

2.3 REVIEW ON TRAIN DYNAMIC

Dynamic characteristics of a train, such as train propulsion and braking are essential to determine the train's maximum speed, acceleration, and power consumption. These values are crucial to assist rail engineers in analysing operational characteristics such as the type of vehicle to use, line alignment, station-to-station distance, and travel time and to estimate operating costs.

Train propulsion creates acceleration, and braking deceleration is affected by friction between the vehicle wheel and the running surface. The adhesion (attraction of two surfaces) and friction (resistance to the relative motion or adjacent surface) are two phenomena that lead to the acceleration and deceleration of rail vehicles (Vukan, 2007).

Tractive and braking forces must be transferred between the train wheel and the rail track through friction or resistance between two surfaces to achieve acceleration and deceleration. The basic equation of train motion is affected by these three forces acting on the rail vehicle: tractive, resistance and braking forces.

The train total resistance comprises running resistance and acceleration resistance. Running resistance can be differentiated between vehicle and line resistance, where the results are comprised of gradient and curvature resistance on track curves. Aerodynamic resistance and several additional resistances, such as rolling resistance and impact resistance, arise from the oscillatory movement of the train in a transverse direction, which forms running resistance (Ihme, 2022).

Figure 2.11 is the composition of train total resistance,

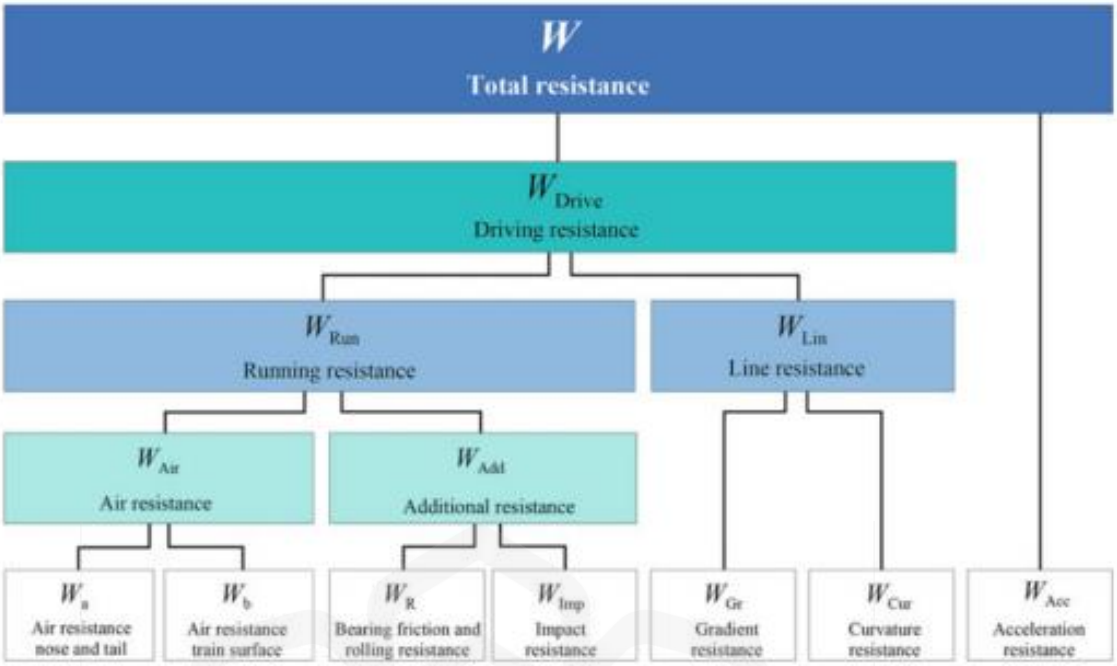

Figure 2.11: Composition of train total resistance (Ihme, 2022).

The coefficient of friction of the rail track surface may affect the tractive, resistance and braking forces hence affecting train acceleration and deceleration. The force acting on a gradient track involves several components, each contributing to the train motion along an inclined track. The primary force components include gravity and resistance. Figure 2.12 is the force acting on a train on a gradient track,

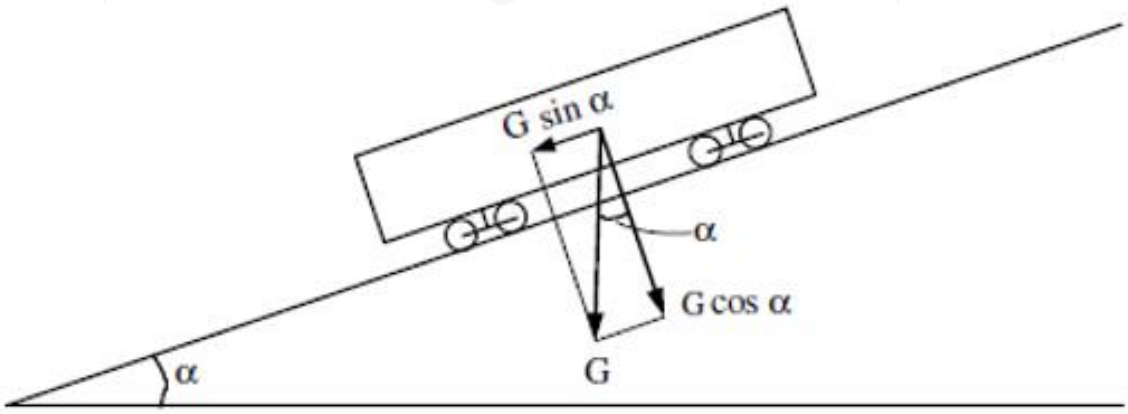

Figure 2.12: Force act on train in gradient track (Vukan, 2007).

The net force acting on train motion is the difference between tractive force and resistance force (Vukan, 2007). Total net force for the train dynamic characteristic is as the following,

$$\sum F = T_e - R = m\,\frac{dv}{dt} \tag{2.1}$$

Where T_e is the tractive force and R is the resistance force respectively measure in N. In addition, m is the train mass in kg and v is the train velocity in km/h.

To analyse of the train dynamic characteristic, it can be performed by the velocity-time graph. According to the velocity-time graph of train operation, the following elements can be constructed: the effects of acceleration, maximum speed, coasting travel time, the interstation distance, average speed, and the influence of travel stage on power consumption (Vukan, 2007).

The power consumption value for each point of train motion can be constructed based on the velocity-time graph. This is because the power a train consumes depends on the train's velocity and acceleration at each instant of time. Its computation is based on the traction force characteristic of the rail vehicle propulsion system, resistance force (mass, friction, aerodynamic drag), and station distance (Rios & Ramos, 2012).

Therefore, based on the velocity-time graph, a power consumption profile can be constructed using the following formula,

$$P = \frac{T_e v}{n},\ T_E = 2650\,\frac{nP}{v} \tag{2.2}$$

Where P is the power consumption in hp and n is the engine efficiency. P is multiply by 0.74 to get in kW.

2.3.1 Train station to station movement

Most train interstation movement consists of different regimes of motion such as acceleration, constant speed, coasting, braking, and station stop. According to Vukan, 2007, there are four types of station-to-station movement. The station-to-station distance, *s* and travel time, *t* depend on whether the transit vehicle reaches maximum speed. Vukan, 2007 added, let critical distance, s_c is the distance required by the train to accelerate to maximum velocity and then immediately apply brakes and come to a complete stop. As the regime consists of $s < s_c$, the travel only consists of acceleration, deceleration, and station stop. In addition, if $s \geq s_c$, the travel regime will compromise acceleration, deceleration, constant speed, coasting region, or both. The differences in travel regime produce four different types of station-to-station movement. Figure 2.13 is the velocity profile of four types of station-to-station movement,

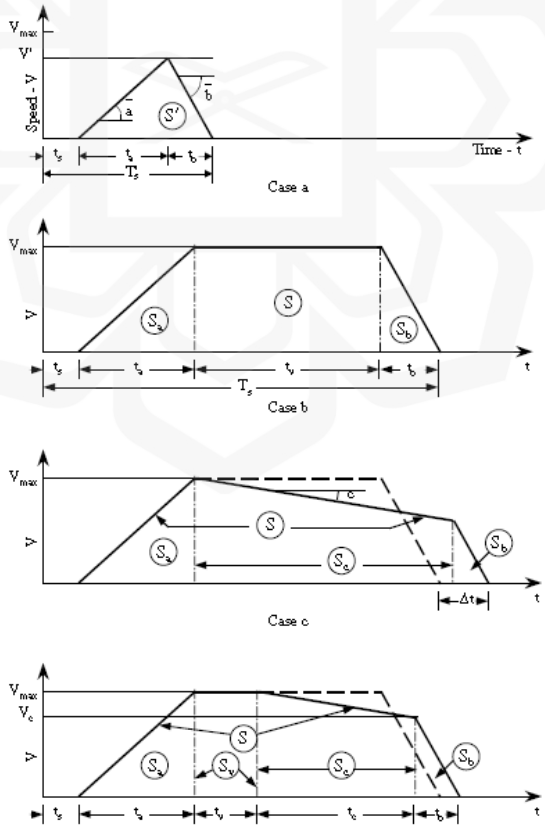

Figure 2.13: Four types of station-to-station movement (Vukan, 2007).

Referring to Figure 2.13, the type of station-to-station travel consists of acceleration and deceleration regions. Type b of station-to-station travel consists of acceleration, constant speed, and station stop region. For type c, station-to-station travel consists of acceleration, coasting, and station stop region. In addition, type d station-to-station travel consists of acceleration, constant speed, coasting, and station stop region.

One train operation cycle between two stations consists of acceleration, constant speed, coasting, deceleration, and station stop. During the first stage of the operation, the rail vehicle moves with positive acceleration, and the vehicle speed increases. During the second stage of operation, the acceleration starts to decrease as it approaches the constant speed region. In the third stage, the vehicle reaches its constant speed, and acceleration is zero. In the fourth stage, the train propulsion system is shut off, the train coasts to its specific distance and braking operation start, and the rail vehicle decelerates until it stops momentarily at the station platform.

The basic cycle of station-to-station operation consists of acceleration, constant velocity, deceleration, and station stop region. Table 2.3 shows the difference between each region of station-to-station travel (Xing *et al.*, 2023; Rios & Ramos, 2012).

Table 2.3: Table of different train operation and its net force (Rios & Ramos, 2012).

Operation	Net Force	Velocity
Acceleration	$T_e\,(v) - R(v) - B_e(v) > 0$	$0 < v < v_{max}$
Constant Velocity	$T_e\,(v) - R(v) - B_e(v) = 0$	$v > 0$
Deceleration	$T_e\,(v) - R(v) - B_e(v) < 0$	$0 < v < v_{max}$
Stop	$T_e\,(v) - R(v) - B_e(v) = 0$	$v = 0$

The power consumed by the train depends on the velocity and acceleration. It is determined based on the traction force of the train, loading, and mode of operation. Figure 2.14 shows the power consumption and tractive force profiles obtained from the train's velocity profile at each operation stage (Hsiang & Chen, 2001).

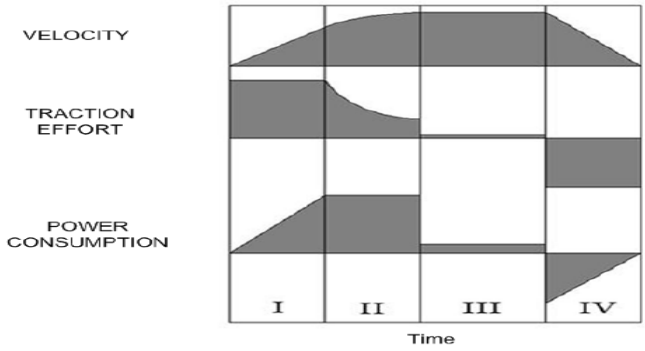

Figure 2.14: Graph of velocity, traction effort, and power consumption of a train for acceleration (I & II), constant speed (III) and braking (IV) region (Rios & Ramos, 2012).

2.3.2 Train electric propulsion system

Many types of electric propulsion systems are used in rail lines worldwide. Among the most popular propulsion systems are the DC and AC rotary motor propulsion systems and Linear induction motor (LIM) propulsion systems.

The difference between a diesel train propulsion system and an electric propulsion system is that the operation of an electric propulsion system makes it possible to regulate speed through electrical voltage and current rather than through mechanical such as gear change. This is because electric motors do not have geared transmissions like conventional engines. Still, their motor is connected with axles via a fixed pair of gears, and the required tractive force is controlled through changes in voltage and current during acceleration from standing to maximum speed or in braking of the vehicle from high to very low speeds (Vukan, 2007). Figure 2.15 shows the power consumption profile of the electrical propulsion system.

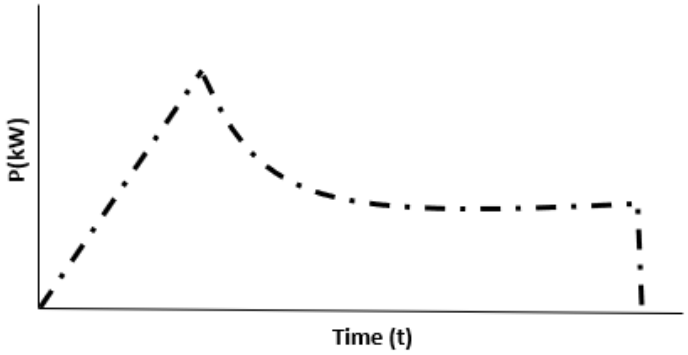

Figure 2.15: Graph of DC LIM propulsion system operation power consumption (Vukan, 2007).

According to section 1.5, the scope of the study is using the LIM propulsion system. LIM propulsion system can be represented as a set of linear induction motors mounted underneath the train and acting as a stator, and a LIM rail laid between the track act as the rotor. The magnetic interaction between the stator and rotor results in tractive force for the train propulsion to move forward. The difference between the LIM and the conventional rotary motor is that the rotor and stator are in a set of the engine that produces rotary force and transfer it to the train wheel axile. Figure 2.16 shows the difference between a conventional rotary motor and a LIM propulsion system.

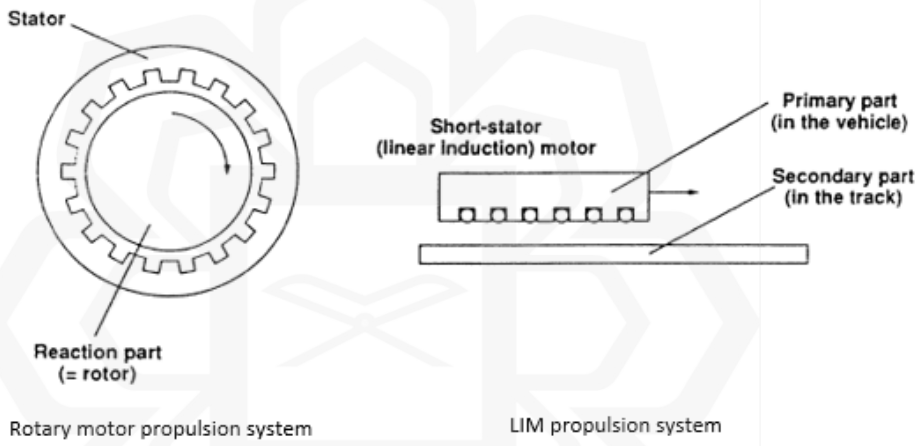

Figure 2.16: The different between conventional rotary motor and LIM propulsion system (Vukan, 2007).

2.3.3 Running Resistance

According to section 2.2, train motion resistance compromise a major percentage of the overall traction power losses. Therefore, running resistance is an important value that needs to be focused on in the study. It has an enormous impact on train performance and traction losses. The running resistance is a set of forces that must be overcome by tractive forces to set the train in motion at a constant speed or to accelerate it to a higher speed (Ihme, 2022; Vukan, 2007).

The running resistance of a train have been addressed in numerous studies in the last two centuries. Early measurements of the running resistance were performed in 1818 by Stephenson and Wood (1855) but were investigated in more detail in the 1840s by Harding (1846) and Gooch (1848). The latter studies lead to early predictive equations for the running resistance by Clark (1855). These early measurements reached velocities up to about 100 km/h, and during the next half-century, the velocity range for resistance measurements was expanded, reaching up to 210 km/h in 1904 (Hansen *et al.*, 2017).

Various tests have been made over the years and have come out with a final empirical formula used in rail industries. This equation is commonly known as the Davis equation (Hansen *et al.*, 2017), as the coefficients of the Davis equation are related to different resistance contributions, as train resistance can be expressed in the following form,

$$R = A + Bv + Cv^2 \tag{2.4}$$

Where R is the train resistance force in N, A is the resistance component independent of train speed, such as rolling and track resistance, contacts between the wheel and track surface. B is the coefficient used to define train resistance dependent on train speed, such as flange friction, wave action, and oscillation, and C is the streamlining and aerodynamic coefficient used to define train resistance dependent on the square of the train speed, such as air or aerodynamic resistance.

The A value consists of the mechanical friction value related to weight which is the rolling resistance. Rolling resistance results from the friction between the wheel and the rail track and its component of the force opposing the train's motion due to car weight. The B value is related to train truck design that affects the ride quality of the train, such as flange friction and oscillation effect due to the nosing force of the train track, and wheel flange to the rail track (Edwards, 2010). Meanwhile, the C value is the aerodynamic resistance of the train body and design.

The impact of the respective Davis equation on resistance is shown in the Figure 2.17,

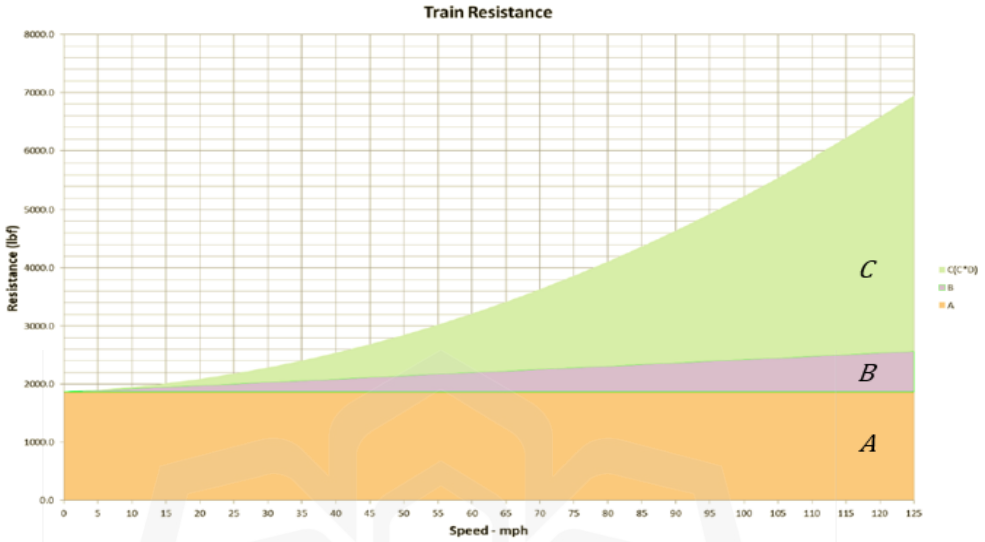

Figure 2.17: Graph of relationship between train resistance and speed (Rochard & Schmid, 2000).

From Figure 2.17, according to Davis equation the value of *A* and the friction elements that contribute to it remain static regardless to the speed of the train. The value of *B* can be seen to slowly increase with speed. For The value of *C*, it shows that the value of *R* increases at significant rate at certain speed as the speed increases. The value of *C* represents the aerodynamic resistance; hence, this also explains why so much attention is taking care of if it related to high-speed train. Good aerodynamic design of vehicle and track is very important for high speed train because the influence of the value of *C* in Davis equation increases with square of the train speed (Rochard & Schmid, 2000).

However, aerodynamic resistance only becomes dominant in high-speed rail operations and freight train operations. For example, the aerodynamic resistance of an open-top empty wagon is higher than that of a closed-top and loaded wagon due to the increase in air turbulence inside the wagon (Sapronova *et al.*, 2017). According to Davis's equation, the value of *A* and the friction elements that contribute to it remain static regardless of the train's speed. The value of *B* can be seen to increase with speed. The value of *C* shows that the value of *R* increases at a significant rate at a certain speed

as the speed increases. The value of *C* represents the aerodynamic resistance; hence, this also explains why so much attention is paid to it if it is related to high-speed trains. The good aerodynamic design of vehicles and tracks is essential for high-speed trains because the influence of the value of *C* in the Davis equation increases with the square of the train speed (Rochard & Schmid, 2000).

For this study, due to the main scope of the study being for low-speed metro rail operation, the study is only taking consider of the resistance component that is independent of training speed, the value of *A* as the research only takes part in low-speed train operation and the aerodynamic of the train is neglected to achieve the objective of the research is to identify how the coefficient of friction between vehicle wheel and rail track affects the rail operation energy consumption.

By the regression of the Davis equation with the net force equation, the change in Power consumption, *P*, in relation to the Davis equation is as the following.

$$P = (\sum F + A + Bv + Cv^2 + B_e)v \qquad (2.5)$$

Where v is the train velocity in km/h and Be is the Braking force in N.

Nevertheless, throughout the world, the calculation formula for running resistance differs significantly. This is due to the difference in parameters used in the Davis equation (Sapronova *et al.*, 2017). Table 2.4 is the summary final form of the Davis equation based on country,

Table 2.4: Summary final form of Davis equation based on country.

Country	**Equation**
Chinese National Railway (N/kN)	$0.92 + 0.0048.V + 0.000125.V^2$
Czech Railway (daN/ton)	$1.3 + 0.00015 \cdot V^2$
German Railway (daN/ton)	$1.0 + 0.0001 \cdot V^2$
Serbian Railway (daN/ton)	$0.0483 + 0.0183.V + 0.00001 \cdot V^2$
French National Railway (daN/ton)	$1.0 + V^2 / 400$
Australian Railway (N/ton)	$5.17 + 0.010997.V + 0.00051.V^2$

Despite the different forms of the Davis equation from all over the world, not all forms of the Davis equation can be used in estimating the operation power consumption saving due to the differences in the equation parameters. According to research at the University of Genoa, Italy, an Amstrong-swift approach is used in the Davis equation to compare the resulting variability. The result shows a slight difference in the value and slope of the result (Boschetti & Mariscotti, 2012). For this study, a set of parameters for the Davis equation is chosen based on the Association of American Railroads for passenger trains. This is due to the parameters being well known for train performance analysis studies, and many references can easily be acquired in literature form.

The comprehensive form of Davis equation representation formed the total train resistance, taking into account three main components of total resistance encountered by a train: train running resistance, line resistance, and acceleration resistance (Ihme, 2022). It compromises by considering these factors, providing a holistic perspective on the forces opposing the motion of the train.

Running resistance in the Davis equation addresses the resistance faced by the train as it moves at a constant speed. It distinguishes between the running resistance of the individual vehicles within the train and the resistance imposed by the track. Factors such as aerodynamic resistance and rolling and track resistance contribute to the overall running resistance.

Line resistance in the context of the comprehensive Davis equation encompasses the resistance encountered by the train due to the characteristics of the track. This includes the effects of gradient resistance, which is the resistance caused by changes in the elevation of the track, and curvature resistance, which arises when the train traverses curved sections of the track.

Acceleration resistance refers to the force opposing the acceleration or deceleration of the train. It is a crucial aspect of the comprehensive Davis equation, recognising that changes in speed also contribute to the overall resistance experienced by the train.

Therefore by incorporating these three types of resistance into a single equation, the Davis equation offers a more comprehensive and nuanced understanding of the complex forces influencing the movement of trains. It provides a practical and

mathematical framework for engineers and researchers to analyse and optimise the performance of trains, taking into consideration various factors that affect their resistance and overall efficiency.

2.3.4 Reduction of resistance

According to Davis equation, there are several ways to reduce Resistance, *R* value. Based on the literature review in section 2.2.2, operation power consumption is reduced by lowering the resistance.

The first way to reduce resistance is by reducing the *B* value of the Davis equation, the coefficient used to define train resistance dependent to train speed, such as wave action and oscillation effect, by applying suitable track alignment and flange design. The second way is by reducing the *C* value of the Davis equation, streamlining, and aerodynamic coefficient used to define train resistance dependent on the square of the train speed (air resistance) by applying an excellent aerodynamic design of the train. Third, by reducing the *A* value of the Davis equation, the resistance component independent of training speed, such as track friction, by adjusting track characteristics, such as track coefficient of friction.

However, reducing resistance in *B* and *C* values required alteration to the existing design (International Union of Railways, 2005), therefore, requires a large investment by the company. Moreover, altering existing designs in *B* and *C* values involves product standards and requirement studies. Therefore, reducing the *A* value in the Davis equation seems beneficial in this research since it only alters the existing operation and maintenance procedure.

Two important aspects highlighted in section 2.2.2 in terms of reducing running resistance for power efficient operation are train mass and reduction of track friction coefficient in the *A* values related to rolling friction. In addition, the change in Power consumption, *P*, is due to changes in these two aspects; train mass, *m* in kg, and friction Coefficient, which can be represented by the *A* value in the following formula,

$$P = (\sum F + \boldsymbol{mg\mu} + Bv + Cv^2 + B_e)v \quad (2.6)$$

Therefore, these two aspects is the focus of the research.

2.3.4.1 Train mass

According to section 2.2.2.5, several ways to reduce train mass are developing new optimized rail vehicle structure and material, optimizing component design, and using optimized passenger movement management. The effect of train mass on power consumption in the Davis equation can be observed in equation 2.6.

Despite using advanced weight reduction in train components and materials, optimizing train passengers movement can also assist in reducing train mass during operation. Optimizing train passengers movement is by regulating passenger movement at the platform.

Therefore, research by Sonia, 2012, on how to manage passenger movement during passenger disembarking and boarding movement in such a way as to optimize train loading and fewer collisions between passengers, three different passengers boarding scenarios are suggested; Boarding space division (BASD) - the entrance to and exit out of wagons are isolated through a separator that helps to separate the in-flow and out-flow of passengers, boarding dedicated doors (BADD) - the in-flow and out-flow of passengers are directed through different doors of the wagon as some doors are used for boarding and the others for exit, Boarding time division (BATD) -In-flow and out-flow of passengers are scheduled in different times. According to the simulation results, all scenario successfully regulates passenger movement during train boarding, resulting in reduced passenger collision and train loading. Still, the result shows outperforming of the BASD scenario compared to others where passengers boarding the train are separated using a barrier at each door (Sonia, 2012).

In conclusion, using the idea of BASD, the movement of passenger boarding can be reduced by delaying the build-up of passengers inside the train, hence delaying the train from achieving maximum capacity. The effect of the application of BASD can be simulated in the Figure 2.18,

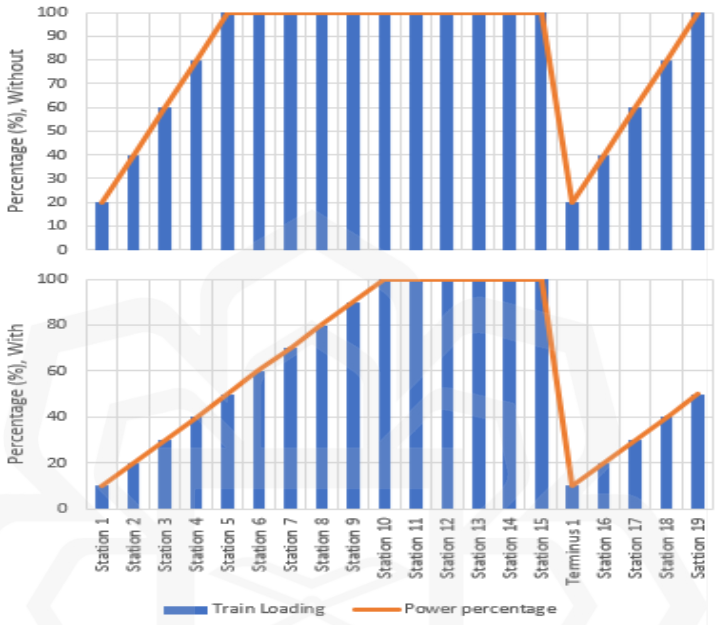

Figure 2.18: Graph of train loading and power consumption percentage without and with the application of BASD.

Based on the graph, instead of the train achieving maximum capacity at the fifth station, due to the application of BASD, the train successfully attained the maximum capacity at the tenth station. The idea of using BASD to regulate the in-flow of passengers during train boarding on peak hours can be introduced by rail operators to manage passenger movement and crowd control. Regulation in-flow of passengers boarding trains not just can reduces train loading and inter-passenger collisions throughout their journey, but it also may increase passengers boarding ability rate at busy front stations, hence increasing passenger satisfaction.

2.3.4.2 Track friction coefficient

The track friction coefficient is an essential value in the Davis equation. Changes in the track friction coefficient will change the overall resistance value. The effect of the track friction coefficient on power consumption in the Davis equation can be observed in equation 2.6. Typical operation conditions of rail track coefficient of friction can be as low as μ 0.05 in ice and snow conditions and as high as μ 0.7 (Vukan, 2007). In typical operation, the track coefficient of friction will range between μ 0.1 to 0.6 for a dry track (Areiza *et al.*, 2014; Wu and Wilson, 2006). However, according to research by the Institute of Rail Transiters in China, it is recommended to maintain the rail track coefficient of friction between 0.2 and 0.3 to ensure good train running performance (Li & Li, 2023).

Two common ways to reduce track surface friction coefficient are rail grinding and rail lubrication. The surface of two objects experiences friction when the surfaces resist one another due to the sticking mechanism at the microscopic scale. Therefore, grinding the surface smoother and applying lubrication reduces the amount of sticking mechanism and reduces the surface friction coefficient. Two everyday rail maintenance activities are practised in the rail industry: rail grinding and rail lubrication.

Rail grinding is a process to improve track profile and ease track corrugation. Moreover, rail lubrication applies grease to the rail vehicle wheel flange and track to minimize contact stress between the rail wheel and the track. The primary function of both processes is to reduce friction and ease wheel and track contact, therefore prolonging rail track life (Ishida *et al.*, 2006; Innotrack, 2006). These two activities ordinarily aim to improve wheel and track contact for safe train operation and reduce the track and wheel wear and tear process. In some rail operators, rail lubrication is used together with rail grinding to extend rail life even more. Rail lubrication can reduce track profile wear and fatigue but not track internal defects and corrugation like rail grinding. The application of rail lubrication together with rail grinding can extend rail life up to 4 years (Zarembski, 2019). Indirectly, these two activities successfully reduced the track friction coefficient, reducing resistance and reducing the operation power consumption, according to the power consumption formula in terms of the Davis

equation. Apart from the positive effect of these two activities, the positive impact of both actions on operation power consumption is seldom neglected by rail operators. Therefore, addressing this study to utilize the existing resources entirely is essential.

Rail grinding and rail lubrication are two distinct maintenance techniques used in the railway industry to enhance the performance, safety, and longevity of rail tracks. The purpose of rail grinding is a corrective and preventive maintenance method used to address issues related to rail profile irregularities, such as corrugations, surface defects, and worn areas. It is performed to restore the rail smooth profile, preventive of further track corrugation, and ensure a safe track surface for trains. The process includes grinding machines equipped with abrasive grinding wheels that are used to remove imperfections on the rail surface. This process results in a smoother rail profile, reducing the impact on rolling stock and improving ride quality. The benefit of rail grinding is it can restore the track's original profile, reduce wear on wheels and track, mitigate noise and vibration caused by irregularities in the rail surface and enhance safety by minimizing the risk of derailments.

Furthermore, the purpose of rail lubrication is primarily to reduce friction and wear between the wheel flange and the rail. It is a preventive measure to mitigate wear and tear on the rail, wheels, and other related components. The process includes lubricants applied to the rail surface. These lubricants form a protective layer that minimizes the friction between the wheel and rail, thereby reducing wear and extending the lifespan of the rail track. The benefit of rail lubrication is that it reduces wear on the rail and wheel flange, reduces noise generated by the train wheels, and enhances fuel efficiency due to decreased friction (Zarembski, 2019; Reddy, 2004).

In comparison, rail lubrication is preventive, aiming to reduce friction and wear in advance. In contrast, rail grinding in Figure 2.19 is corrective, addressing existing irregularities to maintain safety and performance and also preventive to mitigate track corrugation. Rail lubrication is performed as part of routine maintenance, whereas grinding is typically conducted in response to specific rail conditions in certain areas. Rail lubrication may be applied more frequently, depending on factors like weather conditions and traffic volume. Rail grinding is generally done less frequently but is more intensive when performed. Rail lubrication primarily influences the friction between wheel and rail, while grinding impacts the rail profile and the track friction. In

summary, rail lubrication and rail grinding serve different purposes in rail maintenance. Lubrication is a preventive measure to reduce friction and wear while grinding is a corrective action to address existing rail surface irregularities and a preventive measure to mitigate track corrugation.

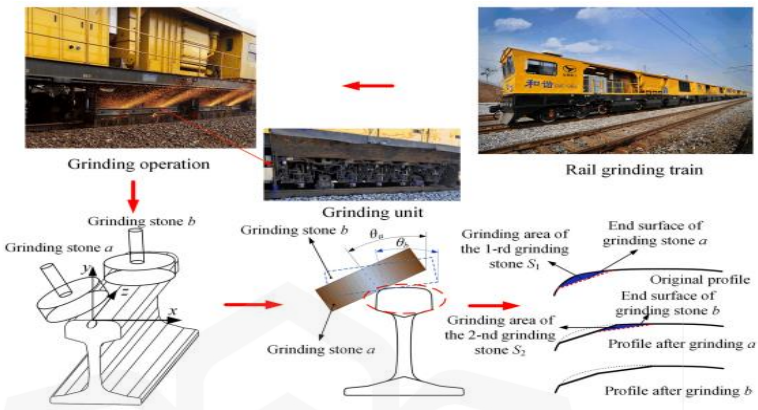

Figure 2.19: Rail grinding techniques illustration (Xie *et al.*, 2020).

However, the application of rail lubrication requires significant investment by rail operators to acquire the lubrication system technology. Figure 2.20 is the example of rail lubrication system using lubrication hole on rail track. In addition, rail lubrication requires extensive study of rail contact limitation and lubricant specification since excessive lubrication of rail tracks can result in wheel slip problems (Charcon *et al.*, 2023). Therefore, this process is neglected in this study. Apart from that, rail grinding is a conventional process in rail maintenance considered in this study; do not require a significant investment to acquire new technology because rail grinding is already being applied in daily rail track preventive maintenance of rail operators.

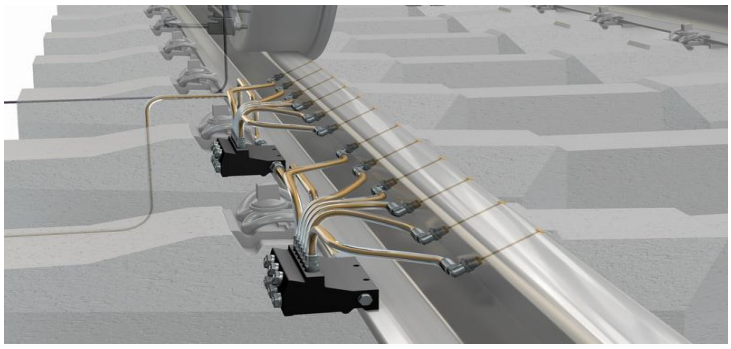

Figure 2.20: Rail lubrication system using lubrication holes (SKF, n.d.).

2.4 REVIEW ON RAIL GRINDING

Rail track surface wear and deterioration may result in rail track profile deformation, corrugation, and shorter rail track life. Rail grinding is a rail maintenance strategy to reduce corrugation and improve track profile for better rolling stock truck steering, dynamic stability, and wheel life.

Rail grinding is a process performed by a Rail Grinding unit, a rail-borne machine (Innotrack, 2006). This machine removes metal from the rail track using a rotating grinding stone to produce the desired rail track surface and profile. The volume of metal that is being removed is dependent on the number and arrangement of stones, the characteristics of abrasive stone, the rate of grinding stone pressure, the forward speed of the machine, and the hardness of the grinding surface (Sroba, 2013; Innotrack, 2006).

There are four types of rail grinding strategies for different rail track defects. The first type is corrective grinding, which is used to eliminate track defects and deformation at the grinding amount of about 0.5 to 6 mm of metal. It requires removing large amounts of metal on the rail tracks. Therefore, it is considered an uneconomical method, but this strategy is suitable at the expense of having a long track life in a short time. The second type is transitional grinding, grinding strategies to reduce track defect and, at the same time, decrease the development of track wear and crack growth rate. It reduces less metal (0.3 to 1.0 mm) than corrective grinding; therefore, it requires several grinding cycles to achieve the same effect as corrective grinding. The third type is preventive grinding, strategies to eliminate track and corrugation, control defect formation by decreasing track wear and crack growth rate, and maintain the track profile and surface appearance. It requires less metal (0.2 to 0.3 mm) than other grinding types; therefore, preventive grinding is economical for a longer track lifespan. The fourth is the particular grinding, a grinding type for a specific location to achieve a particular track profile, shape, and contact surface (Binoj *et al.*, 2022; Innotrack, 2006).

First objective of rail grinding is to restore the optimal rail profile. Surface wear on the wheel and rail contact geometry creates excessive wheel and rail contact stress, which causes rail surface plastic flow and surface fatigue, such as spalling, shelling, and

head checks. This contact geometry increases the internal stresses and may result in transverse defects of the rail track. By improving the track profile with rail grinding, the contact geometry between the wheel and the rail is improved, and this produces relief between the wheel and the rail, reducing contact stresses. In addition, an optimal rail profile will improve vehicle stability in tangent tracks and improve wheelset curving (Xie *et al.*, 2020; Sroba, 2013).

Second objective of preventive rail grinding is to control rail corrugations; rail corrugations initiate from rail head de-carbonization and irregularities such as rail manufacture defects, contact fatigue defects, rail welds, and joints. By grinding a corrugated rail surface, the wheel and track contact stress is reduced. The best practice for rail grinding to ease corrugation is to remove just enough metal to prevent the initiation of rail track surface corrugation and to maintain the optimal profile of the rail track (Binoj *et al.*, 2022).

Despite the two objectives of rail grinding, which are to restore the optimal rail profile and to control rail defects and corrugation, indirectly, the track coefficient of friction is also reduced during the rail grinding process. The typical value for the track coefficient of friction is around 0.1 to 0.6 on a wet and dry rail (Wu & Wilson, 2006). The value may increase due to the rail head corrugation process and decrease due to frost formation during winter. Therefore, maintaining the typical value of the track coefficient of friction is essential to prevent the wheel sliding effect and to optimize train running resistance (Edwards, 2010).

Meanwhile, the advantage of the rail grinding strategy is that it may increase the rail track lifespan, decrease track defect growth rate, reduce rolling noise and vibration, improve wheel and track contact, increase track operation safety and save track replacement cost.

2.4.1 Factor safe rail grinding

Rail track comes with several specification and profile. Each profile comes with its maximum allowable wear and tear value for safe rail operation. Moreover, in term of track coeffiction of friction, μ, there are several value that we must take consider to prevent the effect of wheel slipping and sliding that may affect the safety of the rail operation (Chen *et al*., 2020). Therefore, controlling rail grinding process for operation safety in term of minimum allowable track friction coefficient to prevent train wheel slipping and sliding is a must in this study.

2.4.1.1 Wheel slipping

Monitoring the contact between train wheels and running rail is important to minimize rail contact faulty such as wear and damage. According to the research, maintaining lower resistance between train wheels and rail track make the overall rail operation more efficient in term of operation power consumption. However, the track coefficient of friction, μ should not lower than its minimum value. Lower track coefficient of friction than its minimum value may cause wheel slipping problem.

Wheel slip is due to poor traction control of the train, and it is due to the tractive force exceeds the train adhesive weight (Kumar, 2013). Therefore, adhesive weight play an important role in determining rail grinding minimum coefficient of friction. Adhesive weight, N is defined as the force that can be exerted by a train wheel without slipping and sliding,

$$\text{Adhesive weight, } W_a = \text{Coefficient of friction x Train weight, } W \qquad (2.7)$$

When tractive force is more than adhesive weight, the different in power to weight ratio (power exceeding weight) may result to wheel slipping condition. In addition, when barking force prevent wheel from rotate but with continuation of wheel linear motion due to lower adhesive weight, wheel sliding may occur (Vukan, 2007) (Kumar, 2013). This rubbing effect of wheel in one location may cause the development of wheel flat that may cause hazard to the train operation.

2.5 CHAPTER SUMMARY

Electrical energy is the primary source of train propulsion and traction systems. Reducing rail operation power consumption is essential due to the increase of rail operation daily expenditure due to the expanding rail network size and the electricity tariff increase. Several strategies to reduce rail operation power consumption can be divided into two bases: technology base and operation base. Technology bases such as ECS and hybrid systems require significant investments from rail operators to acquire new applications. Therefore, operation bases such as timetable optimization and track condition management are excellent choices for rail operators because they utilize the existing resources. The fundamental train motion is a compromise of traction effort and resistance force. The resistance value in train motion is based on the Davis equation, the equation of three resistance components of train motion. There are three regimes of station-to-station travel in rail operation: acceleration, constant speed, and braking region. The different trends of the net force equation constitute each region. Reduction of train resistance can be achieved by reducing train mass, also known as train loading, and track coefficient of friction in the *A* value of the Davis equation. Reduction of train loading can be achieved by applying optimized platform management, and reduction of the track coefficient of friction can be acquired using the rail grinding method. Rail grinding is a daily rail preventive maintenance that aims to reduce track corrugation and improve track profile; indirectly, it can also reduce the track coefficient of friction, reducing the train resistance value.

CHAPTER THREE

METHODOLOGY

3.1 INTRODUCTION

This chapter discusses the process throughout the study. The methodology begins with the theoretical analysis of different types of station-to-station travel and operation power consumption and the theoretical analysis of operation power consumption with different train loading and track coefficient of friction. Both theoretical analysis is based on the Davis equation. Next, the study continues with the experimental analysis of train operation power consumption for various train loading and experimental analysis of train operation power consumption for different track coefficients of friction with the application of rail grinding to reduce the track coefficient of friction.

3.2 RAIL OPERATION CONDITION

Rail operation consists of station-to-station movement. According to section 2.3.1, there are 4 different types of station-to-station movement. The most suitable for rail operators to use in their daily operation is based on the type of rolling stock, station distance, and allowable trip time (Vukan, 2007). Table 3.1 is the rail operation condition that is considered in the study,

Table 3.1: Rail operation condition of the study.

Rolling stock	4 Car -Bombardier Innovia Metro 300
	LIM electrical propulsion system
	Low speed operation at 80 km/h
Surrounding	Short inter station distance (1.7 km)
	Short trip time (≈ 3 minutes)

3.3 THEORETICAL ANALYSIS

Two theoretical analysis are done in the study: the theoretical analysis of the station-to-station travel using the Davis equation and the theoretical analysis to investigate the effect of different train loading and track coefficient of friction on rail operation power consumption. Both theoretical analysis is based on the Davis equation (equation 2.4). The following Figure 3.1 is the theoretical analysis flow diagram,

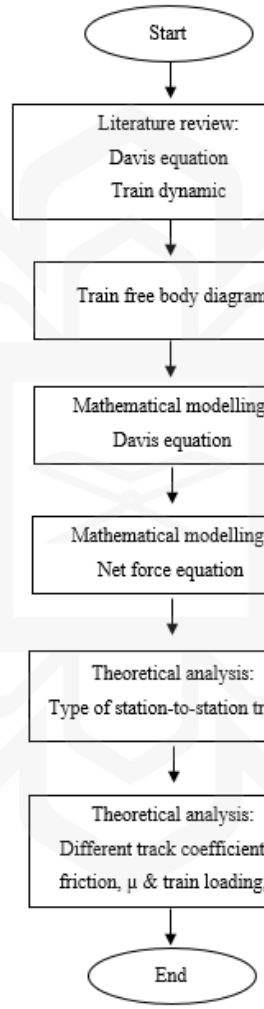

Figure 3.1: Theoretical analysis flow diagram.

Based on the literature review of the Davis equation and train dynamic, a train-free body diagram is established. A mathematical model of the Davis equation and net force equation is established. Theoretical analysis of train station-to-station travel and

operation power consumption of different train loading and track coefficient of friction is done using the mathematical model.

3.3.1 Theoretical analysis of station-to-station travel using Davis equation

According to section 2.3.1, station-to-station travel operation compromise 4 different types of operation; therefore, this methodology aims to understand the difference in these four types of station-to-station travel operation power consumption using the theoretical analysis of the Davis equation. This theoretical analysis is based on section 2.3.1. The following Figure 3.2 shows the four types of station-to-station travel operations,

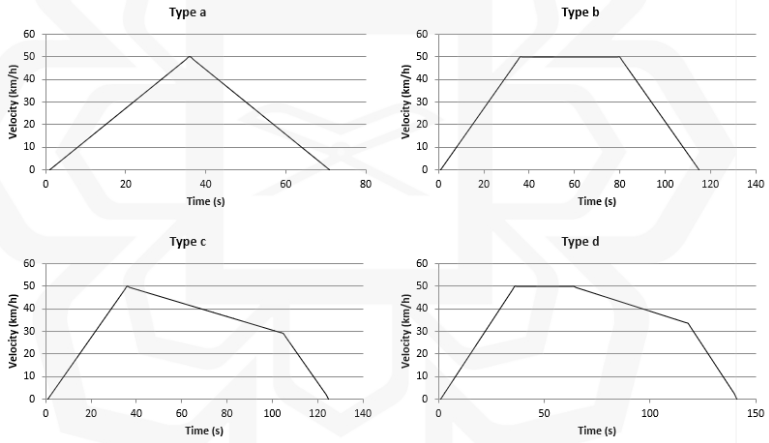

Figure 3.2: Graph of four types of station-to-station movement (Vukan, 2007).

Based on the velocity profile in Figure 3.2, four power consumption graph is constructed using the velocity profile of the four types of station-to-station travel. The power consumption graph is compared and discussed in the next chapter.

Type *A* of station-to-station operation is based on the $s < s_c$, as per section 2.3.1. The station-to-station travel consists of acceleration, deceleration, and station stop only. Type *B, C,* and *D* are based on $s \geq s_c$ station travel. Type *B* consists of acceleration, constant speed, deceleration, and station stop region, and Type *C* consists of

acceleration, coasting, deceleration, and station stop. In addition, type *D* consists of acceleration, constant speed, coasting, and station stop. The four types of station-to-station operation produce four types of velocity profiles.

The four types of velocity profiles are compared, and four power consumption graphs are constructed based on the mathematical model. The data is analysed, and a conclusion is established using the difference in power consumption profile in each type of operation. Based on the four power consumption profiles, one profile will be chosen to represent the actual operation condition in this study. This selected profile is used to compare with a similar power consumption profile produced in other research for validation. Figure 3.3 is based on Vukan, 2007 railway DC power consumption profile,

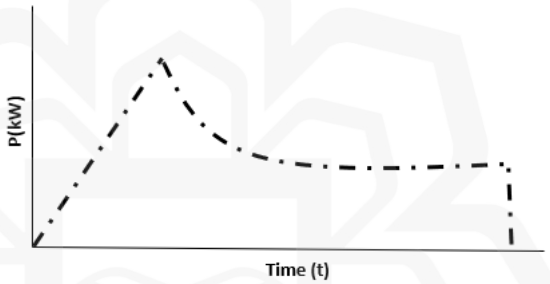

Figure 3.3: Graph of theoretical rail operation power consumption (Vukan, 2007).

3.3.2 Theoretical analysis of train loading and track coefficient of friction

This methodology aims to understand type of station-to-station operation (section 3.3.1) and the effect on operation power consumption with different train loading and track coefficient of friction.

The influence of different train loading and track coefficient of friction can be expressed in terms of power consumption and time. Train loading is the overall train mass, including the percentage of passengers boarding the train, and the track coefficient of friction is the kinetic coefficient of friction of the rail track. The kinetic coefficient of friction is essential in the rail industry because the primary interaction between the wheel and rail track is between steel-to-steel interaction. Therefore, the

static coefficient of friction is almost similar to the kinetic coefficient of friction (Lundberg *et al.*, 2015). The range of kinetic coefficient of friction is taken between 0.2 to 0.8, and this value is the typical rail operation condition based on the literature review. Once the operation power consumption graph is constructed, the data is analysed, and the relationship between the track coefficient of friction, with operation power consumption is established. The finding is validated using the result in the subsequent experimental analysis.

3.4 EXPERIMENTAL ANALYSIS

Several factors such as traction ratio, train loading, track characteristic, propulsion system, and maximum operation speed may affect operation power consumption (Jong & Chang, 2005), but train loading and track coefficient of friction are selected as the variable in this experimental analysis due to the finding in section 2.3.3. The methodology aims to understand the relationship between operation power consumption with train loading and track coefficient of friction, μ.

Two experiments are conducted: Experiment 1 is the experimental analysis of train operation power consumption for various train loading, and Experiment 2 is the experimental analysis of train operation power consumption for different track coefficients of friction with the application of rail grinding to reduce track coefficient of friction.

Train loading in experiment 1 is the total train mass, including the passenger, which varies according to two operation times. The value of the track coefficient of friction in experiment 2 is based on the kinetic coefficient of friction of the rail track. The kinetic coefficient of friction selected instead of the static coefficient of friction in the study is due to the broader range of applications. In addition, the kinetic coefficient of friction is essential in the rail industry because the primary interaction between wheel and rail track is between steel-to-steel interaction. Therefore the static coefficient of friction is almost similar to the kinetic coefficient of friction (Lundberg *et al.*, 2015).

The kinetic coefficient of friction varies with the application of rail grinding to get the lower kinetic coefficient of friction.

3.4.1 Experiment 1- Train loading

The experiment aims to understand the effects of operation power consumption in varying the train loading while maintaining the constant track coefficient of friction, μ.

The test is using a rolling stock unit: 4-Car Bombardier INNOVIA Metro 300 (Width-2.65 m, Length-67.1 m, Mass-20,000 kg per car), 50%=109,400 kg, 100%=138,800 kg operated in 4 ft 8.5 in standard gauge rail track of Kelana Jaya Line that use fourth rail 750 V DC as train electrification with a LIM propulsion system to generate tractive forces. The test is conducted in a low gradient area from Asia Jaya station to Taman Paramount station to represent the study scope best. Figure 3.4 is the experiment flow diagram for variable train loading,

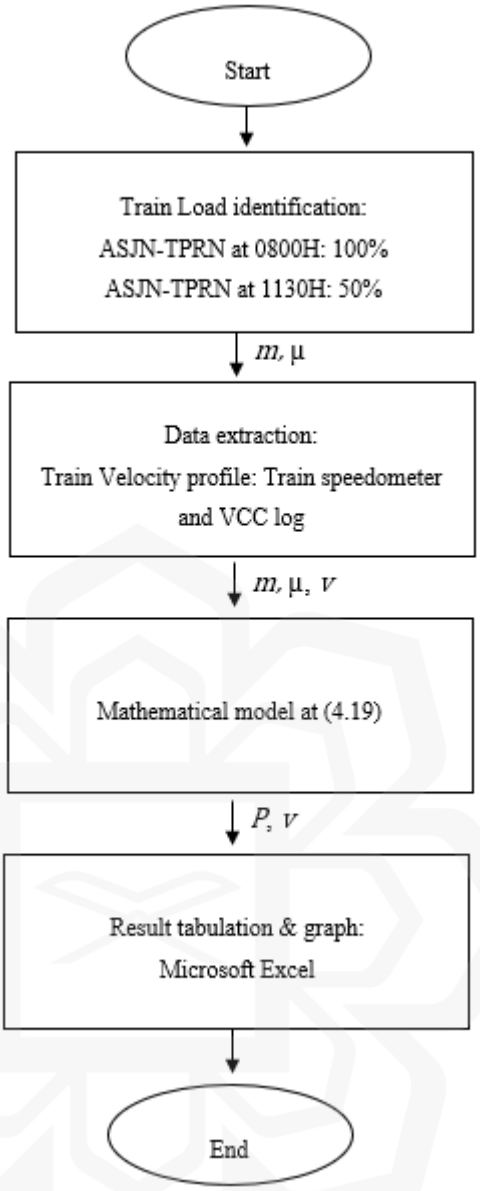

Figure 3.4: Flow diagram of Experiment 1 of experimental analysis of different train loading and the effect to operation power consumption.

Two operational train loading, which is 50% and 100%, is estimated using the percentage numbers of passengers boarding the train and the total weight of the train. Table 3.2 is the summarise of the two trains loading the total train mass,

Table 3.2: Train loading 100% and 50%.

Train loading	Total Passenger	Train Mass (kg)
100%	974	138,440
50%	487	109,400

The track coefficient of friction, μ, is taken and recorded using the weight balance method as in the previous section 3.4.2.1. The train velocity profile is recorded from the train speedometer and the vehicle control centre log as in the previous section 3.4.2.3. Train resistance was calculated using variable train loading. Train loading at the test location varies by taking the reading using two different operation times (0800H and 1130H), in which the two operation time represent various passenger load factors.

The power consumption graph is constructed using the train tractive force, resistance, and velocity profile data. The data is analysed and compared with the theoretical results. The result is discussed and validated with the previous references journal and article.

3.4.2 Experiment 2- Coefficient of friction

The experiment aims to explain the relationship between the kinetic coefficient of friction, μ of rail track, and operation power consumption with constant train loading.

The test uses a rolling stock unit of 4-Car Bombardier INNOVIA Metro 200 (Width-2.65 m, Length-67.1 m, Mass-20,000 kg per car), 50%=109,400 kg, 100%=138,800 kg operated in 4 ft 8.5 in standard gauge rail track of Kelana Jaya Line. The train electrification system uses a fourth rail 750V DC as train electrification with a LIM propulsion system to generate tractive forces. In addition, the rail grinding process is applied at the specific rail track using LORAM Rail Grinding Units. The test occurs from Asia Jaya station to Taman Paramount station in a low gradient area. The track coefficient of friction varies using the rail grinding method to obtain a lower track coefficient of friction. The test begins with the identification of operation power consumption on normal operation conditions before the application of the rail grinding process. Figure 3.5 is the experiment flow diagram for testing before the application of rail grinding,

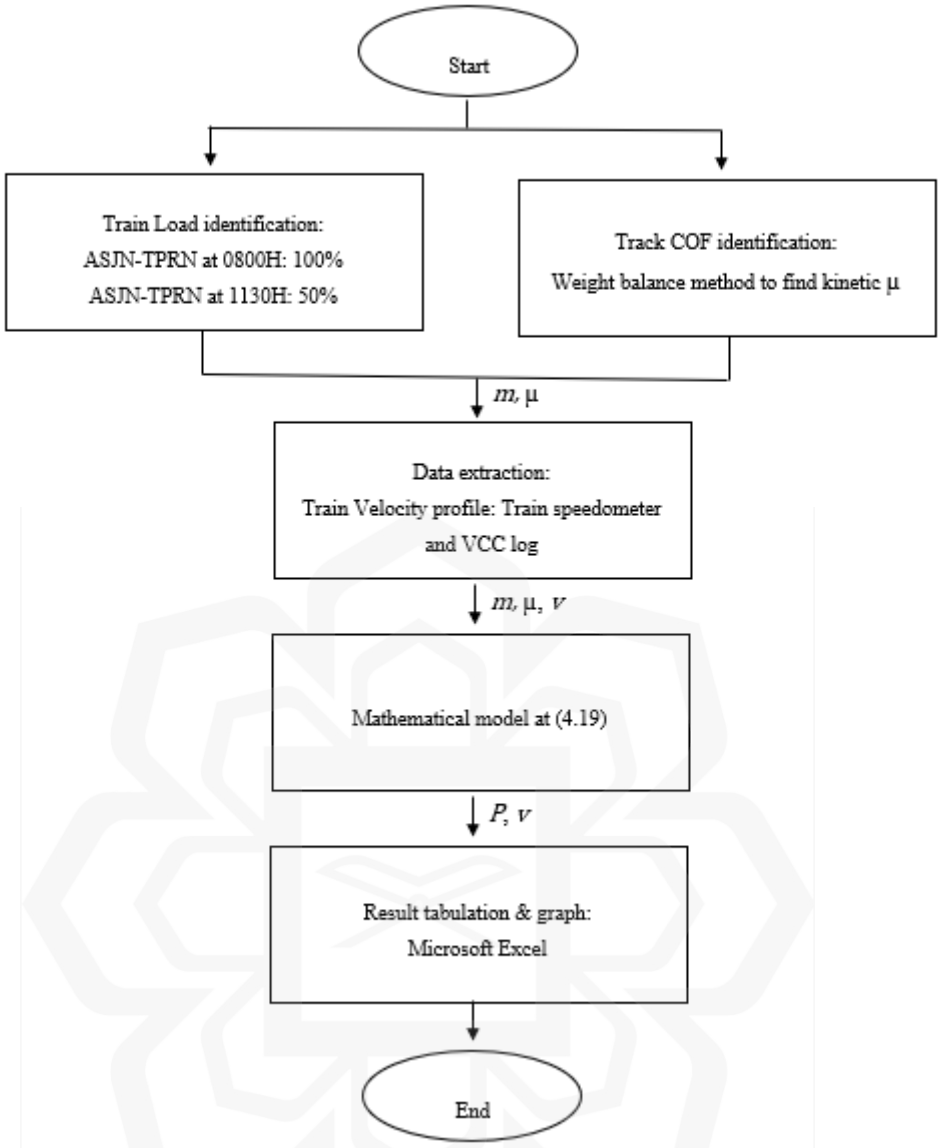

Figure 3.5: Flow diagram of Experiment 2 on experimental analysis of different track coefficient of friction before application of rail grinding.

Rail grinding is an essential rail preventive maintenance to improve track surface; indirectly coefficient of friction is expected to improve, which may reduce rail operation power consumption (Wang & Rakha, 2017). Therefore, the rail grinding is suitable method to reduce track friction coefficient in the study. The testing was carried out with the application of rail grinding to reduce the track coefficient of friction at the test area. The application of rail grinding uses the LORAM rail grinding unit. Figure 3.6 is the experimental testing flow diagram after the application of rail grinding,

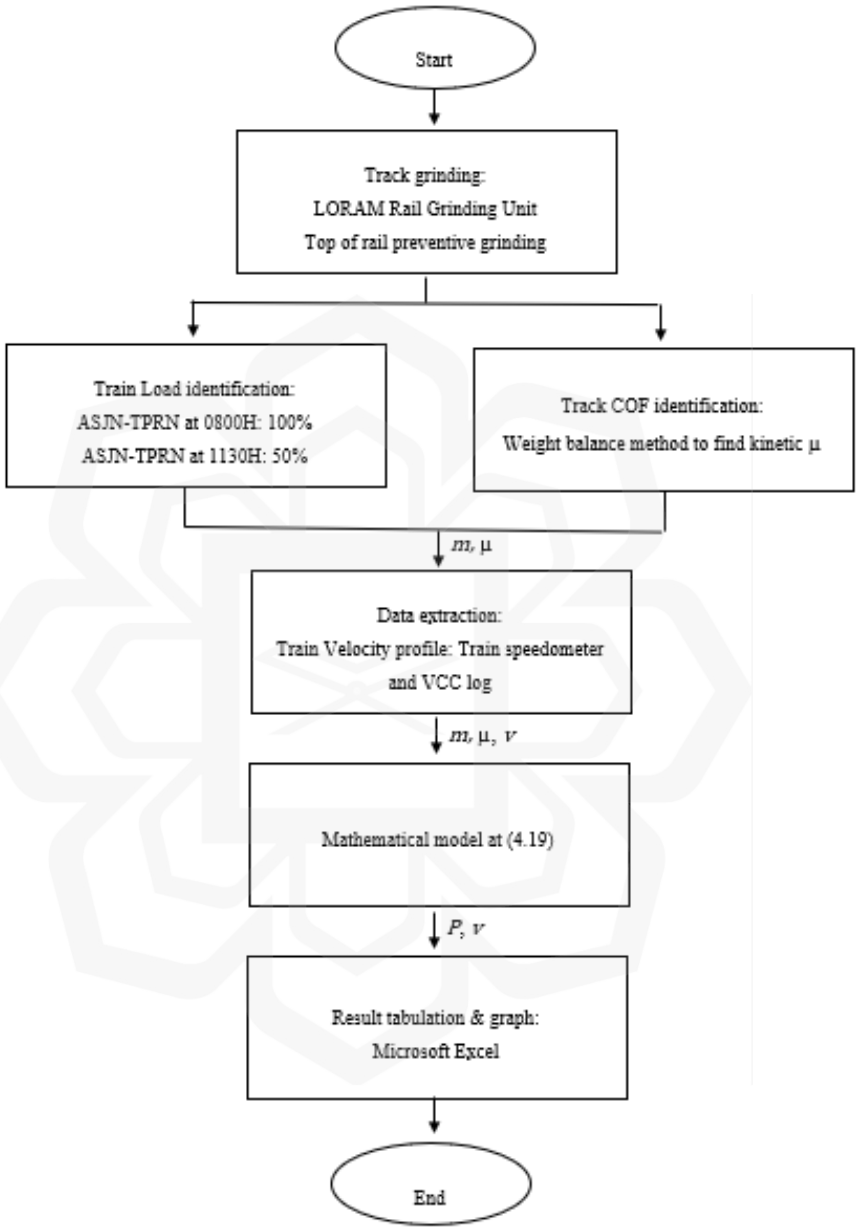

Figure 3.6: Flow diagram of Experiment 2 on experimental analysis of different track coefficient of friction with application of rail grinding.

Two sets of variable track coefficient readings of friction, μ, and train velocity profile, *v* are taken before and after rail grinding is applied. The track coefficient of friction, μ, is taken and recorded using the weight balance method. The train velocity profile is recorded from the train speedometer and the VCC log. The track coefficient of friction is the kinetic coefficient of friction of the rail track, as discussed in section 3.3.2.

The train resistance is analysed using variable train loading and the track coefficient of friction, μ. The variable for the analysis is the track kinetic coefficient of friction before rail grinding and the track kinetic coefficient of friction after the application of rail grinding. Therefore, the testing can be divided into two: before rail grinding (average track coefficient of friction) and after rail grinding (lower track coefficient of friction). The power consumption graph is constructed using the train tractive force, resistance, and velocity profile data. The data is analysed and compared with the theoretical results. The result is discussed and validated with the previous references journal and article.

3.4.3 Equipment and material

Experiments 1 and 2 are carried out at Kelana Jaya Line LRT; therefore, all the equipment and material are based on the LRT line. Some value that needs to be better defined in the experiment is based on the reference journal and article.

3.4.3.1 Type of rolling stock

Rolling stock is also referred to as train or rail vehicles. The Bombardier Innovia Metro 300, manufactured by Bombardier Transportation, is one of the Kelana Jaya Line fleets. The train is operated in the GoA4 level of automation. This driverless metro unit runs on conventional running rail. It uses a third rail system to provide electrical energy (750 VDC) to its linear induction motor, providing traction power to the train propulsion system. It is equipped with MITRAC propulsion technology with a design speed of 90

km/h and an operational speed of 80 km/h. It can operate in a maximum curve radius of 70 m with a maximum track gradient of 62.5%. Figure 3.7 is the train photo at RapidKL Subang depot,

Figure 3.7: Bombardier Innovia Metro 300 train set.

The train is fitted with a 155 kW LIM propulsion system in each bogie resulting in continuous power of 1000 kW with a maximum acceleration rate of 1.25 m/s^2, braking rate of 1.0 m/s^2, and emergency braking rate of 2.4 m/s^2. The overall length of the train is 68.1 m, and the width of 2.65 m with a bogie wheelbase of 1.9 m. The empty weight of each car is 20,000 kg. Figure 3.8 is the diagram of the LIM propulsion system underneath the train,

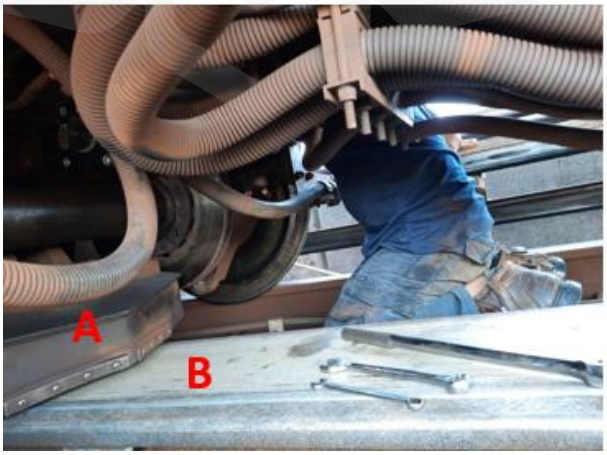

Figure 3.8: LIM propulsion system and LIM rail.

A in Figure 3.8 is the LIM, and B is the LIM rail. According to section 2.3.2, the magnetic induction interaction between the LIM as the stator and LIM rail as the rotor produces tractive force for the train to move forward.

3.4.3.2 Type of rail track

The study uses a standard gauge rail track with a BS113A / 56E1 rail profile and inclination of 1:20 corresponding to the rail head. Standard-gauge rail is a railway running rail that has a track gauge dimension of 1435 mm. It is the most used rail track gauge dimension globally, known as the Stephenson gauge. Figure 3.9 is the running rail gauge illustration.

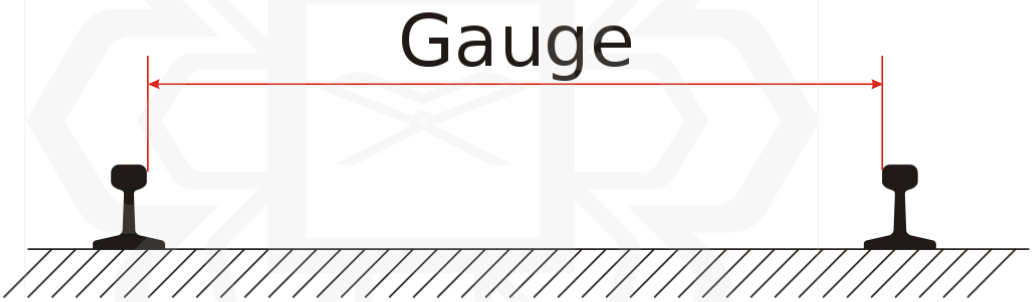

Figure 3.9: Track gauge illustration.

3.4.3.3 Experiment area

The low gradient track of Asia Jaya station to Taman Paramount station (Track section 0154 to 0225) covers about a 1.7 km tangent track (straight track). The train operated in GoA4 level of fully automated mode. The area is selected because the operation condition matches the research scope per section 1.4. Figure 3.10 is the test area illustration,

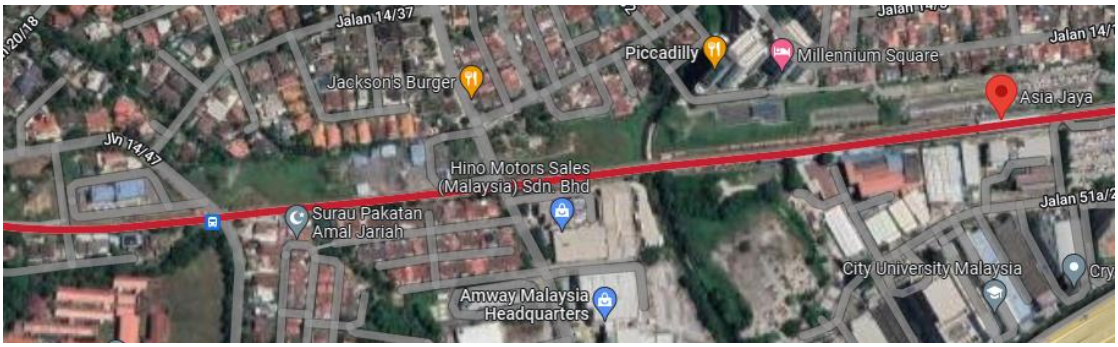

Figure 3.10: Map of test area.

The train operation is operated on a low gradient and tangent track. Therefore, the effect of gradient and track alignment on the study is minimal. The test area also compromises with maximum train loading during a particular hour (08.00 am-09.30 am) and experiences a reduction in train loading. Therefore, the train loading reading can vary throughout the study. In addition, the station-to-station distance also aligns with the study; the train station-to-station operation is included acceleration, constant speed, deceleration, and station stop operation. Therefore the test area simulates the type B of station-to-station operation studied in the theoretical analysis.

3.4.3.4 Rail grinding

The application of rail grinding reduces the track coefficient of friction for the experiment to get different variables of the track coefficient of friction. During the experiment, the rail track undergoes top-of-rail preventive grinding using a rail grinding unit (RGU). The track undergoes corrugation removal, track re-profiling process, and track polishing. Each track section undergoes 12 passes of grinding based on the grinding requirement. The track section is the track label that indicates the track's location, and each track section compromises a distance of 25 m. Table 3.3 summarizes rail grinding activity during the testing.

Table 3.3: Summary of rail grinding activity.

Day	Track section	Distance (m)	Total passes	Type
1	0225-0213	300	12	Tangent
2	0210-0198	300	12	Tangent
3	0195-0183	300	12	Tangent
4	0179-0167	300	12	Tangent

In addition, the following Figure 3.11 is the track condition after grinding process.

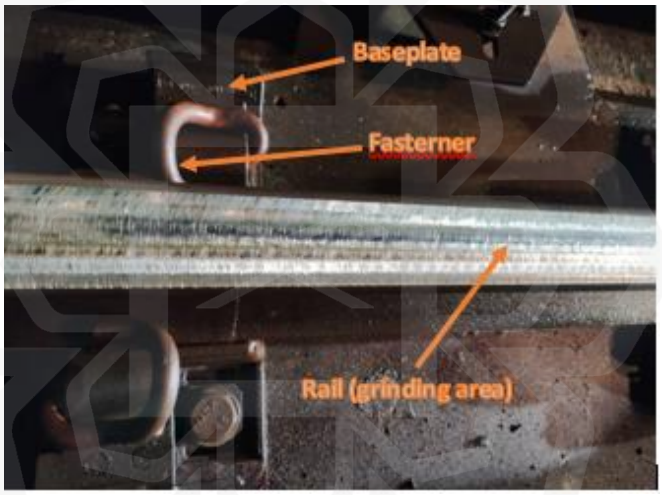

Figure 3.11: Rail track condition after rail grinding process.

LORAM Rail Grinding Units is one of Kelana Jaya line rail grinding units. The propulsion system is using Diesel engine propulsion system. Each operation of the rail grinding unit required three operators to operate the grinding machine. Figure 3.12 is a picture of a rail grinding unit,

Figure 3.12: LORAM Rail Grinding Unit.

3.4.4 Data measurement

Several data measurements are conducted to get the train operation velocity profile, train loading, and track coefficient of friction. This measurement aims to gather all the variables to be inserted into the mathematical model to calculate the power consumption.

3.4.4.1 Measurement of track coefficient of friction.

One conventional way to measure the coefficient of friction is using the weight balance method (Hu and Peachey, 2016; James, 1994). Applying the maximum force needed to move 1 kg of load at the measuring surface. The setup of the experiment is as the following Figure 3.13,

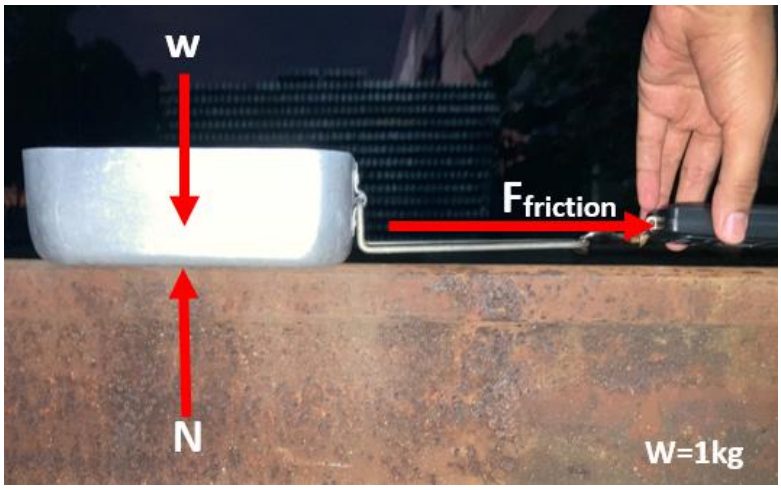

Figure 3.13: Free body diagram of spring balance method

According to Hu and Peachey, 2016, a steady force is applied on the load and the reading of track kinetic coefficient of friction, μ is recorded based on the following formula,

$$F_{friction} = \mu * F_{normal} \quad (3.1a)$$

$$\mu = F_{friction} / F_{normal} \quad (3.1b)$$

The friction shall be measured at the top of the rails as the following Figure 3.14, measured in the centre of the running surface region (nominally zero degrees) for both inner and outer track,

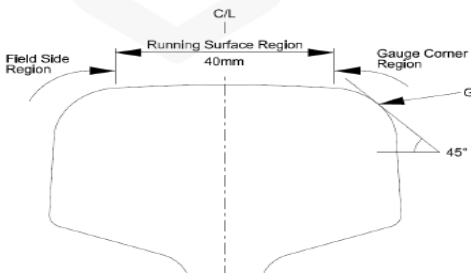

Figure 3.14: Top of rail area

To account for variability in measurements, at least 3 measurements is being made every 100 metres through the area of interest and the average friction level for the top of each rail should be calculated and recorded.

3.4.4.2 Measurement of train loading

The train loading is measured using the data of passenger load factor at instantaneous operation time at a specific location. For example, at 0800H morning rush hour, the passenger load factor onboard a train at Asia Jaya station is 100% capacity, and at 1130H passenger load factor is decreased to 50% capacity. The percentage of passengers boarding the train is illustrated in 25%, 50%, 75%, and 100% train capacity values. The 100% train loading rate represents the maximum 974 passengers capacity boarding the train. Table 3.4 is the table of train loading with the total train mass,

Table 3.4: Table of train loading, total passenger and train mass.

Train loading	Total Passenger	Train Mass (kg)
0%	0	80,000
25%	126	87,560
50%	487	109,400
75%	760	125,600
100%	974	138,440

3.4.4.3 Measurement of velocity profile

Using the train speedometer and vehicle control centre log, train velocity profiles are recorded. At least three measurements are being made to account for measurement variability, and the average reading is taken. The data is viewed in the form of a velocity graph. Figure 3.15 is the train speedometer, and Figure 3.16 is the VCC log view,

Figure 3.15: Speedometer view from Bombardier Innovia Metro 300 hostling panel.

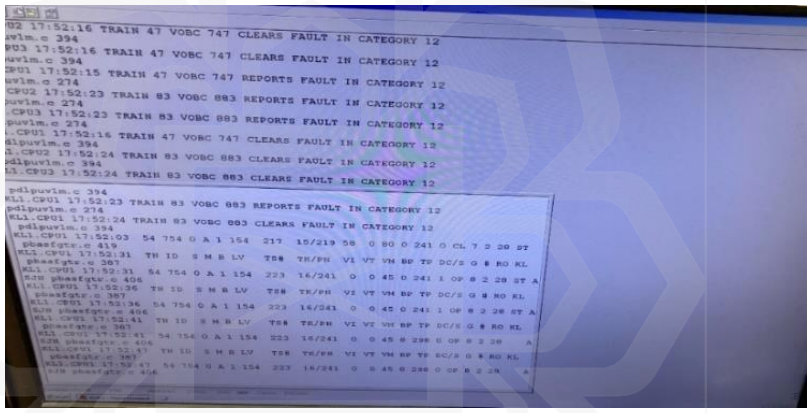

Figure 3.16: Vehicle control centre (VCC) log from the Kelana Jaya Line operation control centre.

3.4.4.4 Measurement of power consumption

The power consumption profile was measured by substituting the train velocity profile to tractive force and resistance into the mathematical model, with the variable of friction coefficient, μ, and train loading, *m*. Thus, an operation power consumption graph is produced. The reduction in operating power consumption is analysed based on the percentage difference in operation power consumption with the different variables of the friction coefficients, μ, and train loading, *m*.

3.5 CHAPTER SUMMARY

In summary, several operation conditions were set in the study to ease the research data collection, such as the rail system operating at a low speed using an ATS moving block signaling system. The study can be divided into two sections, which are the theoretical analysis and the experimental analysis. The theoretical analysis comprises station-to-station travel analysis using the Davis equation and theoretical analysis of operation power consumption using the Davis equation using train loading and track coefficient of friction as the variable. The experimental analysis comprises two tests: experiment 1 of operation power consumption in different train loading and experiment 2 of operation power consumption with the application of rail grinding to lower the track coefficient of friction. The result of the theoretical and experimental analysis is compared with the findings in the literature review and discussed.

CHAPTER FOUR

MATHEMATICAL MODEL

4.1 INTRODUCTION

To study the train motion, a mathematical model was developed based on the Davis equation. Three resistance components that are acting on the train are reflected in the Davis equation. The three resistance components are resistance components that are independent of train speed, such as rolling and track friction, resistance dependent on train speed, and aerodynamic resistance. Through the Davis equation, the net force that is acting on the train can be established.

4.1.1 Mathematical model of net force

A train needs to generate enough tractive force to overcome the resistance force; force that opposing the movement due to gravitational force. As explained in section 3.4.3.1, the train Bombardier Innovia Metro 300 is equipped with LIM propulsion system and tractive force is acting on each LIM at each of bogie. The net force equation can be defined by the following train free body diagram Figure 4.1, where F_a is the aerodynamic resistance, F_{fr} is the friction resistance, a and b is the centre of gravity distance and h is the height.

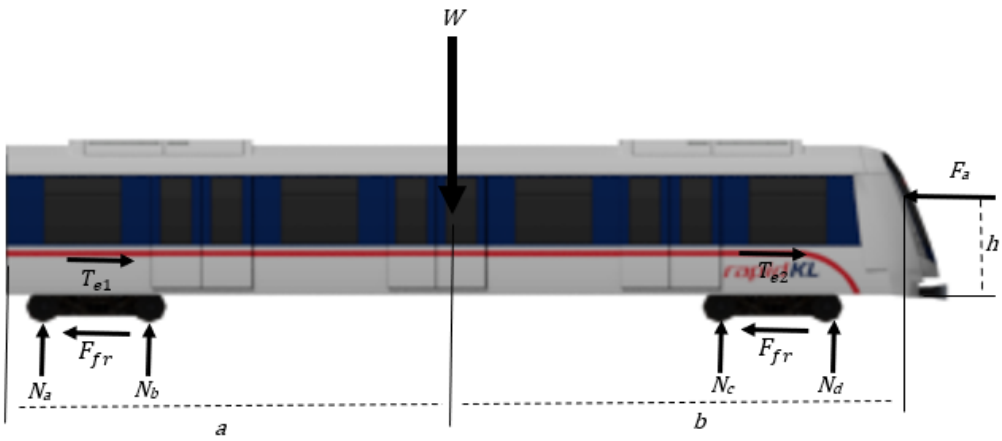

Figure 4.1: Train net force free body diagram.

The net force can be defined as the following equation,

$$\sum F = T_e\,(v) - R(v) - B_e(v) \tag{4.1}$$

Where $\sum F$ is the net force, T_e is the traction force, R is the resistance force and B_e is the braking force in N. The net force is in function of velocity, v in km/h, therefore each of the net force equation is different base on the station-to-station operation. The net force equation for each station-to-station operation can be defined in the following Table 4.1,

Table 4.1: Net force equation for each station-to-station operation.

Operation	Net Force	Velocity	
Acceleration	$T_e\,(v) - R(v) - B_e(v) > 0$	$0 < v < v_{max}$	(4.2)
Constant velocity	$T_e\,(v) - R(v) - B_e(v) = 0$	$v = \text{constant}$	(4.3)
Deceleration	$T_e\,(v) - R(v) - B_e(v) < 0$	$0 < v < v_{max}$	(4.4)
Stop	$T_e\,(v) - R(v) - B_e(v) = 0$	$v = 0$	(4.5)

In the acceleration region, the net force is positive due to the train is in increasing velocity to attain its maximum operation velocity. When the train achieved its maximum velocity, the train operation enter the constant velocity operation. In the constant velocity operation, the net force is equal to 0 due to there are no changes in the value of velocity, v in this operation. In the third operation, deceleration or braking operation, the net force is negative due to the decreasing value of velocity in this region. Lastly, the station stop operation, the net force is 0 due to the train velocity is 0.

The magnitude of velocity, v is according to the instantaneous velocity of the rail system and its varies according to the region of the station-to-station operation. The net force can be define as the following,

$$\sum F = ma \ = m\frac{dv}{dt} \tag{4.6}$$

Where m is the total train mass in kg and a is the acceleration of the train in km/h^2. Therefore, the net force equation can be defined as the following,

$$\sum F = T_e\ (v) - R(v) - B_e(v) = ma \tag{4.7}$$

Where value of velocity, v and acceleration, a change according to the region of the station-to-station operation.

4.1.2 Mathematical model of resistance force

Friction force in a train movement is caused by many factors such as vehicle resistance, aerodynamic resistance, and track alignment resistance (Vukan, 2007). Therefore, according to the governing equation of the study, Davis equation, the net resistance is a composition of all these resistance factors.

According to Davis equation in section 2.3.3, Davis equation can be express as the following in term of train resistance, *R*,

$$R = A + Bv + Cv^2 \tag{4.8}$$

Where value A is the resistance component independent to train speed, such as rolling and friction resistance, contacts between the wheel and track surface. The value B is the coefficient used to define train resistance dependent to train speed such as track alignment resistance, wave action and oscillation effect. Meanwhile, value C is the

streamlining and aerodynamic coefficient used to define train resistance dependent to square of train speed such as air resistance. Nevertheless, value A is the resistance force that being study in this research.

According to Vukan (2017), Davis equation can be generalised into the following equation,

$$R = (c_1^r + \frac{c_3^r}{p} + 10i + c_2^r v)G + c_a^r a v^2 \quad (4.9)$$

Where the value of c_1^r is the coefficient of resistance on track surface or also can be represent as the track coefficient of friction, μ and G is the train weight or can be represent as mg. Values of c_2^r and c_3^r are the coefficient of resistance due to track alignment, p is the train axile loading in N and i is the track gradient percentage. The value of c_a^r is the coefficient of train body smoothness and the value a is the cross-sectional profile of the train frontal.

Therefore, by summarising equation 4.8 to 4.9, the value A, resistance component independent to train speed; rolling and friction is represented in terms of the following equation.

$$A = mg\mu \quad (4.10)$$

Where m is the rail vehicle dry mass in kg, The value of g is the gravitational constant which is 9.81 m/s^2. The value μ is the kinetic coefficient of friction of the running track. Value B is the coefficient used to define train resistance dependent to train speed such as track alignment resistance can be represented in term of the following.

$$B = (\frac{c_3^r}{p} + 10i + c_2^r v)\ G \quad (4.11)$$

Where coefficient c_3^r is 130 and coefficient c_2^r is 0.009 for rapid transit type of rail vehicle (Vukan, 2007). The value i is the percentage of track gradient, due to section 3.2, the study took place in low gradient track, the value is 1 and the train axile weight is 80000 kg. In addition, G is the train weight and the value v is the train speed km/h.

Meanwhile, the value C the streamlining and aerodynamic coefficient can be represent in the following term,

$$C = c_a^r \, a \, v^2 \tag{4.12}$$

Where c_a^r is the rail vehicle body smoothness coefficient in term of 0.013 for rapid transit (Vukan, 2007). The value a is the cross-sectional profile of the rail vehicle frontal area in it represent 8.74 m^2, the train frontal width is 2.65 m and height is 3.3 m. The value v is the rail vehicle speed. Therefore, from equation 4.8 and 4.9, Davis equation can be written as the following,

$$R = mg\mu + 0.0016m + 10mg + 0.009mgv + 0.11367v^2 \tag{4.13}$$

Where the values for m, μ and v are the variables in the study.

4.1.3 Mathematical model for power consumption

Tractive force can be represented in the following equation,

$$T_e\,(v) = 2650 \, \frac{P}{V} \, \eta \tag{4.14}$$

Where P is operation power consumption in hp and η is the electrical propulsion system efficiency ranges between 0.78 to 0.84 for each railway system. Therefore, the rail operation power consumption is the energy consumption rate for the rail operation. It can be represented in the following equation,

$$P = \frac{T_e * v}{2650 * \eta} \tag{4.15}$$

Where power consumption, P is multiply by 0.74 and the train operation power consumption is in kW. Meanwhile, the Tractive force, T_e can be defined using the following formula,

$$T_e\ (v) = ma + R(v) + B_e(v) \tag{4.16}$$

Therefore, the power consumption, P can be defined in term of the following equation,

$$P = (ma + R(v)\ + B_e(v)).v \tag{4.17}$$

Application of Davis equation in the power consumption equation can be defined as the following,

$$P = (ma + mg\mu + Bv + Cv^2 + B_e v).v \tag{4.18}$$

Where the value $B_e(v)$ is equal to 0 for a propulsion system without regenerative braking system (section 3.2), the braking force is neglected. Therefore, the final equation for the rail operation power consumption is,

$$P = (ma + mg\mu + 0.0016m + 10mg + 0.009mgv + 0.11367v^2).v \tag{4.19}$$

Where rail operation power consumption, P is in kW.

4.2 THEORETICAL ANALYSIS OF OPERATION POWER CONSUMPTION

Most rail operations consist of station-to-station movements representing a regime of motion such as acceleration, constant speed, coasting, braking, and station stop regime (Vukan, 2007), (Hsiang & Chen, 2001). This different type of motion regime produces different variables in power consumption trends.

It is essential to analyse the power consumption produced in every station-to-station motion regime to conclude regime of motion to focus on for power consumption reduction (Rios & Ramos, 2012). In addition, the theoretical analysis may also assist future experimental analysis regarding the result validation and suitability of the type of station-to-station movement used for the study. Analysis of rail operation power consumption for the theoretical analysis is based on the net force equation and Davis equation.

4.2.1 Theoretical analysis type of station-to-station travel using Davis equation

This study aims to understand the relationship between different types of station-to-station travel and motion regimes and their effect on operation power consumption. Four types of station-to-station travel are analysed, and each regime of motion is discussed in this chapter.

Analysing the type of station-to-station travel is significant because train operation compromises four different types of station-to-station travel. Therefore it is essential to identify the most similar station-to-station travel type that represents the actual operation condition in the study and to be used in future theoretical analysis. The study's most similar operation style is selected based on the discussed criteria, and the result is compared with the following theoretical rail operation power consumption profile.

According to the four types of station-to-station travel velocity profiles in section 3.3.1, the velocity profile and other variables are substituted into the

mathematical model of equation 4.19, the following Figure 4.2 power consumption profile is produced,

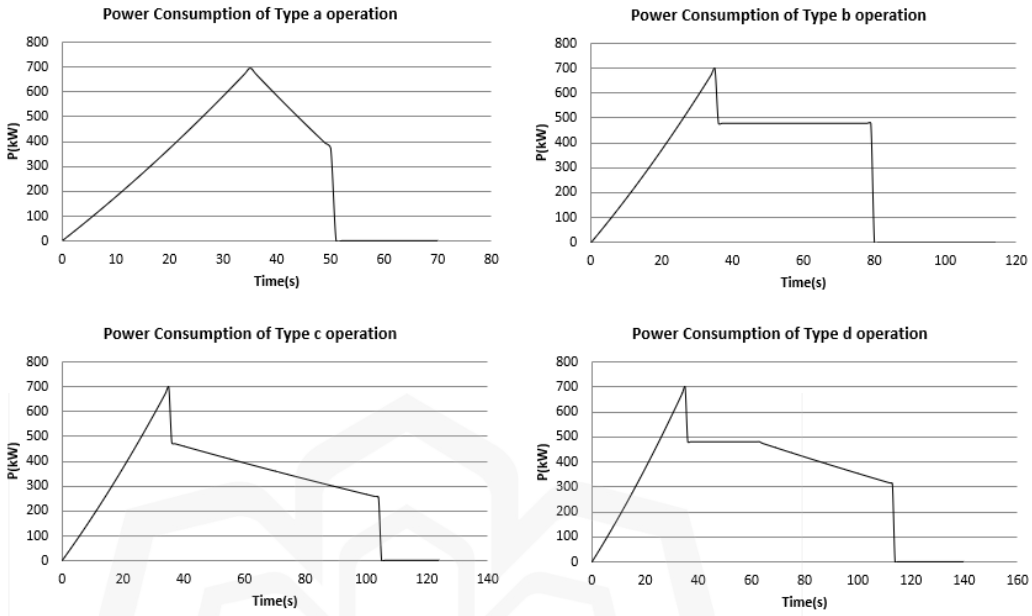

Figure 4.2: Graph of operation power consumption of four types of station-to-station travel.

The power consumption of train is depending on the train velocity and acceleration. It is determine based on the traction force of the rolling stock, train resistance and mode of operation (Hsiang & Chen, 2001). Figure 4.3 power consumption profile (dotted line) is by Vukan, 2007 of rolling stock DC propulsion system is compared with theoretical analysis result of the four types of station-to-station travel,

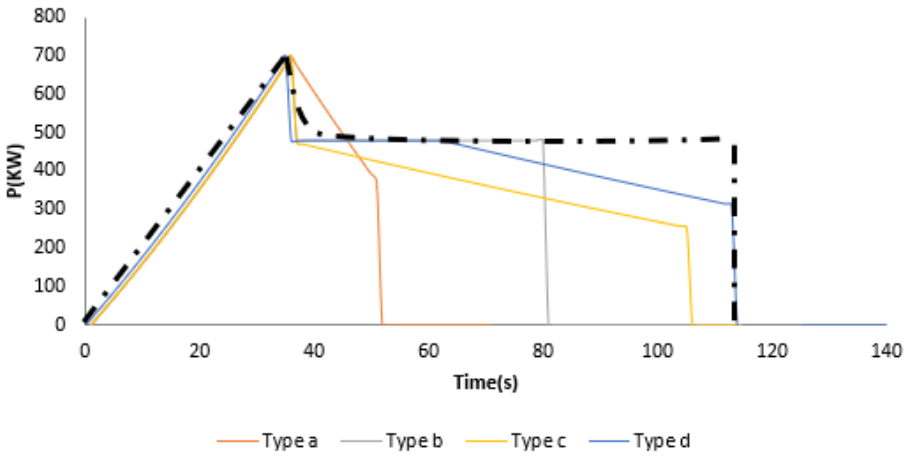

Figure 4.3: Graph of comparison theoretical power consumption of 4 mode of operation with reference graph by Vukan, 2007 (dotted line).

Most rail operation station-to-station movements represent several regimes of motion such as acceleration, constant speed, coasting, braking, and station stop regime (Vukan, 2007), (Hsiang & Chen, 2001). We can see the different trends of operation characteristics from the result as 4 different types of operation are analysed.

During the acceleration regime, the train accelerates at its maximum rate. It maintains it for some time as it gradually decreases its acceleration when approaching the constant speed regime. Maximum power is applied to set the train from a standstill to motion. How fast the train can reach its maximum velocity is commonly affected by its propulsion, resistance, and running track characteristics (Vukan, 2007) (Rios & Ramos, 2012). Therefore, this regime brings the most significant impact on power consumption; research can focus on this regime. Constant speed regime is the interval of the train travel at its constant velocity in some period before braking needs to be applied. The train moves with minimum power consumption due to tractive force being equal to the resistance. Some rail operations with short interstation distances may not reach a constant velocity regime because a brake must be applied earlier to stop. The coasting regime is where the train shuts down its propulsion system and coasts (due to low track resistance) until a brake must be applied to stop. Power consumption is equal to zero, and the train moves in a perpendicular direction. The fourth regime is braking. Regular train dynamic braking (kinetic energy of the train is dissipated as waste in the form of heat) is affected by the maximum braking rate, which is influenced by required braking distance, running surface resistance, and riding comfort (Wang & Rakha, 2017).

For some train equipped with regenerative braking, an electric rotary motor is reversed to slow down the train. The regenerated power can operate train auxiliary equipment (Vukan, 2007).

The train travel time and operation power consumption determine the most efficient rail operation. Efficient rail operation must have lower travel time while maintaining lower operation power consumption (Makovsek *et al*., 2019). Based on the above analysis, the following is the comparison between operation power consumption and travel time for the four types of station-to-station travel,

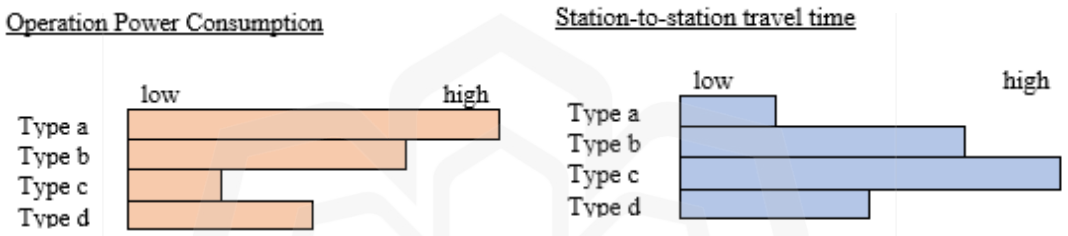

Figure 4.4: Graph of comparison of operation power consumption and travel time for 4 types of operation

According to the result in type a, the interstation distance is shorter, and the interstation travel time is limited; the train only passes two regimes of operation, which are acceleration and braking. Power consumption for this type of operation cannot be compared with another type (Type b,c, and d) due to this operation is only applicable for short interstation distances. Still, the power consumption is higher than the same operation type but with a shorter interstation travel time. For type b (constant speed, no coasting), the rail vehicle accelerates to its maximum velocity and moves at constant velocity until braking must be applied. Power consumption is higher compared to type c and d due to a longer constant speed regime but an advantage of shorter interstation travel time. According to the result in type c (coasting, no constant speed), the train moves with coasting (shutdown of propulsion) after reaching its maximum velocity before braking must be applied. Power consumption is lower than types a and d of operation due to the long coasting regime but with the disadvantage of the longest interstation travel time. For type d (constant speed + coasting), this mode of operation

consists of a constant velocity regime and coasting for some period before braking must be applied. This type of operation considers the most efficient mode of operation; power consumption is lower than type b due to the coasting region, but interstation travel time is longer than type b but shorter than type c.

4.2.2 Type of station-to-station travel for study

Based on the study in section 4.2.1, four different types of operation produced four different velocity profiles. Therefore, it is crucial to find the type of station-to-station velocity profile representing the study operation condition.

The difference in power consumption in all these 4 types of operation shows that it is essential for rail providers to choose the most efficient mode of operation that may result in lower power consumption, thus reducing operating costs. The operation mode with the lowest power consumption is not necessarily the best, and the most important is the operation reliability; lower travel time with the most efficient power consumption. Intercity freight trains with a long interstation distance and long permissible travel time may apply coasting mode in their operation but with a condition of good and low resistance of running track in the coasting area. Urban rail operations are mostly compromised with shorter interstation distances compared with intercity rail operations and a lower requirement for interstation travel time (Shuai *et al*., 2016); thus, the coasting regime could be more suitable. Moreover, rolling stock and CBTC system specifications must meet the coasting operation specification. In addition, research by (Gu *et al.,* 2013*)* on moving block CBTC signalling system power demand and energy reduction strategies highlighted the characteristic of the optimum moving block signalling system acceleration with full power, constant speed with partial power, and braking with no power. Therefore, based on these characteristics, a set of operation power consumption specifications is established as a reference for the study.

Kelana Jaya Line metro rail operation is compromised with shorter interstation distances and capped with a lower interstation travel time to meet its operation reliability and quality. The type b operation power consumption profile is also much represented the reference graph by Vukan, 2007 of power consumption of DC power

train operation; Kelana Jaya Line use DC power for train traction power. Moreover, type b of operation is the most common mode of operation applied in LRT operation worldwide. Type b of operation implies the CBTC system mode of operation implemented on the Kelana Jaya Line operation. Therefore, type b of operation is the reference station-to-station travel type for the study.

4.2.3 Rail operation power consumption for different train loading using theoretical analysis

Based on the previous study on type b of operation, the objective of this section is to understand the 'type b' operation power consumption with different train loading, *m* and track coefficient of friction, μ using theoretical analysis of Davis equation.

The influence of different train loading can be expressed in term of power consumption and time. Various train loading for a train can be express in terms of,

$$T_e = ma + \boldsymbol{m}g\mu + \boldsymbol{B}\boldsymbol{v} + Cv^2 + B_e \quad (4.20)$$

Various track coefficient of friction for a train can be express in terms of,

$$T_e = ma + mg\boldsymbol{\mu} + Bv + Cv^2 + B_e \quad (4.21)$$

The power consumption graph is constructed using train tractive force, resistance, and velocity data. The data is analysed to identify the relationship of train loading, *m*, and track coefficient of friction in the Davis equation. The linear regression of the Davis equation with the net force equation producing variable result of power consumption. The change in power consumption, *P*, is due to a change in train loading, *m*, and track friction coefficient (Shuai *et al*., 2016), (Hansen *et al*., 2017).

The power consumption graph is constructed based on the velocity profile, the reading of resistance, and the tractive force produced. The following is the velocity profile, resistance, tractive force, and operation power consumption for different train loading using the Davis equation,

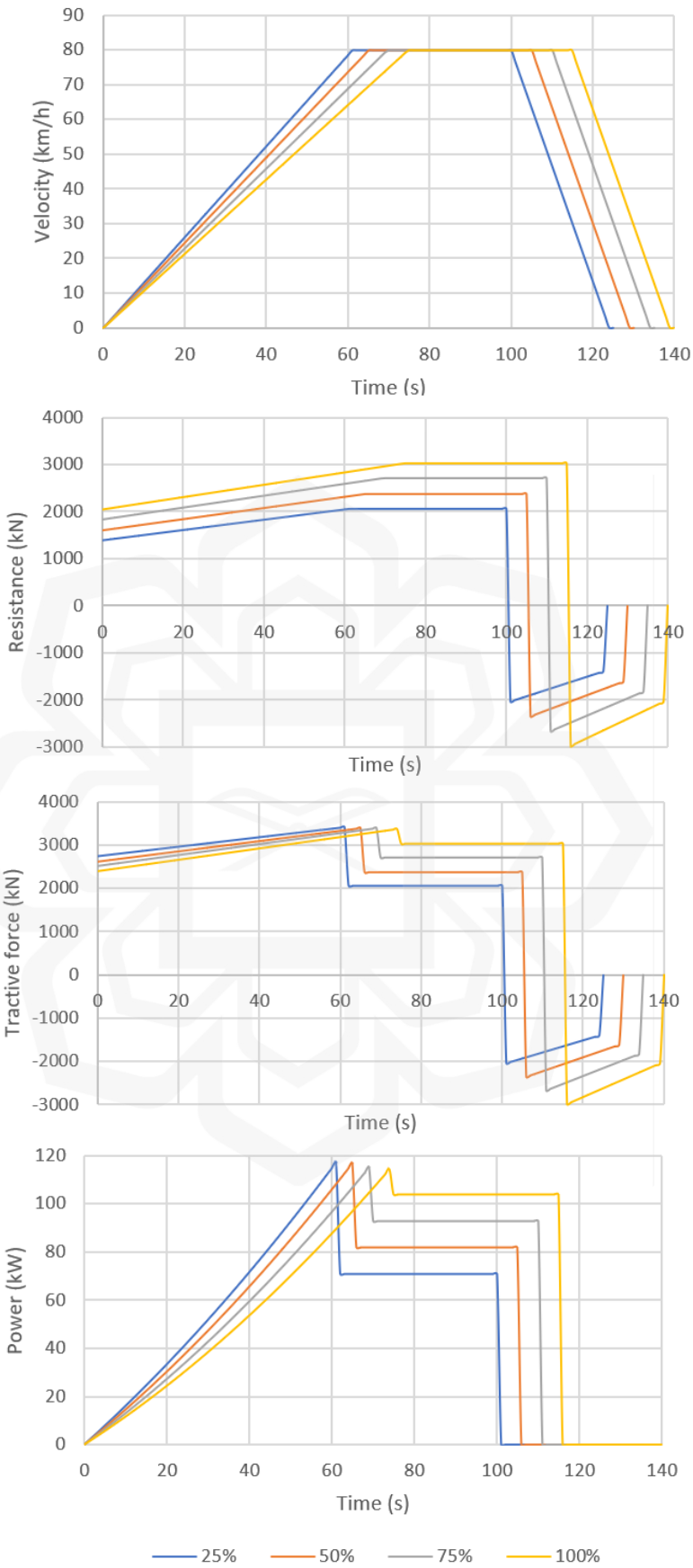

Figure 4.5: Graph of velocity profile, resistance, tractive force and power consumption of different train loading.

The result in Figure 4.5 comprise of four different train loading of 25%, 50%, 75% and 100%. Table 4.2 is the summary of the graph,

Table 4.2: Result summary for different train loading.

Train Loading	Resistance (kN)		Tractive force (kN)		Power consumption (kW)		Travel time (s)
	Stage 1	Stage 2	Stage 1	Stage 2	Stage 1	Stage 2	
100%	3021	3021	3358	3021	114	104	143
75%	2701	2701	3376	2701	115	93	138
50%	2381	2381	3397	2381	116	82	133
25%	2061	2061	3412	2061	117	71	128
↓10%	**↓11%**	**↓11%**	**↑0.5%**	**↓11%**	**↓1%**	**↓11%**	**↓4%**

Where the value of resistance, tractive force, and power consumption is based on the maximum value and consist of two stages of station-to-station operation; Stage 1: acceleration, and Stage 2: constant speed. The difference in the result is shown in terms of percentage.

According to the above resistance-time graph, the resistance for four different train loading increases with increased train velocity. It reaches its maximum value when it reaches the operation's maximum speed. The rate increase of resistance is approximately 10, 11, 12, and 13 kN/s for 25%, 50%, 75%, and 100% train loading. According to section 4.2.1, overall station-to-station travel compromise of four operational stages: acceleration, constant speed, deceleration, and station stop. The effect of deceleration and station stop stage on operation power consumption is neglected due to the scope of the study. Therefore, resistance is reduced by approximately 1% and 11% in stages 1 and 2 of operation in every 25% decrease in train loading.

Furthermore, according to the tractive force-time graph, the tractive force is observed to keep increasing with velocity until it reaches its maximum velocity. The rate increase of tractive force is approximately 10, 11, 12, and 13 kN/s for 25%, 50%, 75%, and 100% train loading. Then, the train operation enters the constant speed region; the tractive force is observed to start to decrease about 40%, 30%, 20% and 10% for 25%, 50%, 75%, and 100% train loading due to the acceleration is equal to zero in

constant speed region. Therefore the tractive force is constant with the resistance. It can be observed that the higher the train loading, the lower the percentage of decrease in tractive force when entering a constant speed region. The theoretical analysis concludes that tractive force increases with every rises in train loading. Meanwhile, the theoretical analysis also shows that the percentage of tractive force reduction decreases when entering a constant speed region with the increase of train loading due to the absence of acceleration in a constant speed region.

Furthermore, based on the above theoretical analysis, in the first stage of the rail operation (acceleration), the train accelerates initially at its maximum rate; the acceleration rate increases for some period and decreases as it approaches its maximum velocity; acceleration starts to decrease as the train approaching its constant speed region. The 25%,50%,75%, and 100% train loading increase its velocity at a rate of 0.35, 0.33, 0.31, 0.29 m/s^2. Lower train loading produces higher acceleration in the first stage of the train operation; hence the lower loading train operation will enter the constant speed region faster. Meanwhile, when the train reaches its maximum speed, it enters its second regime of operation; which is constant speed operation, the operation power consumption drops instantly when the train operation enters the second stage of operation (constant speed); approximate 40%, 30%, 20%, and 10% drops of operation power consumption are observed for 25% ,50%,75%, and 100% train loading. The percentage drop for lower loading train operation power consumption is higher for higher loading train in the constant speed stage.

In the third stage, the braking operation start (deceleration stage), and the train start to decelerate until it stops momentarily at the station. According to the above theoretical result, a reduction of every 25% train loading reduced approximately 5 seconds of station-to-station trip time due to a higher acceleration rate to attain constant speed region in lower loading train. In addition, it can be concluded that a decrease of 11% in operation power consumption is recorded for every 10% decrease in train mass, i.e., 25% train loading, 11% decrease in resistance.

4.2.4 Rail operation power consumption for different track coefficient of friction using theoretical analysis

Moreover, the theoretical analysis is continued with the application of different track coefficient of friction. The range of track coefficient of friction is from μ= 0.2 to 0.8 as per discussed in section 3.3.2.

Figure 4.6 is the velocity profile, resistance, tractive force and operation power consumption for different and track friction coefficient, μ using theoretical analysis,

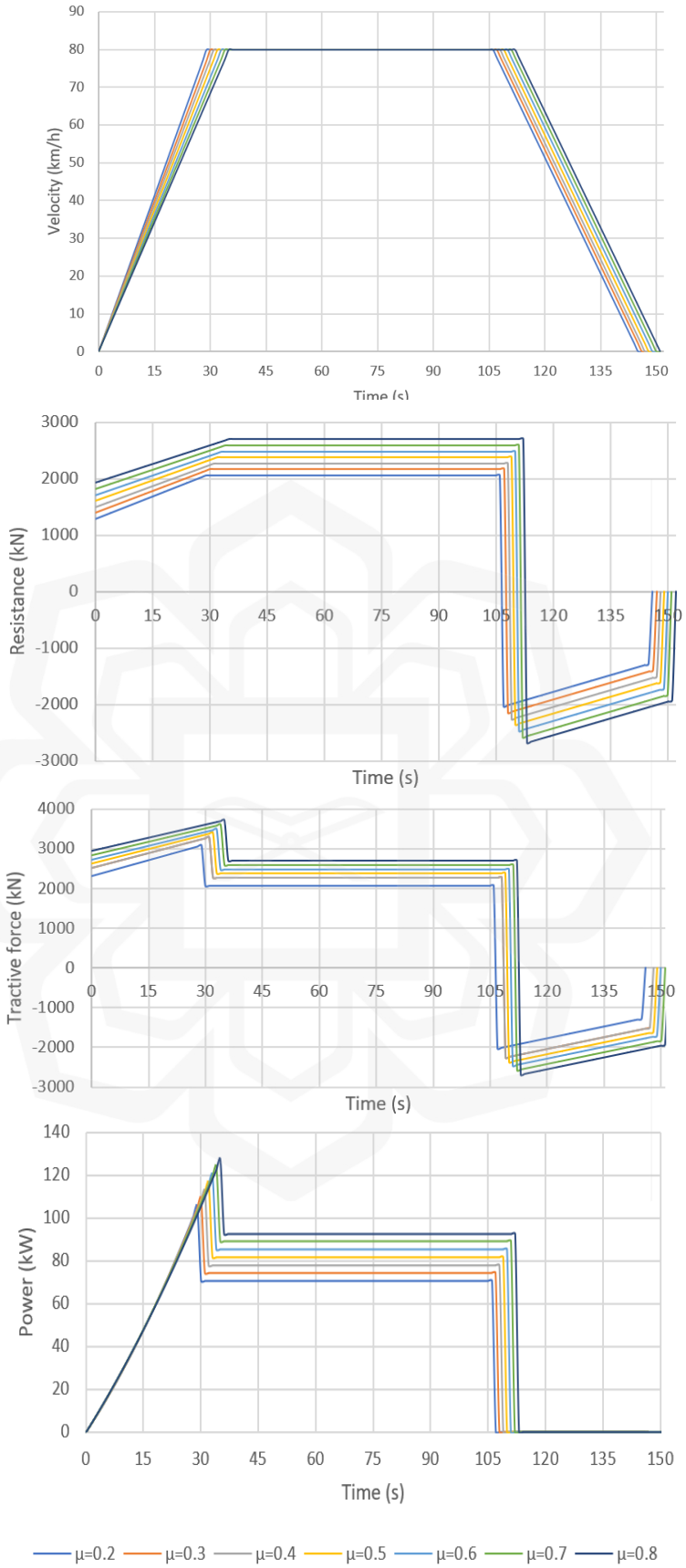

Figure 4.6: Graph of velocity profile, resistance, tractive force and power consumption of different track friction coefficient, μ= 0.2-0.8.

The result in Figure 4.6 comprise of seven different track friction coefficient, μ= 0.2-0.8 based on the normal operation condition. Table 4.3 is the summary of the above graph,

Table 4.3: Result summary for different track friction coefficient.

Coefficient of Friction, μ	Resistance (kN)		Tractive force (kN)		Power consumption (kW)		Travel time (s)
	Stage 1	Stage 2	Stage 1	Stage 2	Stage 1	Stage 2	
0.8	2703	2703	3719	2703	128	93	153
0.7	2595	2595	3612	2595	124	89	152
0.6	2488	2488	3505	2488	120	85	151
0.5	2381	2381	3398	2381	117	82	150
0.4	2274	2274	3290	2274	113	78	149
0.3	2167	2167	3183	2167	109	74	148
0.2	2059	2059	3076	2059	106	71	147
↓0.1	**↓4%**	**↓4%**	**↓3%**	**↓4%**	**↓3%**	**↓4%**	**↓0.6%**

Where the value of resistance, tractive force, and power consumption is based on the maximum value and consist of two stages of station-to-station operation; Stage 1: acceleration, Stage 2: constant speed. The difference in the result is shown in terms of percentage.

According to the above resistance-velocity graph of the theoretical analysis, the resistance is observed to increase with the increase in train velocity. It reaches its maximum value when it reaches the operation's maximum velocity. The rate increase of resistance is approximately 20, 21, 22, 23, 24, 25, and 26 kN/s, i.e., a decrease of 1 kN/s in every velocity increase, is recorded for μ=0.8-0.2. Resistance is observed to reduce approximately 4% at stages 1 and 2 of operation with the decrease of track friction coefficient, from 0.8 to 0.2 of every μ=0.1 decrease of track friction coefficient.

Furthermore, according to the tractive force-velocity graph, the tractive force is observed to keep increasing with velocity until it reaches its maximum velocity and the train operation enters the constant speed region; the tractive force is observed to start to decrease about 33% due to the acceleration is equal to zero in constant speed region. Therefore the tractive force will be similar to the resistance. Meanwhile, increasing resistance in the above resistance-velocity graph decreases about 4% of the tractive

force in every μ=0.1 decrease of track friction coefficient. Therefore, the theoretical analysis shows that tractive force decreases with a reduced track friction Coefficient due to decreased resistance.

According to the Figure 4.6, the rate increase of velocity is approximately 0.70, 0.65, 0.60, 0.55, 0.50, 0.45, 0.40 m/s^2 for μ=0.2, 0.3, 0.4, 0.5, 0.6, 0.7, 0.8. Therefore, it can be concluded that based on the theoretical analysis, a lower track coefficient of friction, μ produces a higher acceleration rate on the first stage of operation due to lower resistance; hence the train operation will enter the constant speed stage faster. Furthermore, during the second stage (constant speed region), operation power consumption drops approximately 33%, 32%, 31%, 30%, 29%, 28%, and 27% for μ=0.2, 0.3, 0.4, 0.5, 0.6, 0.7, 0.8. It can be concluded that based on the theoretical analysis, the percentage drop of operation power consumption during the constant speed region for track coefficient of friction, μ 0.2 to 0.8 is homogenous.

In the third stage of operation, the braking operation start (deceleration region), and the rail vehicle start to decelerate until it stops momentarily at the station. According to the above theoretical result, the acceleration and operation power consumption is negative and can be considered zero in these studies. Meanwhile, according to the theoretical analysis, the reduction of the track coefficient of friction, μ from 0.8 to 0.2, reduced by approximately 1 second in every μ=0.1 reduction of the track coefficient of friction, μ. In addition, based on the above theoretical analysis power consumption graph for μ 0.2 to 0.8 is constructed using linear regression of the Davis equation to net force equation. According to the result, every μ=0.1 reduction of the track coefficient of friction produces a 4% lower operation power consumption rate.

According to the theoretical analysis, higher train loading, *m*, and track coefficient of friction, in Davis equation, produce higher power consumption due to higher running resistance. Therefore, based on this hypothesis, a test is conducted to determine the relationship of train loading, *m*, and track coefficient of friction with operation power consumption.

4.3 CHAPTER SUMMARY

The mathematical model of the study is constructed based on the application of the Davis equation in the net force equation. The theoretical analysis comprise of station-to-station travel analysis using the Davis equation and theoretical analysis of operation power consumption with variable train loading and track coefficient of friction using the Davis equation. The result from the station-to-station analysis shows that type b of the station-to-station operation most resembles the operation condition in the study. Therefore, the type b velocity profile is the reference for the theoretical analysis. Theoretical analysis of different train loading shows that the percentage of power consumption reduction is linear with the percentage reduction of train mass. In addition, theoretical analysis of varying track coefficient of friction shows that reduction of approximately 4% of operation power consumption in every 0.1 drops of μ.

CHAPTER FIVE

RESULTS AND DISCUSSION

5.1 INTRODUCTION

This chapter covers the experimental analysis result and discussion of the studies. These include the elaboration of the research finding of the experimental testing train operation power consumption for various train loading, and experimental testing of train operation power consumption for different track coefficient of friction with application of rail grinding to lower track coefficient of friction. Furthermore, all data collected is tabulated, analysed, and significant and implication of the result is discussed in this chapter.

5.2 EXPERIMENTAL ANALYSIS OF RAIL OPRATION POWER CONSUMPTION

Based on the theoretical analysis, two experiments were conducted to study the relationship between rail operation power consumption to train loading, m and track coefficient of friction, μ.

The objective of the test is to understand the correlation between train loading and operation power consumption and to understand the correlation between track coefficient of friction and power consumption.

5.2.1 Experiment 1- Train loading

Train resistance is a set of forces that must overcome to set the train in motion or to accelerate it to a higher speed. A significant contribution to energy loss is due to energy to overcome the resistance of the train, such as aerodynamic opposition and mechanical friction between wheels and a rail track (Vukan, 2007). Train loading, *m* is the gross weight of the train and passenger in terms of percentage, and it is represented as one of the elements in train resistance. The reduction of 100% train loading to 50% is an approximate reduction of 20% of the overall train mass.

Based on the previous study, each cycle of station-to-station travel consists of 4 operations: acceleration, constant speed, braking, and station stop. Different operation stage with different trend is analysed as the train loading is the variable. Several factors, such as train loading, track characteristic, propulsion system, and operation speed, may affect operation power consumption (Wang & Rakha, 2018), but train loading is selected for sensitivity analysis in this testing.

Theoretical analysis shows that train loading significantly influences operation power consumption and travel time. In addition, the finding in the theoretical analysis is also supported by Jong & Chang, 2005 studies which conclude that power consumption always trades off with running time. Figure 5.1 is the result produced from the experiment,

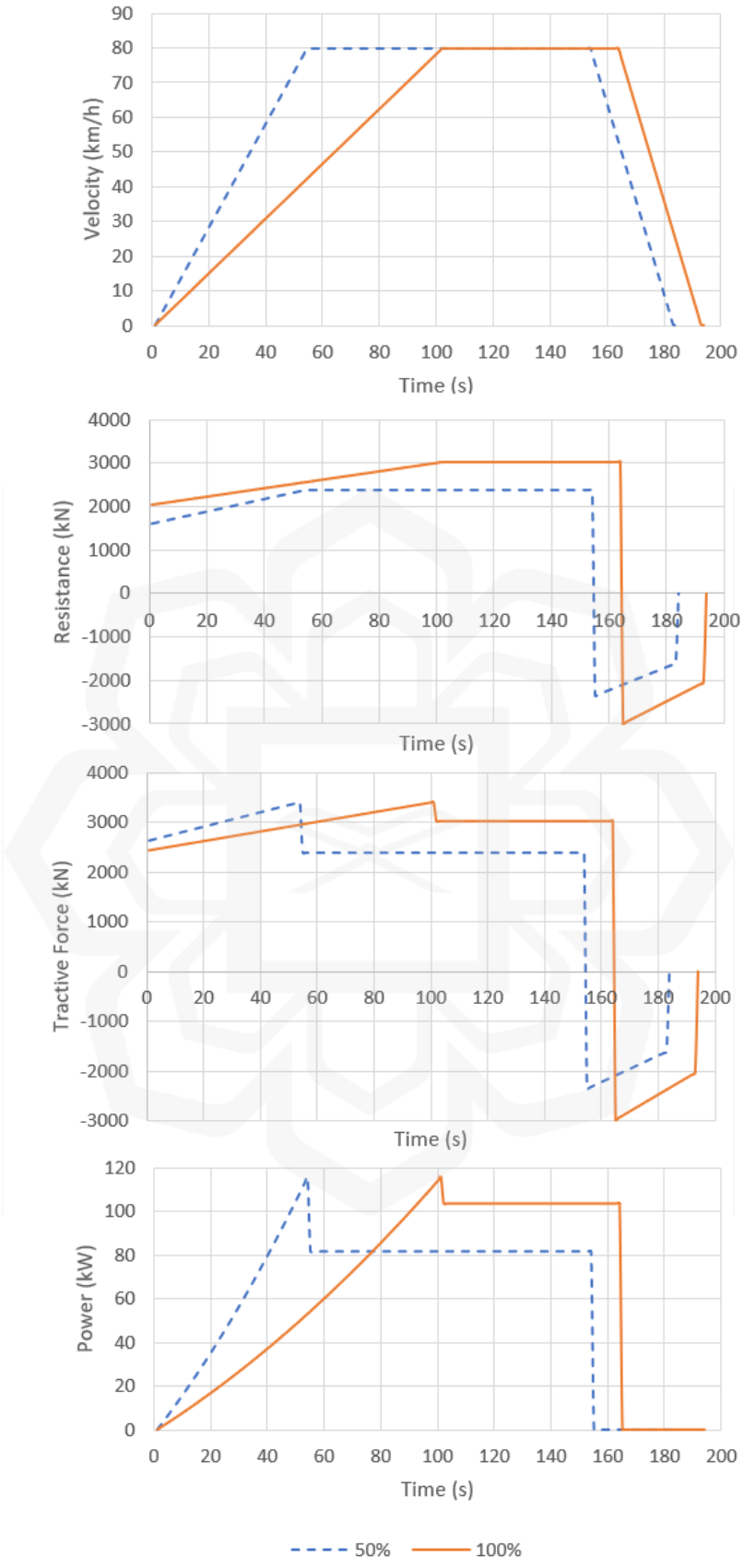

Figure 5.1: Graph of velocity profile, resistance, tractive force and power consumption for 50% and 100% train loading.

The result in Figure 5.1 comprise of two different train loading of 100% and 50%. Table 5.1 is the summary of the result,

Table 5.1: Result summary for 100% and 50% train loading.

Train Loading	Resistance (kN)		Tractive force (kN)		Power consumption (kW)		Travel time (s)
	Stage 1	Stage 2	Stage 1	Stage 2	Stage 1	Stage 2	
100%=138,440 kg	3021	3021	3403	3021	116	104	194
50%=109,400 kg	2381	2381	3393	2381	116	82	184
↓20%	**↓21%**	**↓21%**	**↓0.3%**	**↓21%**	**↓0%**	**↓21%**	**↓5%**

Where the value of resistance, tractive force, and power consumption is based on the maximum value and consist of two stages of station-to-station operation; Stage 1: acceleration, and Stage 2: constant speed. The difference in result is shown in terms of percentage.

Under the above resistance-time graph, the resistance is observed to be increasing with the increase in travel time and reaches its maximum value when it reaches the maximum operating velocity of 80 km/h. The rate increase of resistance is approximately 14 kN/s for 50% train loading and 9 kN/s for 100% train loading in every velocity increase. A total reduction of 21% of resistance is observed when the train loading is reduced from 100% to 50% at stages 1 and 2 of operation.

Furthermore, according to the tractive force-time graph, the tractive force is observed to keep increasing with time until it reaches its maximum velocity. The rate increase of tractive force is approximately 14 kN/s for 50% train loading and 9 kN/s for 100% train loading in every velocity increase. Then, the train operation enters the constant speed region; the tractive force is observed to start to decrease about 29% for 50% train loading and 11% for 100% train loading. The decrease in tractive force is due to the acceleration being equal to zero in the constant speed region. Therefore, the tractive force will be equal to the resistance. At the speed of 60 km/h, both 50% and 100% loading trains reached the optimum tractive force where both train operations operated with the same tractive force and kept increasing until both train operations

reached the maximum tractive force; both train operations differed by time to reach the optimum velocity.

According to Davis equation, the difference in the number of passengers boarding the train produces different values of *A* and *B*, which results in increasing train resistance. According to the finding in the theoretical analysis, lower train loading produces lower train resistance, therefore producing lower operation power consumption; this reflects the above experimental result. Based on the velocity-time graph, 50% and 100% train operation cover the acceleration, constant speed, and deceleration stage, type b of operation. During the first stage of the operation (acceleration), both trains move with positive acceleration and speed increase. During this stage of operation, the train accelerates initially at its maximum rate; the acceleration rate increase for some period and decreases as it approaches its maximum velocity; acceleration starts to reduce as the train approaches its constant speed. The rate increase of velocity is approximately 0.4 m/s^2 for 50% train loading and 0.2 m/s^2 for 100% loading train. The experimental result reflects the theoretical analysis in section 4.2, where lower train loading produces a higher acceleration rate in the first stage of the train operation. Therefore the train operation enters the constant speed region faster; the acceleration region is the region with the highest operation power consumption, and the constant speed region is the region with the lowest power consumption (Vukan, 2007).

The differences in the train loading affect the running resistance; a train with lower loading achieved its constant speed region faster as its acceleration rate was higher due to the lower resistance value. The finding is consistent with the previous studies by Wang & Rakha, 2017 that state that lowers train loading produces lower resistance and may result in a higher acceleration rate. However, a higher acceleration rate may result in higher operation power consumption; the ATS system regulates the station-to-station trip time to the minimum trip time to cope with the daily schedule, and with a restricted maximum speed, the train will always accelerate to its limited speed during acceleration region so that they can achieve constant speed region faster (Gu *et al*., 2013). Therefore the acceleration rate will not continue to increase as the train attain its restricted speed. The operation power consumption for lower train loading during acceleration region is higher than higher train loading due to a higher acceleration rate. However, the overall operation power consumption for lower train loading is lower due to lower traction force during constant speed region and lower

overall trip time as trip time always exerts influence on operation power consumption; this reflects the finding by Su *et al*., 2016.

When the train reaches its maximum speed, it enters the second regime of the operation, which is constant speed operation where the net force is zero, and the tractive force is equal to resistance; the vehicle reaches its constant speed regime, and the acceleration is zero (Rios & Ramos, 2012). Therefore, for the train with lower train loading; lower resistance, the tractive force is at the lowest and equal to the resistance. This reflects the result in the above experimental analysis; the power consumption drops instantly when the train operation enters the second stage (constant speed). The 50% loading train drops approximately 27% of operation power consumption, and the 100% loading train drops around 10%. The percentage drop of 50% loading train operation power consumption is higher compared with 100% loading train; this reflects the finding in the theoretical analysis section 4.2, where the lower the train loading, the higher the percentage drop of operation power consumption during the constant speed region. In the third stage, the braking operation start (deceleration stage), and the train start to decelerate until it stops momentarily at the station platform. According to the above experimental result, the train propulsion system is not exerting any tractive force due to braking operation. The acceleration is at a negative rate, and the operation power consumption is considered zero in these studies. The braking rate is the same for both train operations due to the same braking point for both train operations already being set by the ATS system. Therefore, the fastest train operation that reaches the breaking point will produce lower station-to-station travel time.

Meanwhile, according to the above finding, the implication of reduction in 50% of train loading reduced approximately about 10 seconds of station-to-station trip time due to a higher acceleration rate to attain constant speed region; 50% of train loading achieved the breaking point faster compared to 100% train loading. During the first and second stages of train operation, 50% of train loading moves in lower traction force, hence consuming lower operation power consumption than 100% of train loading. Since lower traction force and shorter trip time for the traction are being applied to achieve the same train speed for lower train loading, an approximately 21% lower operation power consumption rate is produced in a 20% lower total train mass (50% lower train loading). Therefore, based on the finding, 50% lower train loading reduced approximately 21% of operation power consumption and around 5% of travel time. Meanwhile, according to a study in the Yizhunag Line China metro system, the

operation power consumption rate of a metro train is nearly doubled when the train mass increases by double (Shuai *et al*., 2016). Consequently, the finding in test 1 aligns with the study by Shuai *et al*., 2016 on China's metro system. The reduction of 20% in total train mass (50% lower train loading) decreased by 21% in operation power consumption.

The changes in train resistance affect the tractive force in acceleration and constant speed region, producing a different operation power consumption trend for both operation regions. According to a study by Jong & Chang, 2005, train usually operates with a low track friction coefficient. Therefore, the operation power consumption will be very sensitive to train loading factors. Jong & Chang, 2005 added sensitivity analysis shows that power consumption is a convex function (U shape) of track friction coefficient and train loading. The train specification on the wheel slip and slide effect determines the ideal track friction coefficient to operate the train during the acceleration regime. An ideal track friction coefficient rail system may result in lower operation power consumption and lower rail vehicle resistance, giving an advantage to the operation power consumption during constant speed region (Jong & Chang, 2005). Therefore based on the experimental analysis, lower resistance train operation will tend to be more sensitive in reducing operation power consumption than higher resistance train during the constant speed region.

In summary, according to the above experimental analysis on the operating power consumption of 50% and 100% train loading, a 20% decrease in train mass and a 21% decrease in train resistance, an approximate 21% decrease in operating power consumption is produced from 50% train loading to 100% train loading. This finding is supported by the theoretical analysis and a previous finding by Shuai *et al*., 2016. In addition, a reduction of 10 seconds of station-to-station trip time is recorded for every 50% lower train loading due to the higher acceleration rate for lower loading trains during the acceleration region.

The difference in resistance at the first and second stage of operation affect the power consumption. According to the funding in this section, research on reducing operation power consumption should focus on resistance value; to get optimum resistance value for lower power consumption rail operation. Therefore, it is significant to study the other factor to reduce resistance, such as track friction coefficient, μ, as mentioned in section 2.3.3. In addition, the primary effect on operation power consumption lies in the constant speed region. Therefore, finding in this analysis

suggests to focus on this region to reduce train resistance and operation power consumption. Several options to reduce train loading, as per discussed in section 2.2.2, can be implemented with a focus on this region.

5.2.2 Experiment 2- Coefficient of friction

The objective of the experiment is to understand the correlation between train resistance and operation power consumption with the effect of rail grinding to lower the track coefficient of friction. The application of the Davis equation to the net force equation, the change in power consumption is due to a change in friction coefficient. The difference in track friction coefficient in resistance is made by applying rail grinding.

Based on the application of weight balance method to measure the track kinetic coefficient of friction in section 3.4.4. Figure 5.2 is the measurement of the track kinetic coefficient of friction before and after rail grinding is applied,

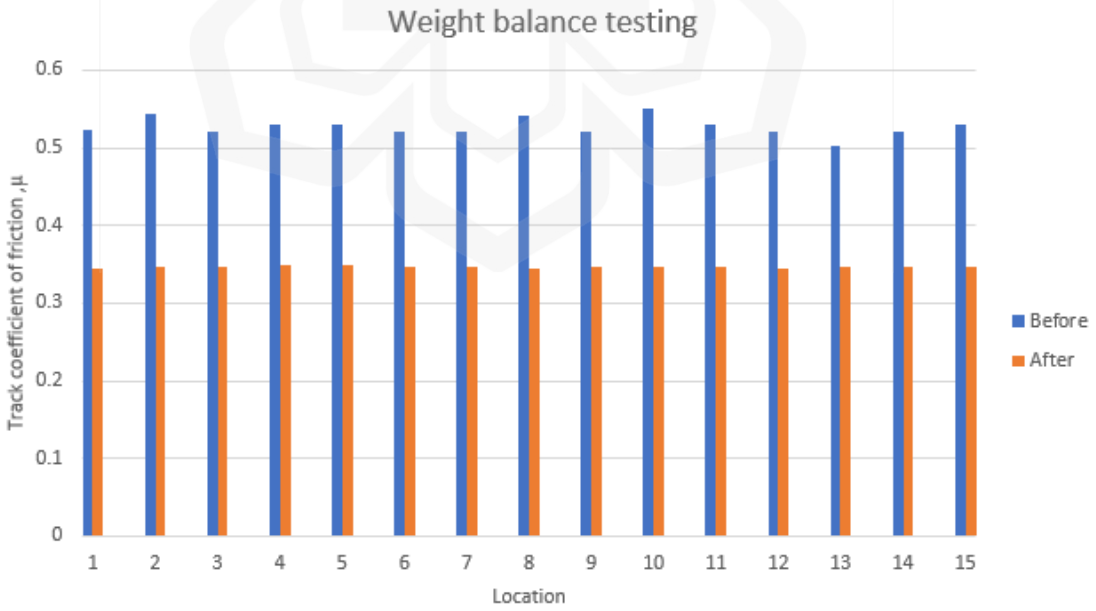

Figure 5.2: Graph of weight balance testing for before and after the application of rail grinding to find μ.

Measurement is taken at 15 locations as per in section 3.4.4. Based on the finding, the track coefficient of friction before rail grinding is being applied is approximately μ=0.5 and after rail grinding being applied is approximately μ=0.3.

When the rail grinding is executed, it results in a smoother and more uniform track surface. This smoother profile significantly impacts the coefficient of friction between the train wheels and the rail. The coefficient of friction, which represents the resistance encountered when two objects move against each other, is influenced by the state of the contacting surfaces.

In the context of rail grinding, the reduction in surface irregularities and imperfections leads to a lower coefficient of friction. A smoother rail surface minimizes the resistance that the train wheels encounter during movement along the tracks. Surface irregularities can create friction as train wheels move over them. Smoothing out the surface by the grinding process reduces the contact points where friction is generated. When the contact point is reduced, the energy required to overcome friction is minimized. The frictional force between two surfaces is directly proportional to the force pressing them together. Lowering the contact point between the track and the wheel decreased the force acting perpendicular to the surfaces.

Meanwhile, the following Figure 5.3 and 5.4 are the graph of velocity profile, resistance, tractive force and power consumption of Experiment 2, before (μ=0.5) and after (μ=0.3) rail grinding being applied for constant train loading condition, 50% and 100% train loading,

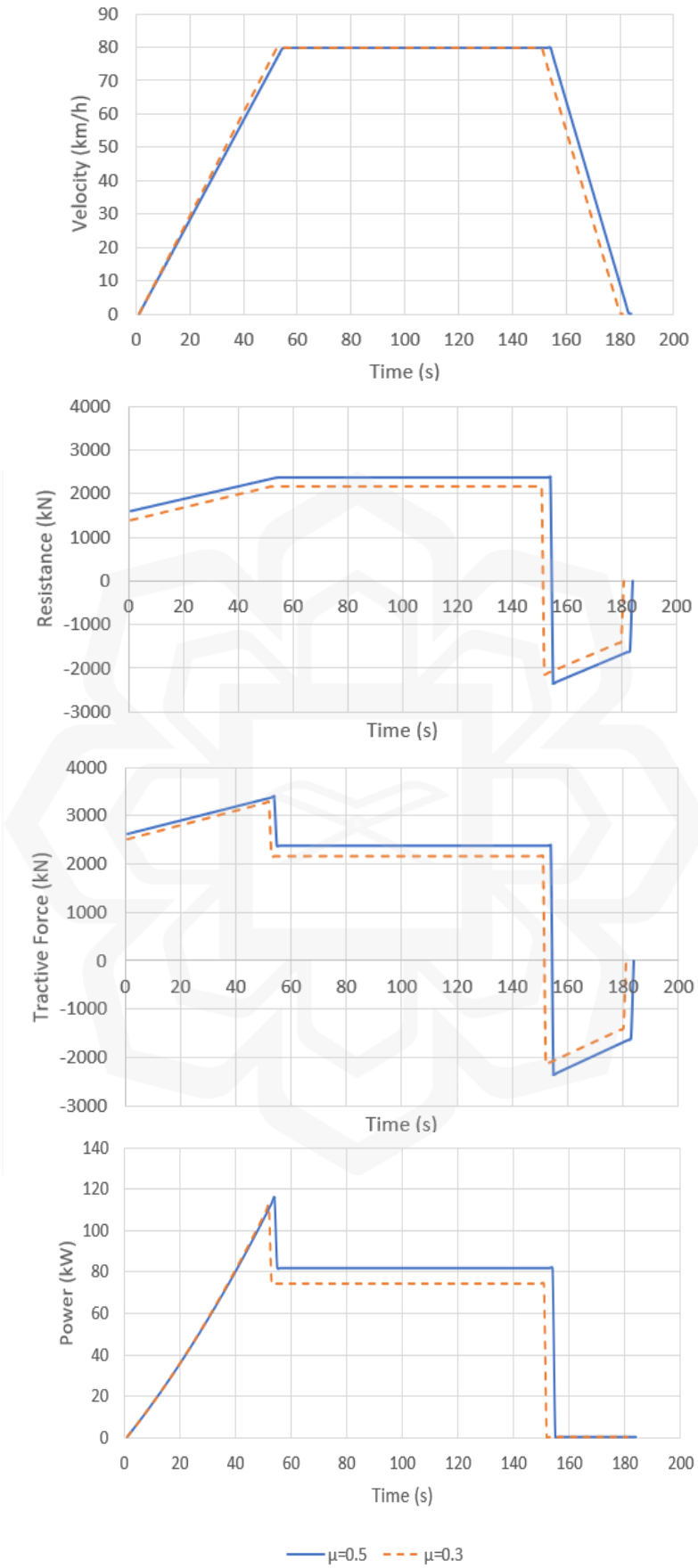

Figure 5.3: Graph of velocity profile, resistance, tractive force, and power consumption for 50% train loading before and after rail grinding.

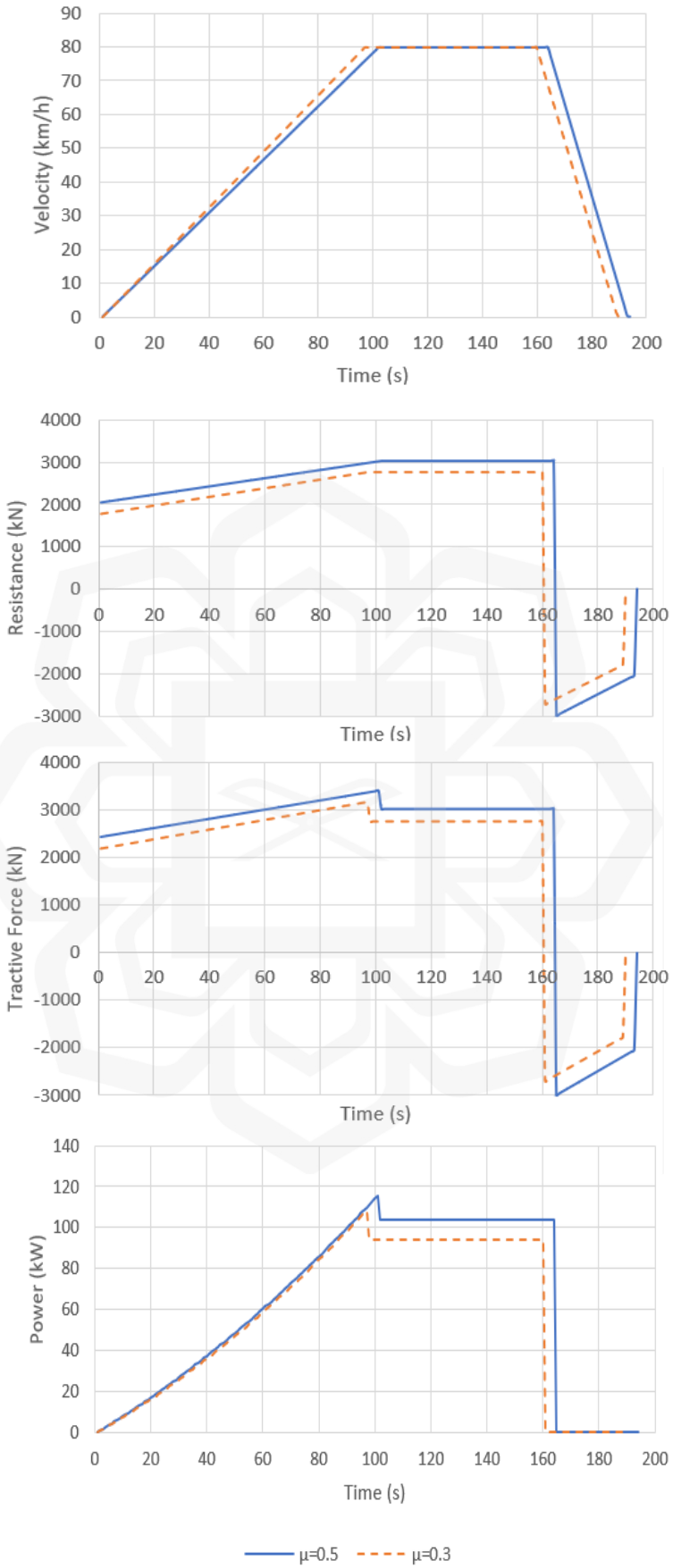

Figure 5.4: Graph of velocity profile, resistance, tractive force, and power consumption for 100% train loading before and after rail grinding.

The result in Figures 5.3 and 5.4 comprise of two different track coefficient of friction, μ=0.5 and μ=0.3. The following Table 5.2 and 5.3 is the summary of the above graph,

Table 5.2: Result summary for 50% train loading.

Coefficient of Friction, μ	Resistance (kN)		Tractive force (kN)		Power consumption (kW)		Travel time (s)
	Stage 1	Stage 2	Stage 1	Stage 2	Stage 1	Stage 2	
0.5	2381	2381	3393	2381	116	82	184
0.3	2167	2167	3288	2167	112	74	181
↓40%	**↓9%**	**↓9%**	**↓3%**	**↓9%**	**↓3%**	**↓9%**	**↓1.6%**

Table 5.3: Result summary for 100% train loading.

Coefficient of Friction, μ	Resistance (kN)		Tractive force (kN)		Power consumption (kW)		Travel time (s)
	Stage 1	Stage 2	Stage 1	Stage 2	Stage 1	Stage 2	
0.5	3021	3021	3403	3021	116	104	194
0.3	2749	2749	3157	2749	108	94	190
↓40%	**↓9%**	**↓9%**	**↓6%**	**↓9%**	**↓6%**	**↓9%**	**↓2%**

Where the value of resistance, tractive force, and power consumption is based on the maximum value and consist of two stages of station-to-station operation; Stage 1: acceleration, and Stage 2: constant speed. The difference in the result is shown in terms of percentage.

Under the above resistance-time graph, the resistance is observed to be increasing with the increase of train velocity and reaches its maximum value when it reaches the maximum operating speed of 80 km/h. The rate increase of resistance is approximately 14 kN/s and 15 kN/s for μ=0.5 and μ=0.3 in 50% train loading operation in every increase of velocity. In addition, the rate increase of resistance is approximately 9 kN/s and 10 kN/s for μ=0.5 and μ=0.3 in 100% train loading operation in every increase of velocity. The decrease of track friction coefficient from 0.5 to 0.3 decreases resistance by approximately 9% for both train loading.

Furthermore, according to the tractive force-time graph, the tractive force is observed to keep increasing with velocity until it reaches its maximum velocity. The

rate increase of tractive force is approximately 14 kN/s and 15 kN/s for μ=0.5 and μ=0.3 in 50% train loading in every velocity increase. In addition, the rate increase of tractive force is approximately 9 kN/s and 10 kN/s for μ=0.5 and μ=0.3 in 100% train loading in every velocity increase. Then, the train operation enters the constant speed region; the tractive force is observed to start to decrease about 29%, and 33% for μ=0.5 and μ=0.3 in 50% train loading, and 11% and 13% for μ=0.5 and μ=0.3 in 100% train loading due to the acceleration is equal to zero in constant speed region. Therefore the tractive force will be equal to the resistance. The implication of both resistance and tractive force is interconnected; the rate increase of both forces is similar.

Tractive force is transferred between the train wheel and the rail track through friction force or resistance between two surfaces to achieve acceleration and deceleration. The basic equation of the rail vehicle motion is affected by these two forces acting on the train: traction and resistance (Vukan, 2007). According to Davis Equation, the difference in track coefficient of friction, μ, produces difference values of *A* due to increasing or decreasing train resistance. According to the finding in the theoretical analysis, a higher track coefficient of friction, μ, produce higher train resistance, therefore producing higher operation power consumption (Su *et al*., 2016; Wang & Rakha, 2017). Therefore, the above finding is significant with the experimental result.

During the first stage of the rail operation, the train moves with positive acceleration and the vehicle speed increases. During this stage of the operation, the train accelerates initially at its maximum rate; the acceleration rate increases for some period and decreases as it approaches its maximum velocity; acceleration starts to decrease as the train approaches its constant speed region. Higher maximum speed might be achieved with higher acceleration, but the ATS maximum speed restricts the rail system. Therefore, the train enters its constant speed region when it reaches the ATS maximum speed (Feng *et al.*, 2014). In the first stage of rail operation for 50% train loading, μ=0.5 train operation increases its velocity at a rate of 0.41 m/s^2, and μ=0.3 increase its velocity at 0.46 m/s^2. Meanwhile, in the first stage of rail operation for 100% train loading, μ=0.5 train operation increases its velocity at a rate of 0.21 km/h^2, and μ=0.3 increase its velocity at 0.24 km/h^2. The experimental result reflects the theoretical analysis in section 4.2, where a lower track friction coefficient produces a higher acceleration rate in the first stage of the train operation; therefore, the result implies that the train operation enters the constant speed region faster. In addition, according to the

above experimental result, the 50% train loading operation shows a higher difference in a change of acceleration rate on the first stage of the operation when the track friction coefficient is reduced compared with 100% train loading. According to Jong & Chang, 2005, as a train operated with a low track coefficient of friction, μ, a train with lower loading will be more sensitive to changes in acceleration rate. Nevertheless, let's compare 50% and 100% train loading in the first stage of operation. The result shows similar trends in increasing acceleration even though the result sensitivity is different. The differences in the track coefficient of friction, μ affect the running resistance; a train with a lower track coefficient of friction, μ, achieved its constant speed region faster as its running resistance is lower, producing a higher acceleration rate on the first stage of operation. Therefore, the trip time in the acceleration region is reduced, producing lower operation power consumption as trip time always exerts influence on operation power consumption (Su *et al*., 2016; Vukan, 2007).

As the rail vehicle reaches its maximum velocity, it enters its second stage of the operation, which is constant speed operation, the net force is zero, and the tractive force is equal to resistance; the vehicle reaches its constant speed regime, and acceleration is zero. The train operates with the lowest operation power consumption in this region, lower track coefficient of friction, μ producing lower operation power consumption due to lower running resistance value and longer trip time. This reflects the result in the above experimental analysis; the power consumption drops instantly when the train operation enters the second stage (constant speed). In the second stage of rail operation for 50% train loading, μ=0.5 operation power consumption drops approximately 27%, and μ=0.3 operation power consumption drops approximately 30%. Meanwhile, in the second stage of rail operation for 100% train loading, μ=0.5 operation power consumption drops by approximately 10%, and μ=0.3 operation power consumption drops by approximately 13%. The drop in operation power consumption for μ=0.3 is more than μ=0.5, and 50% train loading is more than 100% due to the implication of the above train loading and resistance sensitivity.

In the third stage of operation, the braking operation start (deceleration stage), and the rail vehicle start to decelerate until it stops momentarily at the station platform. According to the above experimental result, the train propulsion system is not exerting any tractive force due to braking operation. The acceleration is at a negative rate, and the operation power consumption is considered zero in these studies. The braking rate is the same for both before and after rail grinding train operations due to the same

braking point for both train operations that is already being set by the ATS system. Therefore, the fastest train operation that reaches the breaking point will produce lower station-to-station travel time. Meanwhile, according to the above finding, the reduction of track coefficient of friction, μ from 0.5 to 0.3 reduced approximately about 3 seconds of station-to-station trip for 50% & 100% train loading due to higher acceleration rate to attain constant speed region; μ=0.3 achieved the breaking point faster compared to μ=0.5. According to research by Su *et al*., 2016, an average reduction of 5 seconds is recorded in their research in a decrease of 40% of friction coefficient.

Changes in train resistance affected rail tractive force in acceleration and constant speed stage (Wang & Rakha, 2017). In addition, it also may affect the changes in power consumption in acceleration and constant speed stage. Lower track coefficient of friction, the rail system reaches the constant speed stage faster; the acceleration stage is the region with the highest operation power consumption, and the constant speed stage is the region with the lowest operation power consumption; operation power consumption is lower due to lower running resistance and lower trip time in acceleration region. In addition, it also uses less operation power consumption during the constant speed stage compared to a higher track coefficient of friction due to lower running resistance (Jong & Chang, 2005).

It is clearly shown in the experimental result that the implication of the above finding, the operation power consumption during acceleration and constant speed stage decreased with the decrease of track coefficient of friction, μ from 0.5 to 0.3 from the effect of rail grinding procedure. In addition, the finding also reflects the result in the theoretical analysis, lower track coefficient of friction, μ producing lower operation power consumption. According to the power consumption profile before and after rail grinding, a reduction of 9% lower operation power consumption in a 9% reduction in resistance and a 40% reduction in track coefficient of friction. Meanwhile, according to research in Yizhuang Line China metro, which uses a similar track gauge, type of rolling stock, and maximum operation speed, on the influence of running resistance on operation power consumption, an average of 3% of operation power consumption rate is reduced by every 20% reduction of track coefficient of friction (Shuai *et al*., 2016). Therefore, the finding in experiment 2 reflects the finding of Shuai *et al*., 2016 in the China metro system as an average reduction of 9% is recorded for a 40% (μ= 0.5 to 0.3) reduction of friction coefficient; in addition, according to research on top of rail friction modifier using rail lubrication, an average of 5.3% and 7.8% reduction of

operation power consumption rate is recorded in the research for curve and a tangent rail track (Vandermarel *et al*.,2013).

Moreover, based on the finding in the experimental analysis, the acceleration region covers approximately 250 m from the station for 50% of train loading and 500 m from the station for 100% of train loading, producing a slightly identical value of operation power consumption with and without the application of rail grinding. This is due to the reduction of resistance in the application of rail grinding is contrariwise by the increase of train acceleration in this stage. The reduction of operation power consumption can only be observed when the train operation enters the constant speed region where the acceleration equals zero. Therefore, it is significant to focus on the constant speed region only for a reduction in operating power consumption activities.

In summary, according to the above experimental analysis, approximately 9% lower operation power consumption is produced in a reduction of 40% of the track coefficient of friction and 9% of the resistance. This finding is supported by the theoretical analysis and a previous finding by Shuai *et al*., 2016. In addition, a reduction of 3 seconds of station-to-station trip time is recorded in every 40% lower track coefficient of friction and resistance due to the higher acceleration rate for lower loading trains during acceleration region. In alignment with the train loading and track coefficient of friction analysis, every decrease in the percentage of resistance will decrease an approximately similar rate of operation power consumption. In addition, the effect of reduction in track coefficient of friction to operation power consumption in the acceleration region is small and only can be observed in the constant speed region.

The power reduction percentage in the reduction of track coefficient of friction is smaller than other strategies due to low-speed metro operation, and train resistance in aerodynamic drag is neglected. In high-speed rail operations, train resistance will cover much of the total traction power consumption (Su *et al*., 2016). However, the small percentage of reduction in operating power consumption may increase further with the proper implementation of rail grinding strategies.

5.2.3 Comparison of experimental and theoretical result

Based on the finding in experimental analysis, a reduction in operating power consumption from 100% train loading to 50% train loading (21% reduction in total train mass) is an approximate 21% reduction in operating power consumption. Meanwhile, a reduction of operation power consumption after rail grinding is implemented is about 9% for μ=0.5 to μ=0.3, approximately 40% reduction of track coefficient of friction, and a 9% reduction in resistance. If we compare it with the result of theoretical analysis, we can identify that every decrease in resistance will decrease the same amount of operation power consumption. In addition, the experimental analysis is also parallel with the hypothesis being introduced in the theoretical analysis.

Therefore, the finding in theoretical and experimental analysis agrees relatively well; reducing 50% of train loading, i.e., a reduction of 21% in train mass production, 21% reduction in resistance, and approximately 21% saving in operating power consumption, will be achieved. Every 40% reduction of the track coefficient of friction produces a 9% reduction in resistance, producing a 9% saving in the operating power consumption rate. In addition, the finding in the experimental analysis is also in good agreement with the study in the previous literature review and research discussed above.

5.2.4 Safe application of rail grinding

However, it is essential to strike a balance in achieving the desired level of friction. Excessively low friction may lead to challenges in braking efficiency and train control, potentially compromising operation safety.

Therefore, rail engineers should carefully consider and optimize the coefficient of friction after rail grinding to ensure it aligns with safety standards, operational requirements, and the overall efficiency of the rail system. According to section 2.4.1, there is a minimum allowable coefficient of friction for rail grinding application to prevent wheel slipping problems.

Based on equation 2.7, experimental analysis shows the minimum permissible coefficient of friction, μ, to be taken to consider preventing the wheel slipping problem for a maximum T_E of 3500 kN is μ=0.02. The track coefficient of friction, μ lower than this value, may cause hazards to the train operation. Therefore, studying the minimum track coefficient of friction before applying rail grinding activities is crucial because each rail operation has a different maximum tractive force and adhesive weight.

5.2.5 Influence of rail grinding to running resistance

According to the finding in the above section on operation power consumption before and after rail grinding was applied, it can be concluded that rail grinding had successfully lowered the track coefficient of friction, μ=0.5 to μ=0.3, reducing the resistance value in the Davis equation.

The operation power consumption after rail grinding is about 9% lower than before. The train station-to-station trip time is also reduced due to the increase in acceleration rate during the first stage of the rail operation (acceleration region). The changes in track coefficient of friction, μ from a higher value to a much lower value, had successfully lowered the operation power consumption by decreasing the traction force due to the reduction in resistance.

In addition, changes in the A value of the Davis equation using the rail grinding method successfully lower the power consumption value in the study, and it can be concluded that the A value of the Davis equation brings a significant effect to operation power consumption by reduction of 4% of operation power consumption in μ=0.1 reduction in track coefficient of friction, μ.

However, some considerations should be considered to maximize the efficiency of a grinding method, such as minimizing the specific grinding area to optimize manpower and resources. Hence, two factors must be regarded to make the rail grinding application safe and cost-effective for daily train operation.

5.2.6 Application of rail grinding to lower operation power consumption

Rail grinding is an essential rail preventive maintenance to ease track surface from corrugation and improve track profile; achieve the longest possible rail life by reducing the cycle of rail track replacement and maintaining a good track profile for rail operation safety. Indirectly, this activity may improve the track friction coefficient, and seldom being neglected by rail engineers, that lower track friction coefficient may reduce operation power consumption.

Applying rail grinding to a not corrugated and good rail profile track to achieve a lower track friction coefficient wastes grinding resources. Still, the outcome can be beneficial to rail operators. Nevertheless, applying an excellent grinding resource plan may improve these activities in even future. Therefore, a comprehensive grinding plan must be set up before proceeding with the application.

Improving the grinding process to reduce the rail grinding cost and resources is important. Based on the above finding, several can way be implemented to reduce the rail grinding resources. For example, based on the implication of the experimental result shows, the percentage drop in operation power consumption can only be visualized in the constant speed region after the application of rail grinding; the focus region can now be identified to apply the rail grinding process. The improvement of rail grinding process by minimizing the grinding area may improve rail grinding even further.

5.3 CHAPTER SUMMARY

During the acceleration region of operation, a lower train loading and track coefficient of friction, μ producing lower operation power consumption due to lower rail running resistance and trip time. Nevertheless, the difference in running resistance at the acceleration and constant speed region in the study are affected by the *A* value in the Davis equation that affects the power consumption. In addition, the effect of reduction in track coefficient of friction to operation power consumption in the acceleration region is small and only can be observed in the constant speed region. Based on the study of operation power consumption before and after rail grinding is applied, a successful change of resistance value in the Davis equation, the operation power consumption rate after rail grinding is about 9% lower compared to before rail grinding due to the decrease in track coefficient of friction after the application of rail grinding. Therefore, changes in the resistance value of the Davis equation using the rail grinding method successfully lower the power consumption value in the study. Still, some consideration should be taken to maximize the efficiency of a grinding process, such as minimizing the specific grinding area to improve manpower and resources.

CHAPTER SIX

CONCLUSION AND RECOMMENDATION

6.1 CONCLUSION

In conclusion, this research had achieved the three objectives of research. This research had successfully evaluate the dynamic characteristics of train motion, including acceleration, constant speed, cruising, and braking, through precise measurements and analysis of operational data in order to enhance understanding of rail operation dynamics. Improve the power consumption profile of the train under various operating conditions and to establish a quantitative understanding of power consumption patterns and analyse the impact of rail track coefficient of friction on rail operation power consumption, hence to assess the correlation between train running resistance and operation power consumption using theoretical and experimental analysis.

Four types of station-to-station travel produce different rail operation power consumption profiles. This is due to different types of station-to-station travel motions consisting of the different regimes of operation, i.e., acceleration, constant speed, cruising, and braking regimes. The type of station-to-station travel motion is determined according to the allowable trip time, station distance, and type of operation. The study resembles type b of station-to-station travel that consists of acceleration, constant speed, braking, and station-stop regime of motion. This is due to short station-to-station distance, low allowable trip time, and requirement operation reliability of the train operation. The net force equation also varies by acceleration, constant speed, braking, and station stop in the regime of train motion.

The variations in the net force equation in each station-to-station motion produce different power consumption profiles. Reduction in rail operation power consumption is essential for rail operators. Train resistance plays a vital role in reducing rail operation power consumption. Train resistance is directly related to the Davis equation. Reduction in train resistance can be attained by reducing train loading and track coefficient of

friction neglected the train is in low-speed operation where aerodynamic resistance is neglected. Reduction in train loading can be achieved by good passenger platform management. Meanwhile, a reduction in the track coefficient of friction can be obtained using the rail grinding method.

The rail grinding method is a conventional rail preventive maintenance procedure that aims to improve track profile and ease track corrugation; indirectly, it can reduce the track coefficient of friction. However, there is a minimum allowance coefficient of friction that is allowed in this method to prevent train wheel slipping and sliding problems. The minimum permissible coefficient of friction, μ, to prevent train wheel slipping and sliding problems is $\mu=0.02$. According to the study, for every 50% reduction in train loading, a decrease of 20% in total train total mass is attained. Therefore an average of 21% of operation power consumption is reduced. In addition, in every 40% reduction of track coefficient of friction, an average of 9% of rail operation power consumption is reduced. Therefore, reducing the track coefficient of friction by rail grinding has reduced operation power consumption by 9%. Meanwhile, applying the rail grinding method requires extra resources from the rail operator. Therefore, improving rail grinding process by minimizing grinding area is essential in reducing rail grinding resources. Table 6.1 is the summary of the analysis,

Table 6.1: Summary of the analysis.

Variable	**Reduction in**		
	Variable	**Resistance**	**Power consumption**
Train mass	20%	21%	21%
Coefficient of friction	40%	9%	9%

6.2 RECOMMENDATION 1

The following recommendations are suggested to optimize the rail grinding method further to cope with the application to reduce the track coefficient of friction.

6.2.1 Improving rail grinding

Rail grinding aims to achieve the longest possible rail life without affecting the safety risks and costs associated with rail failures and part replacement (Sroba, 2013). In addition, to get an optimal rail grinding result, rail operators must know the cost and safety risks of the grinding process. These two factors must be controlled so that the process will not adversely affect the operator, as rail grinding for lowering operation power consumption is not a priority. Therefore, managing rail grinding costs in terms of resources is essential in this study.

6.2.2 Minimizing rail grinding station

Rail grinding is a complex method that requires manpower, time, and resources, minimizing the grinding area to get optimum results (Sroba, 2013). According to the finding in the experimental analysis, the acceleration region, the region with the highest power consumption, covers approximately 270 m from the station; therefore, this area should be the focus of applying the grinding method.

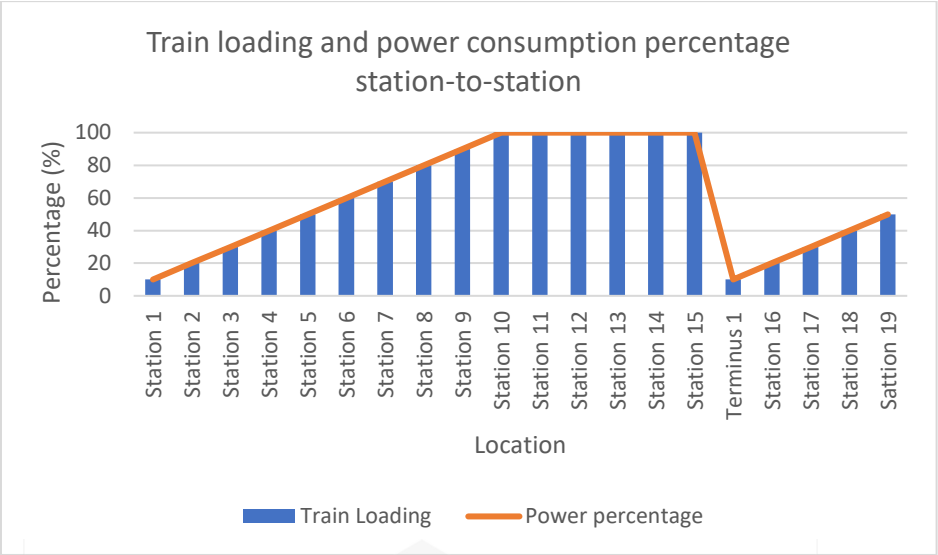

Figure 6.1: Graph of train loading and power consumption percentage station-to-station.

As daily train operation covers several stations with repeated acceleration, constant speed, and breaking region, minimizing grinding station may improve the technique further. In terms of reducing the grinding station, the build-up of passengers inside the train achieves 100% loading at the 10th station.

Based on the above finding in section 5.2, higher train loading produces higher operating power consumption; hence applying rail grinding at the location that exerted the maximum operation power consumption (maximum train loading) may further improve the previous methods. For instance, an 8% reduction of operation power consumption may significantly impact a 200 kW power consumption train operation compared to a 100 kW power consumption train operation. Therefore, if we refer to the above Figure 6.1 train loading by station and power consumption graph, we can conclude that rail grinding should be focused on the 10th station upwards.

6.2.3 Minimizing rail grinding area

Rail grinding is a complex method that requires manpower, time, and resources; therefore, minimizing the grinding area to get optimum results is important (Sroba, 2013).

According to the above finding in the experimental analysis, the acceleration region covers approximately 500 m from the station producing slightly identical values of operation power consumption with and without the application of rail grinding due to the reduction of resistance in the application of rail grinding is contrariwise by the increase of train acceleration in the stage. The reduction of operation power consumption can distinctly be observed when the train operation enters the constant speed region where the acceleration equals zero. In addition, the constant speed region also covers most areas of the rail operation, producing the highest impact on a reduction in operating power consumption.

Therefore, to consider the minimum effect of operation power consumption reduction in the first stage of the train operation (acceleration region), the second stage of operation (constant speed region) area should focus on applying the rail grinding method; hence, to optimize grinding resources. The constant speed region is approximately 500 m from the station to the breaking point location (1500 m from the station) for 100% train loading.

6.2.4 Application of rail grinding improvement

Daily train operation covers several stations with repeated acceleration, constant speed, and breaking region; minimizing grinding stations may improve the method further.

Reducing the rail grinding station, the build-up of passengers inside the train achieves 100% loading at the 10th station; therefore, rail grinding should be focused on

the 10th station upwards till the 15th station. Moreover, in terms of minimizing the rail grinding area, the constant speed region brings the highest impact on reducing operation power consumption. Therefore, rail grinding should be focused in this area, where 500 m from the station to the breaking point location (1500 m from the station).

Consequently, by applying rail grinding only at trains only at the 10th station till the 15th station and only at constant speed region, an area of 500 m from the station to the breaking point location (1500 m from the station) to reduce the rail grinding area. The following figure 6.2 result is produced,

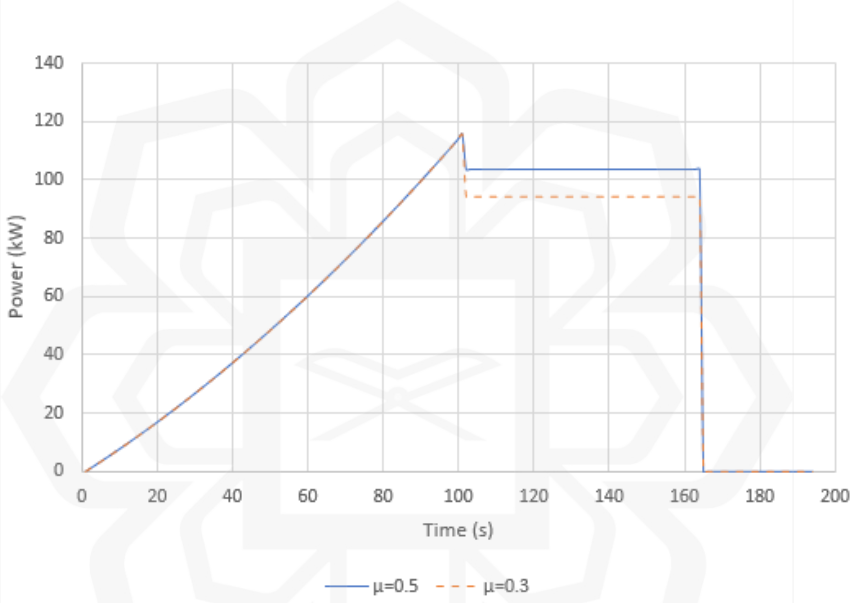

Figure 6.2: Graph of comparison between before and after rail grinding of 100% train loading with grinding optimization in term of travel distance.

According to Figure 6.2, after optimizing the grinding station and area, grinding only at the specific station and area (constant speed region), approximately 5% of the operation power consumption rate is reduced for 100% loading compared to without rail grinding application. Although the reduction is lower than the previous, the manpower and resources are decrepitly lower. For example, by optimizing the grinding area from approximately 1500 m to only 1000 m, roughly about 35% of manpower and resources are expected to reduce and save. Moreover, applying a specific and suitable station to apply rail grinding will also optimize the rail grinding resources.

6.3 RECOMMENDATION 2

In addition, instead of applying optimized rail grinding, the following recommendations are suggested for further investigation based on the problems encountered throughout the study.

6.3.1 Running rail coating and material

According to experimental analysis, an area that brings a significant effect on operation power consumption when the track coefficient of friction is lower is the constant speed region. Therefore, a lower friction coefficient can be attained by applying coating on the rail track at the constant speed region. This process can also be implemented by introducing a lower friction coefficient material rail track in this region.

6.3.2 Aerodynamic resistance

Applying good train body aerodynamic streamlining may further reduce train resistance. The reduction of the *C* value in the Davis equation may enormously impact the overall train resistance value. Therefore, designing a good train body streamlines and will further reduce the train resistance.

6.3.3 Track gradient

According to the literature review, applying the suitable track gradient at the right location may affect the rail operation power consumption. The track gradient is affected by using the gradient equation in the net force equation. Therefore, designing a train

running track with a suitable gradient location may improve overall rail operation power consumption.

6.3.4 Trip time

Based on the literature review, good station-to-station trip time may further improve rail operation power consumption. Trip time may affect the velocity profile of the station-to-station travel. Good trip time may be achieved by optimized platform dwell duration. Therefore, designing a good operation timetable may improve the overall operation power consumption further.

6.4 CHAPTER SUMMARY

Reduction in train resistance can be attained by reducing train loading and track coefficient of friction neglected the train is in low-speed operation where aerodynamic resistance is neglected. It is recommended to apply rail grinding optimization to reduce rail grinding costs and resources. Moreover, the study successfully addresses all the objectives of the study. However, several recommendations can be considered for future research, such as assessing the aerodynamic resistance, track gradient, and trip time to make the analysis more accurate and precise.

REFERENCES

Alexander Hu and Bruce Peachey (2016). *Redesigning an Experiment to Derermine the Coefficient of Friction*

Alex Landex (2012). *Reliability of Railway Operation.*

Allan M. Zarembski (2019). *The Relationship Between Rail Grinding And Rail Lubrication.*

Anupiya Arupiya, Prateek Bansal, Daniel Graham (2020). *Understanding the Cost of Urban Rail Transport Operation.*

B. P. Rochard (2004). *Benefits of lower-mass trains for high speed rail operations.*

Dejan Makovsek, Vincent Benezech and Stephen Perkins (2019). *Efficiency in Railway Operation and Infrastructure Management.*

E. Mikhailov, *S.* Semenov, *V.* Tkachenko and *S.* Sapronova (2018). *Reduction of Kinematic Resistance To Movement Of the Railway Vehicles*

G. Boschetti, A. Mariscotti (2012). *The Parameters of Motion Mechanical Equations as A Source of Uncertainty for Traction System Simulation..*

Galaï-Dol, L., De Bernardinis, A., Nassiopoulos, A., Peny, A., & Bourquin, F. (2016). *On the Use of Train Braking Energy Regarding the Electrical Consumption Optimization in Railway Station. Transportation Research Procedia, 14(Supplement C), 655-664.*

González-Gil, A., Palacin, R., & Batty, P. (2014*). Optimal energy management of urban rail systems: Key performance indicators. Energy Conversion and Management, 90(Supplement C), 282-291.*

González-Gil, A., Palacin, R., Batty, P., & Powell, J. P. (2014). *A systems approach to reduce urban rail energy consumption. Energy Conversion and Management, 80, 509-524.*

H.Chen, T.Furuya, S.Fukagai, S.Saga, J.Ikoma, K.Kimura, J.Suzumura (2020). *Wheel slip/slide and low adhesion caused by fallen leaves.*

Hansen, H. S., Nawaz, M. U., & Olsson, N. (2017). *Using operational data to estimate the running resistance of trains. Estimation of the resistance in a set of Norwegian tunnels. Journal of Rail Transport Planning & Management, 7(1), 62-76.*

Hongxiao Li & Li Li (2023). *Influence of Wheel Profile Wear Coupled with Friction coefficient on the Dynamic Response of Subway Vehicles.*

Hsiang P. & Chen S. (2001). *Electric Load Estimation Techniques for High-Speed Railway (HSR) Traction Power Systems.*

Huan Xie, Xiang Chen, Wei Zeng, Wensheng Qiu, Tao Ren (2020). *A novel prediction method for rail grinding profile based on an interval segmentation approach and accurate area integral with cubic NURBS.*

Innotrack (2006). *D4.5.5 - Guidelines for Management of Rail Grinding.*

International Union of Railways (2005). *Energy Efficiency Strategies for Rolling Stock and Train Operation*.

Irvin A. Vasquez-Chacon, Pedro Sanchez-Tizapantzi, Mario A. Gomez-Guarneros, Mauro A. Enciso-Aguilar, Ezwquiel A. Gallardo-Hernandez (2023). *Runninh-in Evaluation after a Rail Grinding Process Using a Pin-on-disk Tribometer*.

J. Riley (2010). *Rail Transportation CEE 220: Train Energy, Power and Traffic Control.*

James, C. (1994). *Hands-on Physics Activities with Real-life Applications, John Wiley & Sons.*

Jan Lundberg, Matti Rantatalo, Christina Wanhainen, Johan Casselgren (2015). *Measurements of friction coefficient between rail lubricated with a friction modifier and the wheel of an IORE locomotive during real working condition.*

Jean Paul (2015), *The Geography of Transportation System- Rail Transportation and Pipelines.*

Jinghui Wang, Hesham A. Rakha (2017). *Electric Train Energy Consumption Modelling.*

Joachim Ihme (2022). *Running Resistances of Rail Vehicles. In: Rail Vehicle Technology. Springer, Wiesbaden.*

Joel Vandermarel, Donald T. Eadie, Kevin D. Oldknow, Simon Iwnicki (2013). *A Predictive Model of Energy Savings from Top of Rail Friction Control.*

Jong & Chang (2005). *Models for estimating energy consumption of electric trains, Journal of the Eastern Asia Society for Transportation Studies, Vol. 6, pp. 278 – 291.*

Joseph Selvi Binoj, Vijesh Yogesh Shah, Bhavna Chhatwani, Rahul Chhikara (2022). *Influence of grinding on rail surface and profile – A review.*

Jun Yang, Yinghao Tang, Tan Ye, Xiao Han, Mengjie Gong (2022). *Optimization of Metro Trains Operation Plans Based on Passenger Flow Data Analysis.*

M. Ishida, T. Ben, F. Aoki (2006). *The effect of Lubrication on Vehicle/Track Interaction and Performance of Friction Moderator.*

Mahesh Kumar (2013). *Rail Electrica- Wheel Slipping and Sliding.*

Ministry of Transportation Malaysia (2019). *Overview of Railway Industry-Railway Development in Malaysia.*

M V Konstantinova, V I Varavin, R R Dagaev (2022). *Application of Regenerative Braking on Electric Rolling Stock.*

P Rochard, B., & Schmid, F. (2000). *A review of methods to measure and calculate train resistances (Vol. 214).*

Patrick Bochmann & Birgit Jaekel (2022). *Measures and methods for the evaluation of ATO algorithms.*

Peter Sroba (2013). *Rail Grinding Best Practice For Committee 4, Sub-Committee 9.*

Qing Gu, Toa Tang, Yong-duan Song (2010). *A Survey on Energy-saving Operation of Railway Transportation system.*

Qing Gu,Tao Tang,Fang Cao,Hamid Reza Karimi and Yongduan Song (2013). *Peak Power Demand and Energy Consumption Reduction Strategies for Trains under Moving Block Signalling System.*

Rios, M., & Ramos, G. (2012). *Power System Modelling for Urban Massive Transportation Systems.*

S. Yu. Sapronova, V. P. Tkachenko, O. V. Fomin, I. I. Kulbovskiy, E. P. Zub. (2017). *Rail Vehicles: The Resistance to The Movement and The Controllability.*

Satoshi Koizumi (2013). *Advance in Railway Vehicle Technology and Future Prospects Mainly in Relation to Bogie*

Shuai Su, Tao Tang and Yihui Wang (2016). *Evaluation of Strategies to Reducing Traction Energy Consumption of Metro Systems Using an Optimal Train Control Simulation Model.*

Shuai Su, Tao Tang, X. Li, Z. Goa (2014). *Optimization on multi-train operation in subway system.*

Shuqi Liu, Fang Cao, Jing Xun, Yihui Wang (2015). *Energy-efficient operation of single train based on control strategy of ATO.*

SKF (n.d.). *Rail lubrication through lubrication holes. https://www. https://www.skf.com/sg/industries/railways/solutions/lubrication-holes/*

Sonia (2012). *Passenger Boarding/Alighting Management in Urban Rail Transportation*.

Takafumi Koseki (2010*). Technologies for Saving Energy in Railway Operation: General Discussion on Energy Issues Concerning Railway Technology.*

VanderMarel, J., Eadie, D. T., Oldknow, K. D., & Iwnicki, S. (2013). *A predictive model of energy savings from top of rail friction control. Wear, 314(1), 155-161.*

Venkatarami Reddy (2004). *Modelling and Analysis of Rail Grinding & Lubrication Strategies for Controlling Rolling Contact Fatigue (RCF) and Rail Wear.*

Vukan, R. (2007). *Vehicle Motion and Performance. In: Urban Transit Systems and Technology. John Wiley & Sons, Inc. Hoboken.*

Wolfram Heineken, Marc Richter, Torsten Birth (2023). *Energy-efficient Train Driving Based on Optimal Control Theory.*

Wu and Wilson (2006). *Handbook of Railway Vehicle Dynamics, S. Iwnicki.*

Xing Du, Xuesong Jin, Guotang Zhao, Zefeng Wen, Wei Li (2021). *Rail corrugation of high-speed railway induced by rail grinding.*

Xujie Feng, Quanxin Sun, Lu Liu, Minggao Li (2014). *Assessing Energy Consumption of High-speed Trains Based on Mechanical Energy.*

Y.A.Areiza, S.I.Garcés, J.F.Santa, G.Vargas, A.Toroa (2014). *Field measurement of coefficient of friction in rails using a hand-pushed tribometer.*

Ziyou Gao & Lixing Yang (2019). *Energy-saving Operation Approaches for Urban Rail Transit Systems.*

Zhao, Y., Liang, B., & Iwnicki, S. (2012). *Estimation of the friction coefficient between wheel and rail surface using traction motor behaviour (Vol. 364).*

Zongyi Xing, Zhenyu Zhang, Jian Guo, Yong Qin, Limin Jig (2023). *Rail train operation energy-saving optimization based on improved brute-force search.*